NICOTINE AND POLYCYCLIC AROMATIC HYDROCARBONS MODULATE JUNCTIONAL PROTEINS AND PARACELLULAR PERMEABILITY OF RAT CEREBRAL ENDOTHELIAL CELLS

Miss Pilaiwanwadee Hutamekalin

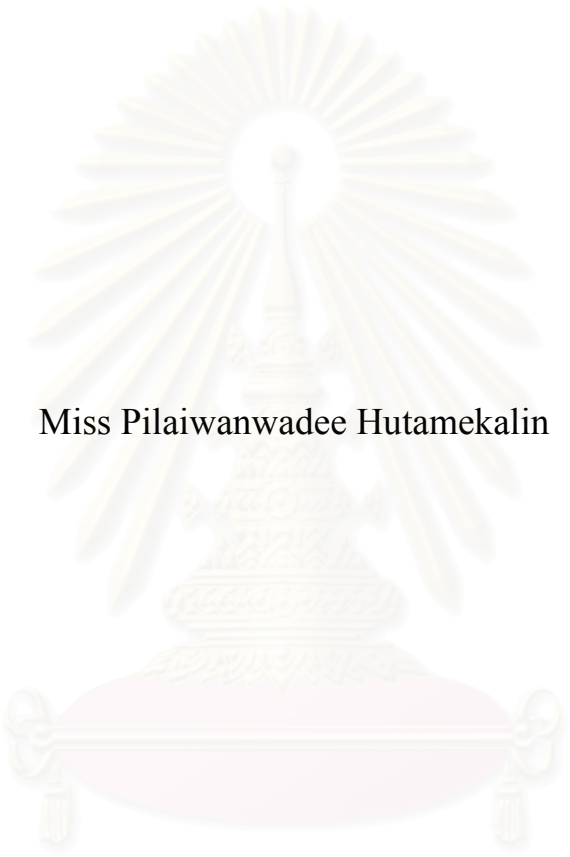

A Dissertation Submitted in Partial Fulfillment of the Requirements
for the Degree of Doctor of Philosophy Program in Biomedicinal Chemistry
Department of Biochemistry
Faculty of Pharmaceutical Sciences
Chulalongkorn University
Academic year 2006

นิโคตินและพอลิไซคลิกอะโรมาติกไฮโดรคาร์บอนเปลี่ยนแปลงการทำงานของโปรตีนที่เชื่อมระหว่างเซลล์หลอดเลือดจากสมองหนูขาว

นางสาว พิไลวรรณวดี หุตะเมขลิน

วิทยานิพนธ์นี้เป็นส่วนหนึ่งของการศึกษาตามหลักสูตรปริญญาวิทยาศาสตรดุษฎีบัณฑิต
สาขาวิชาชีวเวชเคมี ภาควิชาชีวเคมี
คณะเภสัชศาสตร์ จุฬาลงกรณ์มหาวิทยาลัย
ปีการศึกษา 2549

Thesis Title	NICOTINE AND POLYCYCLIC AROMATIC HYDROCARBONS MODULATE JUNCTIONAL PROTEINS AND PARACELLULAR PERMEABILITY OF RAT CEREBRAL ENDOTHELIAL CELLS
By	Miss Pilaiwanwadee Hutamekalin
Field of study	Biomedicinal Chemistry
Thesis Advisor	Associate Professor Duangdeun Meksuriyen, Ph.D.
Thesis Co-Advisor	Istvan A. Krizbai, M.D., Ph.D.

Accepted by the Faculty of Pharmaceutical Sciences, Chulalongkorn University in Partial Fulfillment of the Requirements for the Doctoral Degree

.....Dean of Faculty of Pharmaceutical Sciences
(Associate Professor Pornpen Pramyothin, Ph.D.)

THESIS COMMITTEE

.....Chairman
(Assistant Professor Niyada Kiatying-Angsulee, Ph.D.)

.....Thesis Advisor
(Associate Professor Duangdeun Meksuriyen, Ph.D.)

.....Thesis Co-advisor
(Istvan Krizbai, M.D., Ph.D.)

.....Member
(Associate Professor Thitima Pengsuparp, Ph.D.)

.....Member
(Associate Professor Vimolmas Lipipun, Ph.D.)

.....Member
(Associate Professor Banthit Chetsawang, Ph.D.)

พิไลวรรณวดี หุตะเมฆลิน: นิโคตินและพอลิไซคลิกอะโรมาติกไฮโดรคาร์บอนเปลี่ยนแปลงการทำงานของโปรตีนที่เชื่อมระหว่างเซลล์หลอดเลือดจากสมองหนูขาว (NICOTINE AND POLYCYCLIC AROMATIC HYDROCARBONS MODULATE JUNCTIONAL PROTEINS AND PARACELLULAR PERMEABILITY OF RAT CEREBRAL ENDOTHELIAL CELLS) อ.ที่ปรึกษา: รศ.ดร. ดวงเดือน เมฆสุริเยนทร์, อ.ที่ปรึกษาร่วม: Dr. ISTVAN A. KRIZBAI, 105 หน้า

การสูบบุหรี่ก่อให้เกิดโรคทางระบบประสาทมากมาย รวมทั้งส่งผลกระทบต่อความบกพร่องทางหน้าที่ของเซลล์เยื่อบุผนังหลอดเลือดในสมอง อย่างไรก็ตามความรู้เกี่ยวกับผลกระทบของการสูบบุหรี่ต่อเซลล์เยื่อบุผนังหลอดเลือดยังมีน้อยมาก ดังนั้นวัตถุประสงค์ของการวิจัยนี้จึงมุ่งเน้นศึกษาถึงผลขององค์ประกอบสำคัญของบุหรี่คือ นิโคตินและพอลิไซคลิกอะโรมาติกไฮโดรคาร์บอนที่มีต่อเซลล์เยื่อบุผนังหลอดเลือดจากสมองหนูขาวที่กั้นระหว่างเลือดและสมอง จากการศึกษาการแสดงออกของโปรตีนที่เชื่อมต่อระหว่างเซลล์เยื่อบุผนังหลอดเลือดด้วยเทคนิค Western blot พบว่าเซลล์ที่ได้รับนิโคตินที่ความเข้มข้น 10 ไมโครโมลาร์ เป็นเวลา 24 ชั่วโมง ลดปริมาณโปรตีน cadherin และ ZO-1 ใน Triton X-100 อย่างมีนัยสำคัญ อย่างไรก็ตามกลับไม่พบการเปลี่ยนแปลงของโปรตีนดังกล่าวเมื่อทดสอบด้วยพอลิไซคลิกอะโรมาติกไฮโดรคาร์บอนคือ phenanthrene และ 1-methylanthracene ที่ความเข้มข้น 30 ไมโครโมลาร์ เป็นเวลา 24 ชั่วโมงจากการใช้วิธี immunostaining เพื่อศึกษาการกระจายตัวของโปรตีนที่เชื่อมต่อระหว่างเซลล์เยื่อบุผนังหลอดเลือด พบว่าการกระจายตัวของโปรตีน cadherin และ ZO-1 เปลี่ยนแปลงไปในสภาวะที่เซลล์ได้รับนิโคติน โดยสังเกตได้จากการเรียงตัวของโปรตีนรอบ ๆ ขอบเซลล์กระจายไม่ต่อเนื่องเมื่อเทียบกับเซลล์ที่ไม่ได้รับนิโคติน ซึ่งสอดคล้องกับผลการทดลองที่ได้จากวิธี Western blot สำหรับเซลล์ที่ได้รับ phenanthrene และ 1-methylanthracene กลับไม่พบการเปลี่ยนแปลงของโปรตีนใด ๆ จากผลการทดลองที่พบการเปลี่ยนแปลงอย่างมีนัยสำคัญของโปรตีน ZO-1 ในเซลล์ที่ได้รับนิโคติน จึงศึกษาหาความสัมพันธ์ระหว่างการจับกันของโปรตีนภายในเซลล์ด้วยวิธี co-immunoprecipitation พบว่าการจับยึดกันระหว่างโปรตีน occludin และ ZO-1 ลดลงเมื่อเซลล์ได้รับนิโคติน จึงทำการศึกษาต่อไปว่าผลการเปลี่ยนแปลงดังกล่าวจะส่งผลกระทบต่อหน้าที่การซึมผ่านระหว่างเซลล์ด้วยการวัดค่าความต่างศักย์ระหว่างเซลล์เยื่อบุผนังหลอดเลือด ไม่พบการเปลี่ยนแปลงของค่าความต่างศักย์ระหว่างเซลล์ที่ได้รับนิโคตินและพอลิไซคลิกอะโรมาติกไฮโดรคาร์บอนแต่อย่างใด จากรายงานวิจัยส่วนใหญ่ระบุว่าความเครียดก่อให้เกิดพยาธิสภาพของระบบประสาทส่วนกลาง ดังนั้นจึงทำการศึกษาถึงผลกระทบร่วมระหว่าง oxidative stress และนิโคตินด้วยวิธี immunostaining พบว่าเมื่อเซลล์ได้รับนิโคตินที่ความเข้มข้น 10 ไมโครโมลาร์ร่วมกับ 2,3-dimethoxy-1,4-naphthoquinone (DMNQ) ที่ความเข้มข้น 10 ไมโครโมลาร์พบโปรตีน ZO-1 กระจายตัวไม่ต่อเนื่องเมื่อเทียบกับเซลล์ที่ได้รับ DMNQ หรือนิโคตินเพียงอย่างเดียว นอกจากนี้ นิโคตินยังทำให้ค่าความต่างศักย์ระหว่างเซลล์เยื่อบุผนังหลอดเลือดเมื่ออยู่ในสภาวะ oxidative stress ลดลงอย่างมีนัยสำคัญ จากการศึกษาครั้งนี้สรุปได้ว่านิโคตินมีผลต่อการเปลี่ยนแปลงต่อการแสดงออกและการกระจายตัวของโปรตีน cadherin และ ZO-1 อย่างมีนัยสำคัญ โดยเฉพาะอย่างยิ่งเมื่อเซลล์อยู่ภายใต้สภาวะ oxidative stress ซึ่งจะส่งผลกระทบต่อการทำหน้าที่ของเซลล์เยื่อบุผนังหลอดเลือดในสมอง

ภาควิชา.....ชีวเคมี.....ลายมือชื่อนิสิต.....พิไลวรรณวดี หุตะเมฆลิน.....

สาขาวิชา.....ชีวเวชเคมี.....ลายมือชื่ออาจารย์ที่ปรึกษา.....

ปีการศึกษา.....2549.....ลายมือชื่ออาจารย์ที่ปรึกษาร่วม.....

4576963533: MAJOR BIOMEDICINAL CHEMISTRY
KEY WORDS: NICOTINE / POLYCYCLIC AROMATIC HYDROCARBONS / BLOOD-BRAIN BARRIER / RAT CEREBRAL ENDOTHELIAL CELLS / TIGHT JUNCTIONAL PROTEINS / ADHERENS JUNCTIONAL PROTEINS

PILAIWANWADEE HUTAMEKALIN: NICOTINE AND POLYCYCLIC AROMATIC HYDROCARBONS MODULATE JUNCTIONAL PROTEINS AND PARACELLULAR PERMEABILITY OF RAT CEREBRAL ENDOTHELIAL CELLS, THESIS ADVISOR: ASSOC. PROF. DUANGDEUN MEKSURIYEN, Ph.D., THESIS CO-ADVISOR: ISTVAN A. KRIZBAI, M.D., Ph.D., 105 PAGES.

Cigarette smoking contributes to the development of several neurological disorders associated with blood-brain barrier (BBB) dysfunction. However, very little is known about the effect of smoking on the BBB. Our work was aimed on the effect of major cigarette smoke components on rat cerebral endothelial cells (CECs). Western blot analysis was used to investigate whether nicotine and polycyclic aromatic hydrocarbons (PAH), cigarette smoke components, had an effect on junctional protein expression. The results revealed that the rat CECs exposed to 10 μM nicotine for 24 h significantly decreased cadherin and ZO-1 protein expression in triton X-100 (Tx-100) soluble fraction while no change was observed either in the case of phenanthrene or 1-methylanthracene exposure at the concentration of 30 μM. Immunostaining experiments were used to determine the possible rearrangement in the subcellular distribution of cadherin and ZO-1. A disruption in the continuity of cadherin and ZO-1 staining along cell-cell contacts were observed, which was correlated with the observation obtained by Western blot analysis. No change of protein distribution after the treatment with either phenanthrene or 1-methylanthracene was observed. Due to the observation of a significant change in ZO-1 protein expression after nicotine exposure, protein-protein interactions within the rat CECs were further investigated using co-immunoprecipitation assay. The results showed that protein-protein interaction between occludin and ZO-1 decreased after nicotine exposure. To assess the potential damaging effect of cigarette smoke components on the barrier function, transendothelial electrical resistance (TEER) was measured in a coculture model using rat CECs and astrocytes. Although nicotine decreased ZO-1 protein expression and localization of junctional proteins, the barrier permeability evaluated by TEER measurements did not change in our study. The barrier permeability was also not affected by the treatment with either phenanthrene or 1-methylanthracene. There are several reports showing that oxidative stress is implicated in pathological processes of the central nervous system. Therefore, the potential cumulative effect of oxidative stress and nicotine on the BBB permeability was investigated. Immunostaining analysis revealed that co-treatment of the rat CECs with 10 μM nicotine in the presence of 10 μM 2,3-dimethoxy-1,4-naphthoquinone (DMNQ) disrupted the continuity of ZO-1 staining along the cell-cell contacts, which was more pronounce compared to DMNQ or nicotine treatment alone. Our results revealed that nicotine treatment under oxidative stress for 24 h increased the transendothelial permeability. In conclusion, nicotine significantly affects the junctional complex of the rat CECs by changing protein expression and protein localization of cadherin and ZO-1. The damaging effects are enhanced by oxidative stress, which can further disturb the function of the BBB.

Department.....Biochemistry.....Student's signature.....P. Hutamekalin.....
Field of study....Biomedicinal Chemistry.....Advisor's signature.....D. Meksuriyen.....
Academic year...2006.....Co-advisor's signature.....Krizbai.....

ACKNOWLEDGEMENTS

I would like to thank my supervisor, Associate Professor Dr. Duangdeun Meksuriyen and my co-supervisor, Dr. Istvan A. Krizbai who have been given me a great advice and helped me develop as a scientist. I will never forget for their kind suggestions, and encouragement throughout this study.

I wish to give a special thank to my co-supervisor, Dr. Istvan A. Krizbai for his hospitality and grant supported by OTKA T037956 and Philip Morris Inc. USA while I was under his supervision in Biological Research Center, Hungary.

Also, I would like to thank Assistant Professor Dr. Niyada Kiatying-Angsulee, Associate Professor Dr. Thitima Pengsuparp, Associate Professor Dr. Vimolmas Lipipun, and Associate Professor Dr. Banthit Chetsawang for being on my dissertation committee and for providing useful suggestions, comments and constructive criticism.

I take this opportunity to thank the entire group of Department of Biophysics, and friends in BRC, Hungary, including friends in Department of Biochemistry, Faculty of Pharmaceutical Sciences, Chulalongkorn University, for their friendship, cheerfulness and moral support.

I am deeply appreciated and owed the entire laboratory animal's life for giving me tools to complete my dissertation. Without them, I would not be able to get this far.

I am highly indebted to my parents, who are always with me, for their selfless love, affection and caring that helped me achieved my educational objectives. I also would like to thank my sister and brother who never let me down, for their love and support.

This work was kindly supported by Graduate School, Chulalongkorn University. I would like to thank the Pharmaceutical Research Instrument Center, Faculty of Pharmaceutical Sciences, Chulalongkorn University, for supporting the instruments.

CONTENTS

Page

CHAPTER **Page**

CHAPTER **Page**

LIST OF TABLES

LIST OF FIGURES

Figure **Page**

LIST OF ABBREVIATIONS

AH	aryl hydrocarbon
AhR	aromatic hydrocarbon receptor
AHRE	aryl hydrocarbon responsive elements
AJ	adherens junction
Arnt	aromatic hydrocarbon receptor nuclear translocator
BBB	blood-brain barrier
bFGF	basic fibroblast growth factor
bHLH-PAS	basic helix-loop-helix period aromatic hydrocarbon receptor nuclear translocator single-minded
BSA	bovine serum albumin
°C	degree Celsius (centrigrade)
CAM	cell adhesion molecule
cAMP	adenosine 3′,5′-cyclic monophosphate
CBD	catenin-binding domain
CBF	cerebral blood flow
C/D	collagenase-dispase
CECs	cerebral endothelial cells
CLS	collagenase
CNS	central nervous system
c-Src	c-terminal-v-src sarcoma (Schmidt-Ruppin A-2) viral oncogene homolog (avian)
CSC	cigarette smoke condensate
Cy3	cyanine 3
Da	dalton
DerP1	dermatophagoides P1 protein
DiL-Ac-LDL	fluorescent-labeled-acetylated low density lipoprotein
DMEM	Dulbecco’s modified Eagle’s medium
DMEM/F-12 HAM	Dulbecco’s modified Eagle’s medium/nutrient mixture F-12 Ham
DRE	dioxin responsive elements
ECAM	epithelial cell adhesion molecule
EDTA	ethylene diamine tetraacetic acid

eNOS	endothelial nitric oxide synthase
ERK	extracellular signal-regulated protein kinase
E-selectin	endothelial selectin
et al.	*et alii,* and others
EVOM	epithelial volt-ohmeter
FBS	fetal bovine serum
g	gram
GFAP	glial fibrillary acidic protein
h	hour
HCl	hydrochloric acid
HEVs	high endothelial venules
H_2O_2	hydrogen peroxide
HRP	horseradish peroxidase
HUVECs	human umbilical vein endothelial cells
ICAM	intercellular adhesion molecule
kDa	kilo dalton
mg	milligram (s)
MLC	myosin light chain
MLCK	myosin light chain kinase
µg	microgram (s)
µl	microlitre (s)
1-MA	1-methylanthracene
MAGUK	membrane-associated guanylate kinase proteins
min	minute (s)
ml	milliliter (s)
mm	millimeter (s)
mM	millimolar
N	nicotine
nM	nanomolar
nAChR	nicotinic acetylcholine receptor
NaCl	sodium chloride
NaF	sodium fluoride
nm	nanometer
OD	optical density

p53	tumor protein p53
PAH	polycyclic aromatic hydrocarbons
PBS	phosphate-buffered saline
PDZ	postsynaptic density 95-discs-large-zona occuldens 1
PECAM	platelet/endothelial cell adhesion molecule
P-gp	p-glycoprotein
%	percentage
Ph	phenanthrene
pH	the negative logarithm of hydrogen ion concentration
PI3K	phosphatidylinositol 3-kinase
PKC	protein kinase C
PLA2	phospholipase A2
PVDF	polyvinylidene fluoride
RO20-1724	4-(3-butoxy-4-methoxybenzyl) imidazolidin-2-one
ROS	reactive oxygen species
rpm	round per minute
RT	room temperature
SDS-PAGE	sodium dodecyl sulfate-polyacrylamide gel electrophoresis
sec	second
S.E.M.	standard error of mean
SPSS	statistical package for social sciences
TBS	tris-buffered saline
TBST	tris-buffered saline, 0.1% tween 20
TCF	T cell factor
TEER	transendothelial electrical resistance
TJ	tight junction
Tx-100	triton X-100
UV	ultraviolet
V	volt
VCAM	vascular cell adhesion molecule
VE	vascular endothelial
VECs	vascular endothelial cells
VEGF	vascular endothelial growth factor
VSMC	vascular smooth muscle cell

vWF	von Willebrand factor
XRE	xenobiotic responsive element
XTT	2,3-bis[2-methoxy-4-nitro-5-sulfonyl]-2H-tetrazolium-5-carboxanilide
ZO	zonula occludens
ZONAB	zonula occludens 1-associated nucleic acid-binding protein

CHAPTER I

INTRODUCTION

According to the World Health Organization, there are 1.1 billion smokers worldwide and 6,000 billion cigarettes are smoked every year. Cigarette smoking is responsible for approximately 5 million deaths a year. However, tobacco consumption is still on the rise. Tobacco smoke affects not only people who smoke, but also passive smokers who are exposed to the combustion products of tobacco. Cigarette smoke is a complex mixture of several chemicals, over 4,000 chemicals, which are present either naturally in the tobacco and transfer into the smoke, or are formed when the tobacco is burnt such as acetone, ammonia, benzene, cadmium, carbon monoxide, formaldehyde, hydrogen cyanide, lead, nicotine and tar (Kilaru *et al*., 2001). Cigarette smoking can damage a number of organ systems both in animal and human such as increasing heart rate, blood pressure and cardiac contractility (Yildiz, 2004). However, one of the well-known reasons, which make cigarette smoking to be worldwide investigated, is tobacco dependent, which activates reward pathway in the brain (Corringer *et al*., 2006; Gardner *et al*., 2006). It is primarily injurious to people because of not only its responsibility for tobacco addiction, but also eliciting the hallmark behaviors observed with addictive drugs, including self-administration, as well as withdrawal symptoms (Dani and de Biasi, 2001). In addition, cigarette smoking is one of the major risk factors in the incidence of cerebrovascular disorders such as stroke, changes in cerebral blood flow, and atherosclerosis (Chen *et al*., 1995; Neunteufl *et al*., 2002; Kurth *et al*., 2003; Ohkuma *et al*., 2003; Tsuneki *et al*., 2004). The high number of patients affected by neurological disorders related to tobacco use suggests that one of the main targets of tobacco smoke components is central nervous system (CNS) including the blood-brain barrier (BBB) (Wang *et al*., 1994; Wang *et al*., 1997; del Zoppo and Hallenbeck, 2000). By restricting the movement of different substances between blood and brain, the mammalian BBB plays an important role in the homeostasis of the CNS, which is crucial for proper neural activity. Cigarette smoking has also been shown to cause a number of endothelial cell alterations in tissue culture, specifically decreased tissue plasminogen production (Newby *et al*., 1999), activated matrix metalloproteinase-9 in brain endothelium, which degraded the vascular basement

membrane and zonula occludens-1 (ZO-1) leading to increase paracellular permeability (Asahi *et al*., 2001). Changes in permeability of the cerebral microvascular endothelium can aggravate pathological processes (Abbruscato and Davis, 1999). Despite the high incidence of cigarette smoking affecting the role of BBB, little is known about the direct effects of smoking on the BBB.

Rationale of the study

The principal anatomical substrate of the BBB is the cerebral microvascular endothelium, which form a single lining the blood vessel of the brain. The main structure responsible for the barrier properties is the tight junctions (TJ), which render the vascular wall impermeable to small and macromolecules. Because of the lack of pinocytotic vesicles in the endothelial cells of cerebral microvessels, there are minor transcellular penetrations of blood-borne substances (Hawkins and Thomas, 2005). In contrast, adherens junctions (AJ), a member of junctional complexes, play an important role in cell adhesion, migration, morphogenesis, and proliferation. AJ represent Ca^{2+} dependent cell-cell contacts localized basolateral of TJ, where transmembrane proteins of the cadherin family mediate adhesion (Bazzoni and Dejana, 2003).

By restrict the movement of different substances between blood and brain, the mammalian BBB plays an important role in the homeostasis of the CNS, which is crucial for proper neural activity. Alteration in permeability of the cerebral microvascular endothelium can contribute to several pathological processes (Abbruscato and Davis, 1999). Nicotine is able to induce a significant increase in vascular endothelial growth factor (VEGF) expression (Conklin *et al*., 2002), which in turn affects on vascular permeability involving its regulation of endothelial tight junction assembly by reducing the expression of occludin and disrupting ZO-1 and occludin organization (Wang *et al*., 2001). Tight junctions are regulated by physiological and pathological states and changes in TJ protein expression and/or organization have been associated with altered paracellular permeability (Huber *et al*., 2001). Hypoxia increases the paracellular flux across the cell monolayer via the release of VEGF, which in turn leads to the dislocalization, decrease expression, and enhances phosphorylation of ZO-1 (Fischer *et al*., 2002). Changes in BBB function are correlated with the alteration of the expression of tight junctional proteins,

occludin and ZO-1 (Huber *et al*., 2002). Hydrogen peroxide increases paracellular permeability of the BBB that is accompanied with redistribution of occludin and ZO-1 and increases protein expression of occludin and actin (Lee *et al*., 2004). Besides association among pathological, pathophysiological states, and junctional proteins, cigarette smoking also plays a role on them. The application of nicotine increases permeability of the BBB to 70-kDa dextran (Schilling *et al*., 1992). Subcutaneous injection of nicotine in rat increases the influx of permeable solutes in brain, related to local increase in cerebral blood flow (CBF) (Chen *et al*., 1995). Long term treatment with nicotine causes the increase in rat BBB permeability to sucrose, a marker for the integrity of TJ within the BBB, decreases ZO-1 protein expression (Hawkins *et al*., 2002), and also alters cerebral microvascular tight junction protein distribution (Hawkins *et al*., 2004). Additionally, nicotine increases the permeability of an *in vitro* BBB model, which is associated with diminished expression and altered distribution of the TJ protein ZO-1 mediated by endothelial nicotinic acetylcholine receptors (Abbruscato *et al*., 2004). It has been noted that nicotine modulated protein expression of junctional protein, ZO-1, via α7 nicotinic acetylcholine receptor (α7 nAChR) (Abbruscato *et al*., 2002). Furthermore, over expression of α7 nAChR induces sustained activation of ERK, which probably promotes N-cadherin expression and differentiation-like transformation in PC12 cells (Utsugisawa *et al*., 2002).

In addition to nicotine, the predominant PAH, phenanthrene and 1-methylanthracene, are abundant in cigarette smoke. PAH may play an important role in endothelial cell damage (Grevenynghe *et al*., 2006). PAH exposure has also been suggested to be involved in human cardiovascular dysfunction (Thirman *et al*., 1994) and vascular cell proliferation (Zhang and Ramos, 1997). It has been reported that PAH induced vasorelaxation in isolated rat aorta in an endothelium dependent manner (Kang and Cheng, 1997). PAH also trigger deleterious effect on mature endothelial cells by causing endothelial cell injury (Tithof *et al*., 2002). PAH activate the endothelial nitric oxide synthase (eNOS) and also up-regulate the eNOS protein expression in human umbilical vein endothelial cells (HUVEC) (Li *et al*., 2004). PAH also have an effect on the brain by changing neurotransmitter level (Gesto *et al*., 2006).

PAH induce DNA damage and disrupt the function in human endothelial cells (Whyatt *et al*., 1998; Annas *et al*., 2000). However, the effect of PAH on cerebral

endothelial cells (CECs) and paracellular permeability has not been reported elsewhere. Despite the possible harmfulness, the direct effect of cigarette smoke on cerebral endothelial cell is still unclear. The purposes of this work were to clarify the structural and functional alteration of rat CECs at interendothelial junction sites elicited by nicotine and PAH using rat CECs model.

Objectives

1. To elucidate the effect of nicotine, phenanthrene, and 1-methylanthracene on junctional protein expression of rat CECs.
2. To study the possible changes in the subcellular localization of interendothelial junctional proteins of rat CECs in response to nicotine, phenanthrene, and 1-methylanthracene.
3. To study the protein-protein interactions of junctional proteins of rat CECs affected by nicotine, phenanthrene, and 1-methylanthracene.
4. To assess the potential damaging effect of nicotine, phenanthrene, and 1-methylanthracene on the barrier properties of rat CECs.

Scope of study

The present study investigated the effect of nicotine, phenanthrene, and 1-methylanthracene on the expression and localization of junctional proteins in rat CECs using Western blot and immunostaining analysis. The protein-protein interaction of junctional proteins affecting by the smoke components were investigated using immunoprecipitation. The TJ assembly was elucidated by transendothelial electrical resistance (TEER) measurement (Figure 1).

To investigate the effects of nicotine and PAH, 1-methylanthracene and phenanthrene, on junctional proteins, a well-defined *in vitro* BBB model based on the culture of rat CECs was used. The methods were designed as the following. Rat CECs were exposed to nicotine or PAH. The effect of nicotine or PAH on the expression of junctional proteins of TJ and AJ such as occludin, claudin-5, ZO-1, and cadherin, were investigated by Western blot analysis. Furthermore, immunofluorescence was used to determine the subcellular localization of the principal protein components of the interendothelial junctions. The interaction of junctional proteins of TJ and AJ were further analyzed by immunoprecipitation

technique. Additionally, paracellular barrier, characteristic of the cerebral capillary endothelium, was investigated using TEER measurement.

Contributions of the study

Understanding the structural-functional relationships between molecular components of junctional complexes of BBB can provide information about various pathological conditions of the central nervous system affecting by cigarette smoke components and might help to elaborate novel therapeutic approaches.

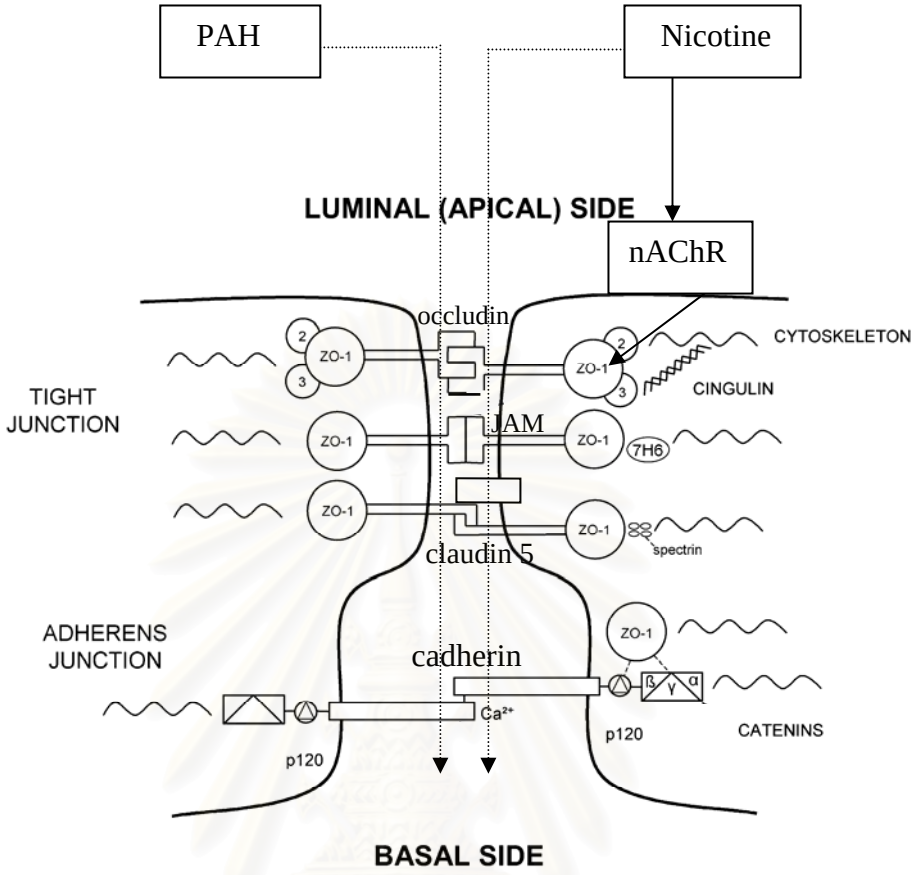

Vorbrodt and Dobrogowska, 2003

Figure 1 Proposed diagram of nicotine and PAH on endothelial cells on junctional protein expression and paracellular permeability.

Previous reports

Present investigation

CHAPTER II

LITERATURE REVIEW

Cigarette smoking

There are over 4,000 different compounds in cigarette smoke. Cigarette smoke is a complex mixture of gases and solid particles. About 10% of these compounds constitute the particulate portion of cigarette smoke, which contains nicotine and tar. Nicotine is a major constituent of tobacco smoke. It is a potent agonist affecting various cellular processes throughout the brain. Tar is the general term for polycyclic aromatic hydrocarbon products. The remaining 90% consist of carbon monoxide, carbon dioxide, cyanides, various hydrocarbons, aldehydes, and organic acids. Both the gaseous and particulate phases have been involved agitating the normal vascular biology, especially causing injury to the endothelium (Zimmerman and MaGeachie, 1987; Lin *et al*., 1992). Cigarette smoking can also cause endothelial dysfunction such as inducing cell proliferation, cell migration, and alterations of adhesion proteins expression of vascular smooth muscle cells (Niermann, *et al*., 2003; Tsuneki *et al*., 2004; di Luozzo *et al*., 2005; Jiang *et al*., 2006). Cigarette smoke extracts generated oxidative stress and caused cytotoxic to endothelial cells via JNK pathway (Hoshino *et al*., 2005). Besides causing endothelial cells injury, cigarette smoking is also associated with various kinds of diseases (Kurth *et al*., 2003, Ohkuma *et al*., 2003). By lining the vascular system, endothelial cells are the first candidate for vascular diseases (Kilaru *et al*., 2001).

Nicotine

Nicotine or 3-(1-methyl-2-pyrrolidinyl) pyridine, an amine composed of pyridine and pyrolidine rings, contains in the moisture of the tobacco leaf. Since nicotine was first identified in the early 1800s, it has been studied extensively and showing a number of complex and sometimes unpredictable effects on the brain and the body. When the cigarette is lit, it evaporates, attaching itself to minute droplets in the tobacco smoke inhaled by the smoker. It cannot be absorbed through the cell membrane in the mouth at the pH of smoke. From the oral cavity, nicotine is inhaled into the smoker's lung, and can be absorbed through pulmonary capillary blood flow. Once the nicotine is absorbed through the alveolar blood flow, nicotine levels

quickly rise in the blood. Nicotine reaches the brain within 10-19 seconds and sends to the body organ very quickly. It is clear that nicotine is a quick acting drug, it is rapid distribution to the brain, this allows the rapid psychological and behavioral effects of nicotine on the brain (Yildiz, 2004).

It has been revealed that nicotine has profound effects on cerebral microcirculation and cerebral arterial tone, which are the sign of endothelial dysfunction (Neunteuft *et al*., 2002; Koide *et al*., 2005; Jiang *et al*., 2006). Nicotine causes dysfunction of vascular endothelial cell (VEC), with a decrease in nitric oxide synthesis in VEC and increase in endothelium-dependent vasodilatation. The primary role of nicotine is the regulation of endothelial function and that functional changes may occur in the absence of accompanying morphological changes. Chronic exposure to nicotine and acute infusion of nicotine cause an impairment of endothelim-dependent arteriolar dilation that can be restored by superperfusion with superoxide dismutase (Mayhan and Sharpe, 1998). Superoxide causes a loss of the vasodilatory action of nitric oxide and yields peroxynitrite at the same time. Indeed, significant functional perturbations in endothelial function have been identified in response to nicotine such as cell proliferation and migration (Tsuneki *et al*., 2004; di Luozzo *et al*., 2005; Jiang *et al*., 2006). In addition, nicotine has the effects on bovine aortic vascular smooth muscle cell (VSMC) migration, mediated via the mitogen-activated protein kinase (MAPK) p38 and p44/42 (di Luozzo *et al*., 2005). Nicotine can induce up-regulation of vascular endothelial growth factor expression in porcine aortic endothelial cells (Conklin *et al*., 2002). Furthermore, many studies have shown that nicotine changes gene expression of intercellular adhesion molecule (ICAM), vascular cell adhesion molecule (VCAM), and endothelial selectin (E-selectin) of human umbilical vein endothelial cells (HUVEC) (Wang *et al*., 2004; Wang *et al*., 2006). Consequently, nicotine also has an effect on cerebral microcirculation; for example, nicotine increases plasminogen activator inhibitor-1 production in human brain endothelial cells (Zidovetzki *et al*., 1999), which leads to reduce brain microvascular tissue plasminogen activator activity in rats that can result in thrombosis (Wang *et al*., 1997). By using microarray technology found that several genes such as rap1, homer, and NF-kB may play significant roles in nicotine dependence in rat brain (Konu *et al*., 2001). It is well known that nicotine is an important risk factor for stroke by breakdown of the BBB and alterations of the cerebral endothelium (Hawkins *et al*., 2002). Several lines of evidence suggest that

nicotine binds to the nAChR. nAChR are members of the ligand-gated ion channel superfamily. Previous result revealed that activation of nAChR cause phosphorylation of MAPK cascade (Heeschen *et al*., 2002). Nicotine can activate endothelial cells and induce the expression of surface/soluble VCAM-1, E-selectin through Ca^{2+} influx and ERK1/2, p38 activation which mediated by α7 nAChR (Wang *et al*., 2006) in HUVEC. It was reported that α3, α5, α7 and β2 but not α4, β2 or β4 nAChR subunits are present in cerebral vessels (Abbruscato *et al*., 2002; Hawkins *et al*., 2005). It was demonstrated that nicotine increased the permeability of the BBB by a redistribution of tight junctional proteins in cerebral microvessels via α7 nAChR (Abbruscato *et al*., 2002). Over-expression of α7 nAChR induces sustained activation of ERK phosphorylation, which promotes differentiation-like transformation and N-cadherin expression.

Polycyclic aromatic hydrocarbons

PAH are a group of over 100 different chemicals that are formed during the incomplete combustion of organic materials. PAH have found at high levels in tobacco smoke (Grevenynghe *et al*., 2006), dominantly is phenanthrene and 1-methylanthracenes (362 ng/cigarette and 1,500 ng/cigarette ng/cigarette, respectively). PAH have a broad impact on health of animal. Several studies have shown that PAH could exert several biological actions on different organ, cells and enzymes (Thirman *et al*., 1994). They also trigger deleterious vascular effect, including mature endothelial cells and smooth muscle cells (Lu, *et al*., 1998; Tithof *et al*., 2002) such as aberrant signaling, gene expression, and proliferation (Ou and Ramos, 1992). PAH binds to the cytoplasmic aromatic hydrocarbon receptor (AhR) in the cytoplasm, a member of the basic helix-loop-helix Per-Arnt-Sim (bHLH-PAS) family of transcription factor, play a central role in cell proliferation, determination, and differentiation in a wide variety of tissues and developmental stages in multicellular organisms (Hassan and Bellen, 2000; Merson *et al*., 2006). The ligand-bound AhR translocates to the nuclease where it binds as a heterodimer with the AhR nuclear translocator (Arnt; another bHLH-PAS protein) to specific *cis*-acting regulatory DNA sequences located in the promoter of its targets (known as AH-, dioxin-, or xenobiotic-responsive elements (or AHRE, DRE, or XRE, respectively)) to enhance their transcription (Okey *et al*., 1994). Previous report indicated that AhR-Arnt-

independent pathway involved p53. Activation of p53 occurs in response to a number of cellular stresses, including DNA damage, and leads to the activation of several genes whose products trigger cell cycle arrest, apoptosis, or DNA repair (Lakin and Jackson, 1999). Several PAH metabolites possess high mutagenic activity that can induce p53 through their DNA-damaging activity (Flesher *et al*., 1998a and 1998b). PAH have been produced cell proliferation by inducing the specific alterations in growth-related gene expression, *c-fos* and *c-jun* (Parrish *et al*., 1998), modified intracellular proliferative steps by phosphorylation, ERK1 and ERK2, via intercellular communication (Denhardt, 1996). It has also been revealed that PAH promoted the inhibitory effect on intercellular junctional protein communication by specifically mutated in the *ras* gene (A to T at the 61st codon) (Yamakage *et al*., 2000). Baylike regions, the angular pocket formed at the top of the benzene ring by an alkyl group of PAH were potent inhibitors of gap junctional intercellular communication leading to modify the intracellular proliferative steps via ERK pathway (Weis *et al*., 1998; Rummel *et al*., 1999). It has been shown that cigarette smoke condensate (CSC) induces the surface expression of a subset of cell adhesion molecules (CAM) like ICAM-1, endothelial leukocyte adhesion molecule-1 (ELAM-1), and VCAM-1 in HUVEC. Other studies have shown that CSC-induced activation of protein kinase C in endothelial cells initiates signaling pathways, leading to increased binding of NF-kappa B to specific DNA sequences, which in turn increases surface expression of the subset of CAM.

Evidence of the changes in TJ or AJ and permeability by nicotine or PAH might indicate the failure of maintaining BBB integrity, which have been described in several neurological disorders (Abbruscato *et al*., 1999; Mark *et al*., 2002).

Blood-brain barrier

The blood brain barrier, the regulated interface between the peripheral circulation and the CNS, is the specialized system of capillary endothelial cells that protects the brain from harmful substances in the blood stream. Unlike peripheral capillaries that allow relatively free exchange of substance across/between cells, the BBB strictly limits transport into the brain. The CNS is extremely sensitive to a wide range of chemicals; many of the substances we consume in our diet, although readily metabolized and excreted without harm to peripheral organ systems, are in fact quite

neurotoxic. It is therefore essential that the interface between the CNS and the peripheral circulatory system functions as a dynamic regulator of ion balance, a facilitator of nutrient transport, and a barrier to potentially harmful molecules (Hawkins and Thomas, 2005). Anatomically, the endothelial cells of the BBB are distinguished from those in the periphery by increased mitochondrial content and increased energy potential required for active transport of nutrients to the brain from the blood; a lack of fenestrations (*i.e.* openings); minimal pinocytotic activity; hollowed out portion of cell membrane filled with fluid, forming a vacuole which allows for nutrient transport; the presence of TJ that result in high TEER of 1,500 – 2,000 Ω cm^2, and multiple transport systems (Crone and Christensen, 1981; Butt, 1995; Huber *et al*., 2001; Petty and Lo, 2002).

The function of BBB can be divided into two-fold: first is to protect the brain from blood-born substances and second is a supply nutrient by specific transport system. The transport at the BBB can be separated into 2 pathways; paracellular pathway (across between the cells) or transcellular pathway (across the endothelial cells). There are four basic mechanisms by which solute molecules move across membranes. First is the simple diffusion, which proceeds from low to high concentrations. Second is the facilitated diffusion, a form of carrier-mediated endocytosis, in which solute of molecules bind to specific membrane protein carriers, also penetrate from low to high concentration. Third is the simple diffusion through an aqueous channel, formed within the membrane. Fourth is the active transport using a protein carrier with a specific binding site that undergoes a change in affinity. In general, the transcellular pathway permits entry by passive diffusion, but only neutral lipophilic substances with a molecular weight of less that 450 daltons can gain access by this route. However, small and large hydrophilic molecules can penetrate the brain by transcellular active transport. In the case of paracellular route, ions and solutes are allowed to diffuse across. However, this paracellular route is almost completely obstructed, *i.e.* the molecular weight should not be greater than 180 daltons, by tight junction complexes in the apical region of the cell membrane (Mitic and Anderson, 1998; Stevenson and Keon, 1998; Petty and Lo, 2002).

The CECs are interconnected by complex arrays of TJ. The BBB is characterized by the presence of TJ, which result in high TEER. Values of electrical resistance in endothelial vary greatly depending on location, which has important functional consequence. For example, human placental endothelial cells have TEER

value of 22-52 Ω cm^2, which permits rapid paracellular exchange of nutrients and waste between the mother and fetus; urinary bladder epithelium, however, has a very high TEER value of 6,000-30,000 Ω cm^2, which is necessary for preserving urine composition (Huber *et al*., 2001). The TEER value of BBB is around 1,500–2,000 Ω cm^2 *in vitro*. TJ causes decrease in paracellular permeability of BBB. TEER, which is reciprocal to ionic conductivity across cellular sheets, characterizes the integrity of TJ is terms of their relative permeability to ions. The TEER varies by several orders of magnitude between so-called tight and leaky endothelium (Huber *et al*., 2001).

Cellular structure of the blood-brain barrier

The BBB is formed by a complex cellular system of endothelial cells, astroglia, pericytes, and a basal lamina (Abbott *et al*., 2006). Astrocytes project their end feet tightly to the endothelial cells, influencing and conserving the barrier function of these cells. Astrocytes, which have foot ending process invested in the abluminal surface of capillaries (Goldstein and Betz, 1986; Abbott *et al*., 2006), are believed to confer the proper function of BBB (Hurst and Fritz, 1996; Bauer *et al*., 1999; Cucullo *et al*., 2002). Endothelial cells are embedded in the basal lamina, a membrane 30-40 nm thick composed of collagen IV, heparin sulfate proteoglycans, laminin, fibronectin, and other extracellular matrix (ECM) protein, together with pericytes (Graeber *et al*., 1989). The role of pericytes is still controversial. Pericytes are characterized as contractile cells that surround the brain capillaries with long processes, and are believed to play a role in controlling the growth of endothelial cells (Hatashita and Hoff, 1990; Hori *et al*., 2004). Platelet-derived growth factor-B knock-out mice lack brain pericytes, and die due to hemorrhage (Lindahl *et al*., 1997). Therefore, it is believable that paracrine interactions between CECs and pericytes, play important roles in maintaining TJ at the BBB. *In vitro* BBB model studies revealed that the pericyte-derived multimeric angiopoietin-1/Tie-2 pathway induces occludin expression (Hori *et al*., 2004).

On the other hand, pericytes in contact with microvascular endothelial cells inhibits endothelial growth in which produce an active form of transforming growth factor type-β (TGF-β) (Orlidge and D'Amore, 1987), which inhibits cell growth and cell proliferation; increasing the permeability of the CECs monolayer (Parkinson and Hacking, 2005; Perriere *et al*., 2005; Calabria *et al*., 2006). BBB disruption induced by TGF-β1 occurs partly by a reduction in occludin mRNA level (Hori *et al*., 2004).

Blood-brain barrier and diseases

Failure of the BBB formation is a critical event in the development and progression of several diseases that affect the CNS. BBB dysfunction by disruption of tight junctional protein integrity has been observed in the majority of neurological disorders including stroke (Heo *et al*., 2005), Alzheimer's disease (Fiala *et al*. 2002), multiple sclerosis (Huber *et al*., 2001; Opdenakker *et al*. 2003), and hypoxia/aglycemia (Park *et al*., 1999; Abbruscato and Davis, 1999). The previous investigation demonstrated that λ-carrageenan-induced inflammatory pain elicited a biphasic increase in BBB permeability. *Campylabacter jejuni*, a leading cause of human enterocolitis, results in a time-dependent loss of TEER and marked decrease in the level of hyperphosphorylated occludin (Chen *et al*., 2006). Hyperpermeability under hypoxia/reoxygenation stress is caused by the reorganization of both the actin cytoskeleton, as well as AJ and TJ proteins (Witt *et al*., 2003). Oxidative stress-induced increase in permeability is associated with Tyr-phosphorylation, redistribution from the cellular junctions of occludin and ZO-1, and dissociation of these proteins from the cytoskeleton (Rao *et al*., 2002). Disruption of TJ by oxidative stress is mediated by the activities of phosphatidylinositol 3-kinase (PI3K) (Sheth *et al*., 2003) and c-Src (c-terminal-v-src sarcoma (Schmidt-Ruppin A-2) viral oncogene homolog (avian) (Basuroy *et al*., 2003).

Several studies have shown that exposure of endothelial cells to reactive oxygen species (ROS) is one of the main causes of endothelial dysfunction. Oxidative stress-mediated disruption of BBB was shown in experimental models *in vivo* (Parathath *et al*., 2006) or by injury of endothelial cells *in vitro* (Blasig *et al*., 2002). By using primary human brain microvessel endothelial cells, alcohol-induced loss of BBB integrity is associated with increased production of ROS, activation of myosin light chain (MLC) kinase (MLCK) and phosphorylation of MLC and TJ proteins (Haorah *et al*., 2005). BBB damage is mediated by oxidative stress (Haorah *et al*., 2005) via stimulation of inositol 1,4,5-triphosphate-gated intracellular Ca^{2+} release resulting in MLCK activation and BBB dysfunction (Haorah *et al*. 2007). Taken together, oxidative stress emerges as a common underlying cause of BBB dysfunction. DMNQ is a redox-cycling agent that induces intracellular superoxide anion formation and induces cell proliferation or apoptosis or necrosis, depending on the concentration, DMNQ does not react with free thiol groups, is non-alkylating and adduct-forming in contrast to other quinones. Thus, DMNQ is a valuable tool for the

generation of ROS. DMNQ, which generates O_2^- and H_2O_2 continuously through redox cycling, was widely used as source of oxidative radicals (Liu *et al*., 1998; Bresgen *et al*., 2003; Krizbai *et al*., 2005). MAPK activity was also found to the involved in the disruption of TJ by H_2O_2 in the endothelial cell monolayer (Kevil *et al*., 2000).

Tight junctional proteins

The CECs are interconnected by complex arrays of TJ, which is the most apical elements of the junctional complexes and create a barrier to paracellular diffusion of solutes between blood and brain. The TJ regulates the passage of ions and small water-soluble molecules through the paracellular pathway (Gonzalez-Mariscal *et al*., 2003). Therefore, the permeability of the endothelial barrier is largely determined by the integrity of the tight junctions. TJ are associated with numerous intracellular signaling molecules, and are regulated by the activity of signaling transduction pathway (Krizbai and Deli, 2003). The integrity of the TJ is regulated by G-proteins (Nusrat *et al*., 1995; Denker *et al*., 1996), protein kinase C (Stuart and Nigam, 1995), c-Src (Basuroy *et al*., 2003), PI3K (Sheth *et al*., 2003), and phospholipase Cγ (Ward *et al*., 2002). Evidence suggests that these signaling activities may affect TJ by inducing phosphorylation and regulation of protein-proetin interactions. Three types of transmembrane proteins have been found in TJ so far: occludin (Furuse *et al*., 1993), claudin (Furuse *et al*., 1998), and junctional adhesion molecules (JAMs) (Martin-Padura *et al*., 1998).

Occludin, a 60-65 kDa phosphoprotein, contains four transmembrane domains, two extracellular loops, with a short amino-terminal domain and a long carboxy-terminal domain oriented into the cytoplasm. Both extracellular loops are enriched in tyrosine residues, and in the first one more than half of the residues are tyrosines and glycines (Gonzalez-Mariscal *et al*., 2003). Occludin can be detected on the SDS gel with the cluster of 62-82 kDa as a result of phosphorylation of serine, threonine, and tyrosine residue (Sakakibara *et al*., 1997). Occludin is associated mainly with TJ, which is essential for maintenance of the barrier function of the endothelial lining in brain capillaries. There are some evidences showing that occludin is a key tight junction protein whose expression level dictates tissue barrier properties, such as, cleavage of occludin by the cysteine proteinase allergen DerP1

resulted in occludin degradation and increased paracellular permeability to mannitol (Wan *et al*., 2000). In addition, a high expression of occludin in brain capillaries, observed by immunofluorescence and electron microscopy, indicated that occludin could be considered as a sensitive and reliable marker of TJ (Vorbrodt and Dobrogowska, 2003). The over-expression of mutant forms of occludin leads to disrupt TJ structure and function (Bamforth *et al*., 1999). The administration of synthetic peptides corresponding to the extracellular loops of occludin, results in the disappearance of TJ, leads to inhibition of cell adhesion and up regulation of β-catenin and of the β-catenin/TCF downstream target gene c-myc (Vietor *et al*., 2001). The sequence of the COOH-terminal, around 150 amino acids, is relatively conserved among species. It interacts directly with F-actin (Wittchen *et al*., 1999). This constitutes a property for actin association. Furthermore, occludin also binds directly to the membrane-associated guanylate kinase-like proteins (MAGUK) ZO-1 through this carboxyl segment (Furuse *et al*., 1994). The expression of occludin correlates with barrier properties in various tissues. For example, arterial endothelial cells express 18-fold greater occludin protein levels than venous endothelial cells and form a tighter solute barrier (Kevil *et al*., 1998). Similarly, occludin is highly expressed in brain endothelium, which forms a very tight barrier, but occludin is expressed at much lower level in endothelial cells of non-neuronal tissue, which have lower barrier properties than brain endothelium (Hirase *et al*., 1997).

At the cytoplasmic face, occludin is connected to TJ plaque proteins, ZO-1, -2 and -3 (ZO-1, 220 kDa; ZO-2, 160 kDa; ZO-3, 130 kDa), cingulin, and several others. ZO, a phosphoprotein, has sequence similarity with each other and belong to the family of proteins known as MAGUK. ZO-1 is the cytoplasmic protein link membrane proteins to actin, the primary cytoskeleton protein for the maintenance of structural and functional integrity of the endothelium. The C-terminus of occludin binds to ZO-1 and is required for occludin localization at tight junctions (Mitic *et al*., 1999). In particular, ZO-1 might organize occludin at junctional sites, since transfected occludin usually co-localizes at cell-cell contacts with endogenous ZO-1 (Van Italie and Anderson, 1997). The presented study found that ZO-1 links between occludin and actin cytoskeleton (Fanning *et al*., 1998).

Claudins are small transmembrane proteins (20-27 kDa) that span the membrane four times, two extracellular loops, and a short carboxyl intracellular tail. The amino acids of this tail are highly conserved within the family and constitute PDZ

binding domain. Up to now, at least 24 members of claudin family have been identified. Different claudin species are capable of generating in different cell type (Furuse *et al*., 1999). Claudins have been identified as important structural and functional components of TJ involved in paracellular transport (Tsukita and Furuse, 2000; Matter and Balda, 2003). Among these integral membrane proteins, claudin-5 seems to play the most important role on the BBB function (Morita *et al*., 1999). The claudin-5 was first specifically found in endothelial cells, predominantly expression in the brain endothelial cells. Mice deficient in claudin-5 showed barrier failure (Nitta *et al*., 2003). These proteins are integral membrane proteins that share the four transmembrane domains of occludin, but do not contain any sequence homology to occludin (Morita *et al*., 1999; Liebner *et al*., 2000; Lippoldt *et al*., 2000). They are detected in all tissues and form a complex with occludin and JAMs.

The JAM family consists of JAM-A, JAM-B, and JAM-C (Bazzoni, 2003). JAM shows only one putative transmembrane sequence (Citi *et al*., 1998). JAM-A localizes at the intercellular junctions of murine and human endothelial and epithelial cells. In these cells, JAM-A localizes in close proximity of tight junction strands. JAM-A is not restricted to cells that form junctions. However, it is also expressed in platelets and cells of the immune system. JAM-B has a more restricted distribution. It localizes at the junctions of endothelial cells from different vessels, but mostly in high endothelial venules (HEVs). JAM-C has a wide distribution. It is expressed in vascular endothelial cells, including HEVs; lymphatic vessels, platelets, natural killer and dendritic cells (Bazzoni, 2003). Claudins, with occludin and JAMs, are considered as transmembrane proteins, which are essential for the formation of TJ and for their barrier and fence functions.

Adherens junctional proteins

Tight and adherens junctions together form the junctional complexes between adjacent endothelial cells. The major barrier in the paracellular pathway is created by the tight junction. The other junctional complex in the BBB is adherens junction (AJ). AJ plays a crucial role in contact inhibition of endothelial cell growth, paracellular permeability to circulating leukocytes and solutes (Bazzoni and Dejana, 2004). AJ connects endothelial cells and provides the structural base for interendothelial mechanical stability. They are composed of major transmembrane glycoproteins, interact homotypically, of AJ, which belong to the Ca^{2+}dependent cadherin superfamily. Cadherin, the adhesive transmembrane proteins are specifically located at intercellular adherens junctions and, once the cells get in contact, form zipper-like structures along intercellular contacts. Each cadherin type has a unique tissue distribution pattern. Endothelial cells have been shown to express N-cadherin (Liaw *et al*., 1990), VE-cadherin (Lampugnani *et al*., 1992), and to a lesser extent, P-cadherin (Liaw *et al*., 1990). Among these, only VE-cadherin is expressed specifically in endothelial cells. Furthermore, VE-cadherin is associated consistently with intercellular junctions. VE-cadherins on adjacent cells bind to one another through their extracellular domains and associated with the actin cytoskeleton via proteins known as catenins (β-catenin, γ-catenin or plakoglobin). Furthermore, this region can bind p120. β-Catenin and γ-catenin bind directly to the cadherin carboxy-terminal catenin-binding domain, further they bind to α-catenin, which is an actin-binding molecule and link adhesive cadherin/catenin complex to the F-actin-based cytoskeleton (Hoschuetzky *et al*., 1994, Jou *et al*., 1995, Knudsen *et al*., 1995). VE-cadherin - catenin complex may change according to the functional state of the cells (Lampugnani *et al*., 1995). The function of β-catenin is regulated by tyrosine and serine/threonine phosphorylation, depending on specific kinases and phosphatases. At early stages of confluency, VE-cadherin is heavily tyrosine phosphorelated and mostly linked to p120 and β-catenin. When the junction stabilizes, the tyrosine residues in VE-cadherin tend to loose phosphorylation. β-catenin and p120 partially detach from the complex and are substituted by γ-catenin (Lampugnani *et al*., 1997). β-catenin is an important mediator in transcriptional regulation and interacts with transcription factors. Free β-catenin can translocate to the nucleus and bind to transcription factors of the high mobility group. After dissociated from junction, β-

catenin becomes available for signaling. This process may regulate the expression and differentiation (Dejana *et al*., 2000), for example, β-catenin directly participates in Wnt growth factor signaling cascade to enter the nucleus by forming a complex with the Lef/tcf family of transcription factors then activated transcription of Wnt target genes (Akiyama, 2000). As α-catenin is too large to diffuse through the nuclear pore, it also enters with this pathway (Giannini *et al*., 2004). ZO-1 also binds to the AJ protein α-catenin (Imamura *et al*., 1999), indicating a general scaffolding function of ZO-1 in junctional complexes. The recent report showed that tight junctional occludin and adheren junctional protein α-catenin interact in a four-helix-bundle motif with the same epitopes of ZO-1 from their C-terminal region as intermolecular association sites and determine their relative spatial orientation (Muller *et al*., 2005). At present, at least three junctional proteins: occludin, ZO-1, and VE-cadherin, detected at the ultrastructural level can be considered to be valuable and efficient markers of the integrity of both TJ and AJ that form the entire interendothelial junctional complexes in BBB microvessels (Vorbrodt and Dobrogowska, 2003). The interactions between TJ and AJ components are important during junction assembly. It has also demonstrated that ZO-1 associates with α-catenin at the AJ and occludin at the tight junction (Muller *et al*., 2005). It has been reported that catenin and ZO-1 form a complex during early stages in the assembly of tight junctions (Rajasekaran *et al*., 1996).

A number of cell surface molecules that mediate endothelial cell-leukocyte interactions are expressed on the surface of activated endothelial cells. Cell adhesion molecules (CAM) that have been characterized to date include E-selectin, P-selectin, VCAM-1, ICAM-1 and PECAM-1. These molecules are of particular importance since the specificity of the transendothelial movement of leukocytes seems to depend on the activation status of the endothelium (Bolton *et al*., 1998; Eden and Parkos 2000).

In vitro model of BBB

The *in vitro* BBB model is an isolated system that capable to study the physiology, pharmacology, and pathophysiology of the BBB. It is a basic tool to monitor drug delivery through the brain microvascular endothelium. Ideally, an *in vitro* model comes as close to the *in vivo* situation as possible, without losing the

advantages of being an *in vitro* system. The system should be flexible, reproducible, abundantly, available and functionally characterized based on specific cell type properties and on the functional expression of specific BBB properties (Gaillard *et al*., 2001).

Different models of the BBB have been established based on immortalized brain endothelial cell lines and primary culture of brain capillary endothelial cells. bEND3 and bEND5 cells, established from the brains of mice using the polyoma virus middle T-antigen, are immortalized brain endothelial cell line, which is available so far. However, no published report exist regarding the use of bEND cells in pharmaceutical studies because they generate TEER values of no greater than 60 Ω x cm^2 although optimizing culture condition, medium, and the presence of differentiating agents have been applied. However, many of the immortalized brain endothelial cell lines, not commercial available, were produced to address questions in cerebrovascular pathophysiology or cell biology, rather than the barrier properties of the brain microvasculature to pharmaceuticals, such as GP8.3, t-BBEC-117, TM-BBB4, and RBE4 (Greenwood *et al*., 1996; Sobue *et al*., 1999; Asaba *et al*., 2000; Gumbleton and Audus, 2001; Friedrich *et al*., 2003). Cell lines are very easy to handle and less time consume, however, they rapidly de-differentiate *in vitro*, losing the characteristics of BBB endothelial cells after a few passages in culture. These cultures would represent a significant advantage if they could be shown to maintain their barrier properties and characteristics. Primary culture of brain capillary endothelial cells is one of alternative models of *in vitro* BBB. The cells were obtained from murine, rat, bovine, feline, and porcine (Abbott *et al*., 1992; Abbruscato *et al*., 2002; Wu *et al*., 2003; Abbruscato *et al*., 2004; Weidenfeller *et al*., 2005; Perriere *et al*., 2005; Roux and Couraud, 2005; Calabria *et al*., 2006; Forster *et al*., 2006; Fletcher *et al*., 2006). Bovine and porcine are the two species that preferable mostly because of the yield of cerebral microvascular endothelial cells. However, most *in vivo* BBB studies have been performed with small laboratory animals, especially rat. Thus *in vitro* model from rat will be able to correlate with *in vivo* model. Disadvantage of primary culture of brain capillary endothelial cells is time consuming and expensive, which may hamper their routine use in nonexpert laboratories, including it is difficult to eliminate all nonendothelial cell contaminations.

These primary cultured cells exhibit the typical properties of microvascular endothelial cells of the BBB. There are several specific properties of BBB, which

could be employed for their characterization (de Boer *et al*., 1999). In particular, endothelial cells may be characterized by their characteristic morphology in culture such as cobblestone shape when the cells growing in a cluster and spindle shape when the cells reach confluent (Abbott *et al*., 1992; Krizbai *et al*., 2000; Wu *et al*., 2003; Perriere *et al*., 2005; Fletcher *et al*., 2006). The endothelial cells may subsequently be characterized by using general endothelial cell-specific properties such as Factor VIII-related antigen or von Willebrand factor (vWF) (Dorovini-Zis and Huynh, 1992; Domotor *et al*., 1999; Calabria *et al*., 2006), uptake of DiL-labeled-acetylated low density lipoprotein (DiL-Ac-LDL) (Fletcher *et al*., 2006), glucose transporter type I (Ghazanfari and Stewart, 2001). In addition, typical barrier makers like the formation of tight junctions, expression of γ-glutamyl-transpeptidase, P-glycoprotein (P-gp) and glucose transporter (GLUT) are the markers. Astrocytes can be identified by the expression of glial fibrillary acidic protein (GFAP), an intermediate filament protein, well documented as one of the hallmark of astrocytes differentiation, and its specific morphology in culture (Abbott *et al*., 1992; Ghazanfari and Stewart, 2001). Pericytes may be characterized by their district irregular morphology (Hayashi *et al*., 2004). By staining, α-actin is specific marker for pericytes. Contaminated cells caused a major problem in developing *in vitro* model. Then methods that can achieve pure CECs culture in a simple and reproducible manner is still need. Techniques for achieving to obtain endothelial cells purity that have been used such as incorporated magnetic bead separation (Abbott *et al*., 1992; Parkinson and Hacking, 2005), the appropriate control of serum and growth supplement concentration (Abbott *et al*., 1992), including employs chemical mediators such as puromycin, a P-gp substrate (Perriere *et al*., 2005; Calabria *et al*., 2006). It is a protein synthesis inhibitor that causes premature chain termination by acting as an analog of the 3’ terminal end of aminoacyl-tRNA, which can bind 70S and 80S ribosomes. It takes part in the ribosomal peptide bound-forming reaction and accepts the nascent peptide chain. As puromycin binds only weakly to ribosomes, the resultant peptidyl-puromycin molecule usually separates from the ribosome almost at once, thus stopping protein synthesis (Perriere *et al*., 2005).

Since astrocytes were known to induce and maintain BBB properties in endothelial cells, these cells have been co-cultured with endothelial cells (Dehouck *et al*., 1990; Gaillard *et al*., 2001). In addition, supplements of culture medium were added to maintain the BBB function, such as hydrocortisone, glucocorticoid (Hoheisel

et al., 1998; Forster *et al*., 2005; Forster *et al*., 2006) or to apply a combination of astrocyte-conditioned medium and agent which elevates intracellular cAMP (Rubin *et al*., 1991). Most of the experiments involving increases in cAMP, cells were treated with a combination of a cAMP analogue (250 μM CPT-cAMP) and a phosphodiesterase inhibitor (17.5 μM RO20-1724). The ability of cAMP to increase resistance is that protein kinase A mediates the phosphorylation of one or more proteins important in regulating the resistance of tight junctions (Rubin et al., 1991), while phosphodiesterase inhibitor blocks the enzyme phosphodiesterase, therefore, preventing the inactivation of the cAMP. With the help of hydrocortisone at physiological concentrations (70-550 nM) induced upregulation of occludin, accompanied by a threefold enhancement of TEER. At the molecular level, hydrocortisone induces increase of occludin at mRNA and protein levels by activation of the glucocorticoid receptor and its binding to putative glucocorticoid responsive elements in the occludin promoter (Forster *et al*., 2005).

CHAPTER III

MATERIALS AND METHODS

Materials

Dulbecco's modified Eagle's medium (DMEM), Dulbecco's modified Eagle's medium/nutrient mixture F-12 Ham, (DMEM/F-12 Ham), gentamycin, collagenase (CLS), collagenase-dispase (C/D), deoxyribonuclease I (DNase I), fibronectin, collagen type IV, albumin from bovine serum (BSA), puromycin, heparin, nicotine, phenanthrene, 1-methylanthracene, 8-(4-chlorophenylthio) adenosine 3′,5′-cyclic monophosphate sodium salt (cAMP), 4-(3-butoxy-4-methoxybenzyl)imidazolidin-2-one (RO20-1724), hydrocortisone, tetrazolium salt (XTT) (2,3-bis[2-methoxy-4-nitro-5-sulfonyl]-2H-tetrazolium-5-carboxanilide), antibody specific for cadherin, and secondary anti-rabbit Cy3 conjugated were purchased from Sigma (St. Louis, MO, USA). Western blotting detection reagent, SuperSignal West Pico chemiluminescent substrate and secondary anti-rabbit IgG (H+L) peroxidase-linked were purchased from Pierce (Rockford, IL, USA). Antibodies specific for occludin, claudin-5 and ZO-1 were obtained from Zymed (San Francisco, CA, USA). Polyclonal rabbit anti-human von Willebrand factor (vWF) was purchased from Dako Cytomation (Glostrup, Denmark). Prestained protein ladder was purchased from Fermentas (Hanover, MD, USA). Basic fibroblast growth factor (bFGF) and Pefabloc FC were purchased from Roche (Penzberg, Germany). Percoll and protein G sepharose 4 fast flow were purchased from Amersham Biosciences (Uppsala, Sweden). Glutamax I supplement was purchased from Gibco (Grand Island, NY, USA). Fetal bovine serum (FBS) was purchased from Biochom AG (Berlin, Germany). Polyvinylidene difluoride (PVDF) membrane was purchased from Pall (Pensacola, FL, USA). All other chemicals used were commercially available reagents or analytical reagent quality.

Methods

Animals

Wistar rats were kept in a controlled environment with free access to food and water. Manipulation of the animals was performed according to the European Union Directive (86/609/EEC), which was approved by Hungary and was applicable in the Biological Research Centre, Szeged, and special care was taken to minimize the number of animals used and their suffering. The animals were also purchased from the National Laboratory Animal Center, Mahidol University. The protocol was approved by the Ethics Committee of the Faculty of Pharmaceutical Sciences, Chulalongkorn University (209/2005). Rats were housed in groups of five with good ventilation at room temperature and 12-hours light/dark cycle.

Isolation of rat cerebral microvessel endothelial cells

Rat CECs were isolated from fresh rat brains as described previously (Deli *et al*., 2003). Wistar rats, 2 week-old were anesthetized with diethylether. The heads of the rats were rinsed thoroughly in 70% ethanol and iodine, respectively, and then the heads were cut with scissors and placed in a sterile glass petri dish. In the laminar flow box, skins were cut with small scissors. Nose and the skin edges were fixed to the dissecting pad with needles. Another pair of scissors was used for cutting the bones with a sagittal incision. The skulls were opened with the curve sterile microdissecting forceps and the forebrains were collected in ice-cold sterile phosphate buffered saline (PBS, without calcium and magnesium, pH 7.4). Meninges were removed on sterile filter paper (Whatman 3M) from each brain hemisphere and at the same time white matter was peeled off with the aid of fine curved forceps. Then, grey matter was separated from the meninges and the white matter by gently rolling on. The grey matter was carefully collected from the filter paper (meninges tend to stick to it), and then put the tissue pieces into a glass petri-dish containing 2 ml DMEM/F-12 Ham and 50 µg/ml gentamycin. The gray matter was minced by scalpels to small pieces (approximately 1 mm^3) and transferred into a 50 ml sterile centrifuge tube. Then the first incubation medium (18 ml DMEM/F-12 Ham, 1 mg/ml CLS2, and 15 µg/ml DNase I) was added for first enzyme digestion. The minced tissue, which transferred into the 50 ml sterile centrifuge tube, was triturated with a 5 ml pipetman,

10 times up and down. The tissue was incubated at 37 °C for 1.5 h in a shaking waterbath (200 rpm). At the end of the incubation, the homogenate looked like creamy and colour looked like milk-coffee. Ten milliliter medium (DMEM/F-12 Ham containing 50 µg/ml gentamycin) was added to the homogenated tissue and centrifuged at 1,000 x g for 8 min at 4 °C, in swing-out rotor. The supernatant was aspirated and the cell pellet was added with 25 ml of 20% BSA- DMEM/F-12 Ham. The tissues were mixed thoroughly with a 5 ml pipetman for 10 times up and down and centrifuged at 1,000 x g for 20 min at 4 °C, in swing-out rotor. The myelin layer at the top (neurons and glia) and the BSA solution were aspirated. The cell pellet, the colour of which was whitish and red, at the bottom of the tube contained the microvessels. One milliter second incubation medium (13.5 ml DMEM/F-12 Ham, 50 µg/ml gentamycin, 1 mg/ml collagenase-dispase, and 15 µg/ml DNaseI) was added to the pellet and mixed thoroughly. The tissue was transferred to a new 50 ml sterile centrifuge tube and the rest of the second incubation medium was added. Then, the second digestion was continued by incubation at 37 °C for 50 min in a shaking waterbath (200 rpm) to remove pericytes from the basal membrane. At the end of the incubation, the solution looked like a rasberry drink. Ten millilitters of DMEM/F-12 Ham containing 50 µg/ml gentamycin was added to the homogenate tissue and centrifuged at 700 x g for 6 min. The supernant was poured out and the cell pellet was added 2 ml DMEM/F-12 Ham containing 50 µg/ml gentamycin. The pellet was mixed thoroughly with 1 ml pipetman by pipetting up and down. Microvascular endothelial cells clusters were separated on a 33% continuous Percoll gradient from pericytes, red blood and other cells by carefully layered onto the top of the Percoll gradient and centrifuged at 1,000 x g for 10 min at 4 °C in a swing-out rotor. After Percoll gradient, the top of the gradient was pinkish from the DMEM/F-12 Ham. Near the bottom of the tube, there was a red layer, consisting of red blood cells and pericytes. Above the red layer, there was an interface where a white-grayish layer contained the microvessel fragments. The band of the endothelial cell clusters was collected with a long pasture pipette and put into a tube containing medium (25 ml DMEM/F-12 Ham 50 µg/ml gentamycin). Then, the cells were centrifuged at 1,000 x g for 10 min at 4 °C. The cells were resuspened and washed again in 15 ml DMEM/F-12 Ham containing 50 µg/ml gentamycin at 700 x g for 8 min at 4 °C. The supernatant was aspirated and at the bottom of the tube, the whitish-yellowish pellet

was the digested- isolated microvessel fraction. The cells were then suspended in 5 ml culture medium (20% FBS, 1 ng/ml bFGF, 100 µg/ml heparin, 2 mM glutamine, 40 µg/ml puromycin and 80 ml DMEM/F-12 Ham containing 50 µg/ml gentamycin). One milliliter culture medium was added per 35 mm culture dish or filters (12 mm Millicell-CM (Millipore) filter insert). Five hundred microliter cell suspensions were added per coating dish or filter. The side of the dish or filter was tapped to disperse the cells evenly. The dishes or filters were incubated in CO_2 incubator. On day 1, rat CECs started to migrate out from microvessel, one milliliter of culture was added per dish. On day 2, medium was aspirated and 1.5 ml fresh medium was added. Medium was changed on every other day. One hundred microliter cell suspensions were dropped on coating coverslips. After the cells attached to the coveslips, 1 ml culture medium was added. The cells were incubated in CO_2 incubator for 1-2 days.

Isolation of rat astrocytes

Rat astrocytes were isolated from fresh rat brains as previously described (Perriere *et al*., 2005). One-day old of a Wistar rat was anesthetized with diethylether. The head of the rat was rinsed thoroughly in 70% ethanol and iodine, respectively, and then the head was cut with scissors and placed in a sterile glass Petri dish. In the laminar flow box, skin was cut with small scissors. Nose and the skin edge were fixed to the dissecting pad with needles. Another pair of scissors was used for cutting the bones with a sagittal incision. The skull was opened with the curve sterile microdissecting forceps and the forebrain was collected in ice-cold sterile phosphate buffered saline (PBS, without calcium and magnesium, pH 7.4). Meninges was removed on sterile filter paper (Whatman 3M) from each brain hemisphere and at the same time white matter was peeled off with the aid of fine curved forceps. Then, grey matter was separated from the meninges and the white matter by gently rolling on. The grey matter was carefully collected from the filter paper (meninges tend to stick to it), and then put the tissue pieces into a glass Petri-dish containing 2 ml DMEM and 50 µg/ml gentamycin. The gray matter was minced by scalpels to small pieces (approximately 1 mm^3) and transferred into a 15 ml sterile centrifuge tube. Then 10 ml of 10% FBS-DMEM was added. Attached a long needle (20G, 700) to a 10 ml syringe and mixed thoroughly 3 times up and down. The cells allowed to sediment by waiting for 1 min. The cell suspension from the top was collected in a 50 ml tube and

aided to filtrate through a 40 μm mess cloth. Fresh 10 ml of 10% FBS-DMEM was added to the sediment tissue, mixed, and collected three more times. A total of 37 ml of cell suspension was collected and added 11 ml 10% FBS-DMEM. Five ml of the cells were seed into 10 flasks of T25 flask. The flasks were not allowed to touch for 5 days, and then the medium was able to change. Thereafter, the medium was changed twice a week. Three-week old culture in T25 flask was used for co-culture with endothelial cells on filter.

Cell viability test

The viability of the endothelial cells in response to nicotine, phenanthere, and 1-methylanthracene were assessed by using XTT assay. Rat CECs were cultured in 96-well plate in DMEM/F-12 Ham culture medium supplemented with 20% FBS, 1 ng/ml bFGF, 100 μg/ml heparin, 2 mM glutamine, 40 μg/ml puromycin and 50 μg/ml gentamycin. After the cell reached confluency, the culture medium was substituted with serum free medium for overnight at 37 °C in a humidified atmosphere of 5% CO_2 and 95% air. To analyze the initial value of nicotine, phenanthrene, and 1-methylanthracene-mediated cell viability, four different concentrations of nicotine (0.01-10 μM), five different concentrations of phenanthrene, and 1-methylanthracene (15-240 μM) were applied to rat CECs for 24 h. The serum free medium was replaced by XTT solution. Then the cells were incubated for 4 h in a humidified atmosphere of 5% CO_2 and 95% air. The plate was shaken for 10 sec on the microplate shaker to disperse the XTT. The optical density (OD) was quantified at an absorbance of 450 nm using a reference wavelength of 620 nm (Lin *et al*., 2001).

Preparation of cell extracts and Western blot

To determine protein expression of junctional proteins and junctional associated proteins by Western blot analysis, after nicotine, phenanthrene or 1-methylanthracene treatment. This procedure was performed as described previously (Farkas *et al*., 2005). Confluent monolayers of rat CECs were treated with 10 μM nicotine, 30 μM phenanthrene or 30 μM 1-methylanthracene for 24 h. Cells were grown on 35 mm culture dishes. After the cells were washed with PBS, protein was extracted in lysis buffer (20 mM Tris-HCl pH 7.4, 150 mM NaCl, 1% sodium deoxycholate, 1% Tx-100, 1 mM sodium orthovanadate, 10 mM NaF, 1mM Pefabloc)

and incubated on ice for 1 h. The supernatant was collected by centrifugation at 10,000 rpm for 10 min at 4 °C. This fraction was defined as the Tx-100 soluble fraction. The pellet was resuspended in SDS sample buffer and used as the Tx-100 insoluble fraction. The protein concentration was determined using Bradford method. Equal amounts of protein samples (10 µg/lane) were loaded and separated on SDS-polyacrylamide gel electrophoresis. The proteins were transferred to PVDF membrane. After blocking in TBST (pH 7.5, 10 mM Tris-HCl, 100 mM NaCl, 0.1% Tween 20) containing 5% skimmed milk for 30 min at room temperature, the membranes were incubated with rabbit anti-occludin, anti-ZO-1 and cadherin for 1.5 h. Blots were then exposed to secondary anti-rabbit horseradish peroxidase (HRP)-conjugated antibody for 30 min at room temperature (RT). After washing three times with TBST, the signal was detected by SuperSignal West Pico chemiluminescent substrate.

Immunofluorescence microscopy

To determine whether nicotine, phenanthrene, and 1-methylanthracene could affect the localization of junctional proteins, immunofluorescence staining was used. Rat CECs were labeled for immunofluorescence as described previously (Farkas *et al*., 2005). Confluent monolayers of rat CECs growing on coverslips were washed three times in PBS, pH 7.4 and then fixed 10 min with ethanol/acetic acid (95:5) solution at -20 °C. After washing, the coverslips were blocked with 3% BSA in PBS for 30 min, then immunostained with primary antibody: vWF, occludin, claudin-5, ZO-1, and cadherin (1:200) in blocking solution for 1.30 h. The cells were washed with PBS and incubated with Cy3 conjugated secondary antibodies. The signal was studied by using immunofluorescence microscopy at the absorbance of 490 mm.

Immunoprecipitation

The protein-protein interaction of junctional proteins was investigated. This procedure was performed as described previously (Farkas *et al*., 2005). Cells were grown on 35 mm culture dishes. Cells were lysed as described above with 300 µl lysis buffer. The supernatant was collected by centrifugation at 10,000 rpm for 10 min at 4 °C. The equal concentration of protein was added the excess antibody concentration. The protein samples were incubated at 4 °C for 2 h by inverting. The

supernatant was collected by centrifugation at 2,000 rpm for 10 sec at 4 °C. The pellets, insoluble form, were added loading buffer and boiled at 4 °C for 3 min. Fourty microlitter of protein G sepharose slurry was added to each sample. The samples were incubated for overnight by gently inverting at 4 °C. The supernatant was collected by centrifugation at 2,000 rpm for 10 sec at 4 °C. The supernatant were kept for checking the immunoprecipitation efficiency. Sepharose beads were washed with ice-cold TBST 5 times. The samples were collected by centrifugation at 2,000 rpm for 10 sec at 4 °C. Then, the samples were added loading buffer and boiled at 4 °C for 3 min.

Measurement of transendothelial electrical resistance

To determine the paracellular barrier properties of TJ, the measurement of TEER was investigated. This method was performed as described previously (Rubin *et al*., 1991; Krizbai *et al*., 2005). Cells were grown until reach confluency on transwell filter inserts (0.4 μM; Costar, USA) coated with collagen type IV and fibronectin. To obtain a better BBB model, endothelial cells were cocultured with astrocytes, which is a widely accepted model of the BBB (Dehouck *et al*., 1990). The filters were moved to the plate containing astrocytes, which reached confluent. Medium volume was adjusted to 0.5 ml in the upper chamber and 1.5 ml in the lower chamber (luminar side) supplemented with 550 nM hydrocortisone (Hoheisel *et al*., 1998). The cells were incubated in CO_2 incubator for 24 h. The day later, 250 μM CPT-cAMP and 17.5 μM RO20-1724 were added to both the upper and lower compartments (Rubin *et al*., 1991). Ten micromolar of nicotine, 30 μM phenanthrene or 30 μM 1-methylanthracene was added in the luminal side of a coculture model at 24 h. The electrical resistance across the membrane was measured by an EVOM resistance meter (World Precision Instruments, USA). For each filter, the electrical resistance was measured using an electrical resistance system with a current-passing and voltage-measuring electrode. TEER was calculated from the displayed electrical resistance on the readout screen by subtraction of the electrical resistance of a blank filter and a correction for filter surface area. The resistance obtained with cells on the filter, which is given by the endothelial monolayer itself. At least five independent TEER measurements were done. The resistance measurement was expressed in ohms square centimeters ($\Omega\ cm^2$).

Cell under stress condition

To determine the effect of oxidative stress on rat CECs, a redox cycling agent, DMNQ was used. This method was performed as described previously (Krizbai *et al*., 2005). The viability of the endothelial cells in response to DMNQ was assessed by using XTT assay. To analyze the initial value of DMNQ-mediated cell viability, six different concentrations of DMNQ (1-100 μM) were applied to rat CECs for 24 h. The serum free medium was replaced by XTT solution. Then the cells were incubated for 4 h in a humidified atmosphere of 5% CO_2 and 95% air. The plate was shaken for 10 sec on the microplate shaker to disperse the XTT. The OD was quantified at an absorbance of 450 nm using a reference wavelength of 620 nm (Lin *et al*., 2001).

Protein localization was detected by immunostaining while paracellular barrier properties of TJ were investigated by the measurement of TEER.

Statistical analysis

For all experiments, the data were presented as the mean ± S.E.M. The reproducibility of the results was confirmed in at least three independent sets of experiments. Student's *t*-test was used for the comparison of two mean values, and statistical significance was taken as * $p < 0.05$.

CHAPTER IV

RESULTS

Isolation of rat cerebral endothelial cells

Primary cultures of rat CECs are widely used as a model of BBB because they preserve the specific BBB characteristics (Perriere *et al*., 2005; Calabria *et al*., 2006). In this study, rat CECs were used to investigate the effect of cigarette smoke components on interendothelial junctions. Rat CECs were isolated from the cerebral cortex of 2-week old Wistar rats. After meninges were removed, a two-step enzymatic digestion was performed to separate the capillaries from the surrounding brain parenchyma. Following two steps of enzymatic digestion and a centrifugation step, cells were resuspended and subjected to further purification on 33% Percoll gradient. Endothelial cells were located in the gradient density between 1.033 and 1.047, whereas non-endothelial cells had different densities. Thus, the red blood cells and contaminating cells such as pericytes and astrocytes were separated from the microvessels containing endothelial cells (Figure 2).

One of the main difficulties with primary CECs is obtaining pure cultures. The variation in purity limits the achievement of *in vitro* models of the rat BBB. As P-gp expression is known to be much higher in CECs than in any contaminating cells, we treated cells with puromycin, P-gp substrate and translation inhibitor, assuming that CECs would resist the treatment, whereas contaminating cells would not. The culture medium containing puromycin was replaced with normal culture medium after 2 days because CECs could not resist to a longer exposure to puromycin. After plating, freshly isolated rat brain microvessel fragments initially attached to the collagen IV/fibronectin-coated plastic culture dishes, including scattered single cells and debris (Figure 3A). The small capillary fragments were around 200 μm long. After being cultured for 1 day, the cells started to migrate out from the capillaries. Groups of cells formed small islands showing the spindle-shaped microvascular endothelial morphology (Figure 3B). Cells were rapidly growing out of the clusters after 2 days, while solitary cells outside colonies generally disappeared (Figure 3C). The predominant cell type in the culture was spindle shaped endothelial one. Cells showed a uniform phase-bright appearance with dark granular inclusions. The cells

grew out from the clusters approximately radially, with some swirling patterns and whorls. Clear alignments of the cells were visible, with neighboring cells tightly packed against each other leaving few gaps (Figure 3D). After reaching confluency in 5-7 days, monolayers of elongated spindle-shaped rat CECs were used for the experiments. On the other hand, cultures in the absence of puromycin treatment predominately contained endothelial cells with contaminating cells becoming apparent on day 2 (Figure 4), which later overgrew by endothelial cells. Based on their morphology, contaminating cells looked like pericytes. Our results showed that the use of 4 μg/ml puromycin in the culture medium reduced the level of contaminating cells, while the proliferation rate of endothelial cells was not affected.

Characterization of rat CECs

To investigate the purity of the cell culture endothelial morphology was examined by phase-contrast microscopy (Figure 3D). The nuclei of rat CECs displayed a characteristic oval morphology in the center of the spindle shaped cells. To determine the endothelial origin of the cells, immunofluorescence characterization was performed. For this purpose rat CECs were stained with an antibody against vWF (or factor VIII). Factor VIII is a multimeric glycoprotein that plays an essential role in primary homeostasis by mediating platelet adhesion to the injured vessel wall and is synthesized by endothelial cells (Argyris *et al*., 2003). The endothelial marker vWF was localized at the perinuclear level of rat CECs (Figure 5).

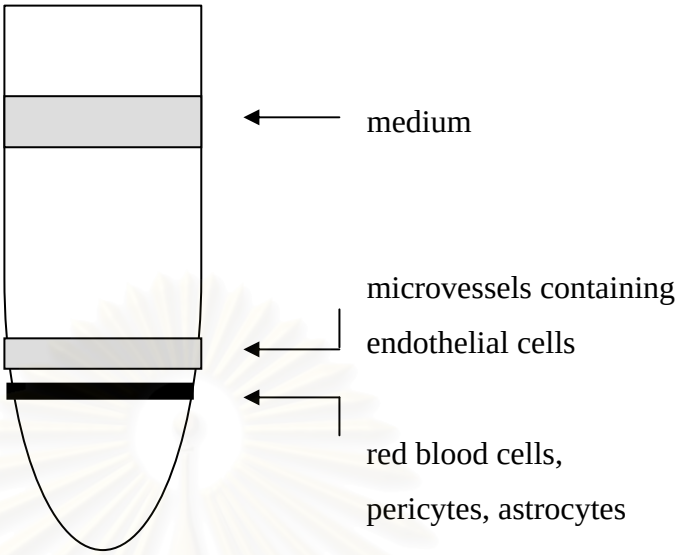

Figure 2 Schematic representation of the localization of microvessel containing endothelial cells after subjected to 33% Percoll gradient centrifugation.

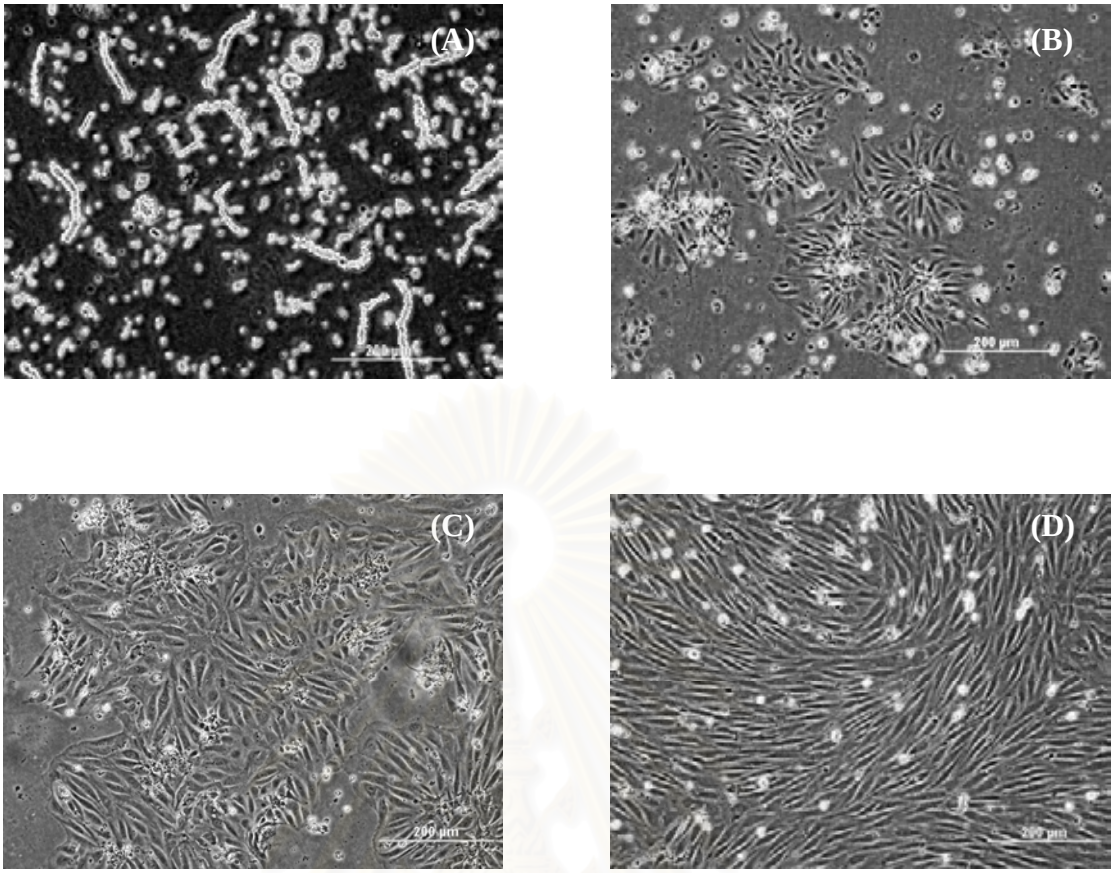

Figure 3 Phase contrast microscopic images of isolated microvessel fragments from rat brain. (A) At the time of plating (day 0). (B) Typical spindle shape of brain endothelial cells growing out of the microvessels (day 1). (C) Spindle-shaped cells growing out of the cell cluster (day 2). (D) Confluent monolayer (day 5). The rat CECs were cultered with media containing 4 μg/ml puromycin. Scale bar = 200 μm.

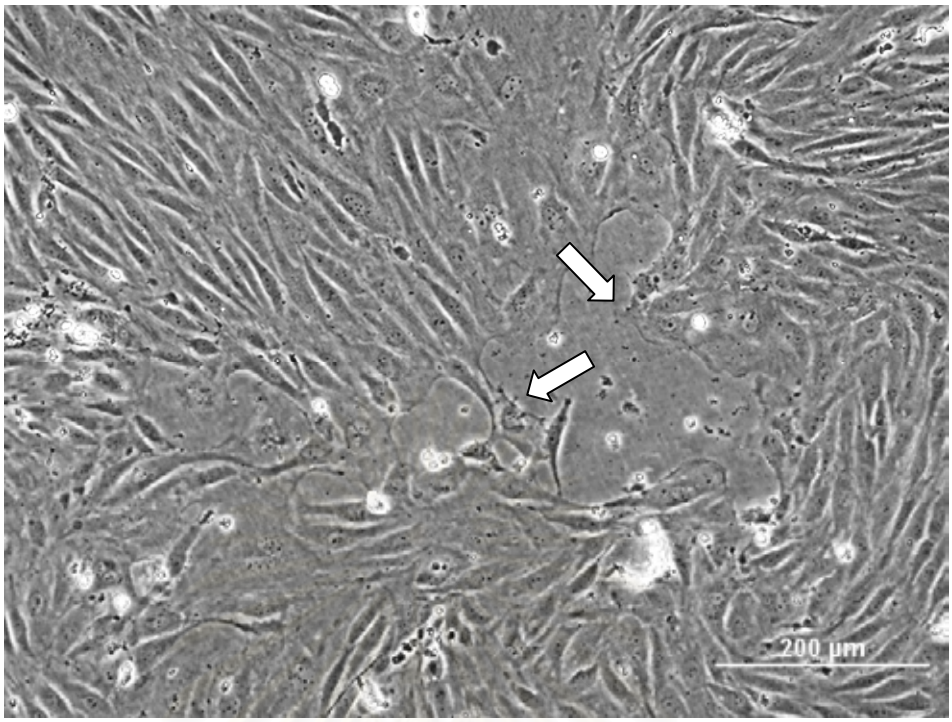

Figure 4 Phase contrast microscopy of rat CECs 5 days after plating. The arrow showed contaminating cells, which were observed in culture of rat CECs without 4 µg/ml puromycin. Scale bar = 200 µm.

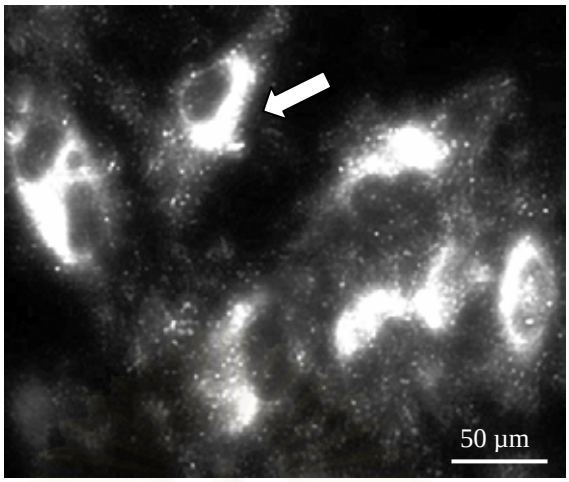

Figure 5 Characterization of rat CECs. Primary rat CECs were positive for vWF by indirect immunofluorescence with rabbit anti-human vWF antibody conjugated Cy3. Labelling was observed in a granular population concentrated in the perinuclear zone (arrow). Scale bar = 50 µm.

Cytotoxic effects of nicotine and PAH exposure

To exclude the changes observed after nicotine, phenanthrene, or 1-methylanthracene treatment, which might arise from nonspecific cell injury, XTT assays were performed in order to assess cell viability and mitochondrial function. The assay with XTT is based on the cleavage of yellow tetrazolium salt XTT to form an orange formazan dye by mitochondrial dehydrogenase in metabolically active cells, which is inactive shortly after cell death. Consequently, this conversion only occurs in viable cells. In this study, XTT assays were performed on rat CECs treated with nicotine, phenanthrene, or 1-methylanthracene. Based on the nicotine concentrations measured in the plasma of smokers (Kilaru *et al*., 2001), we treated cells with nicotine at concentrations of 0.01, 0.1, 1.0, and 10 μM for 24 h. No significant difference was observed in endothelial cells, which the percentage of cell viability was 99.41±3.55, 93.54±5.21, 90.65±6.17, and 89.66±6.93, respectively, compared to control (Figure 6).

We were not able to find reports about plasma levels of phenanthrene and 1-methylanthracene in smokers. However, previous reports used PAH in concentrations ranging up to 120 μM (Rummel *et al*., 1999; Vinggaard *et al*., 2000). In this investigation, the tested concentrations of phenanthrene and 1-methylanthracene were 15, 30, 60, 120, and 240 μM for 24 h. The percentage of cell viability according to the phenanthrene treatment was 93.86±0.32, 86.75±1.97, 67.95±6.93, 64.12±3.28, and 47.12±2.64, respectively. The percentage of cell viability according to the treatment of 1-methylanthracene was 89.80±2.56, 87.16±2.99, 84.54±7.01, 67.86±4.90, and 56.56±5.90, respectively. The results suggested that phenanthrene and 1-methylanthracene at the concentrations above 60 and 120 μM significantly reduced the cell viability in a concentration-dependent manner (Figure 7). For further investigation, noncytotoxic concentration of nicotine, phenanthrene, and 1-methylanthracene treatment were used at 10 μM, 30 μM, and 30 μM, respectively.

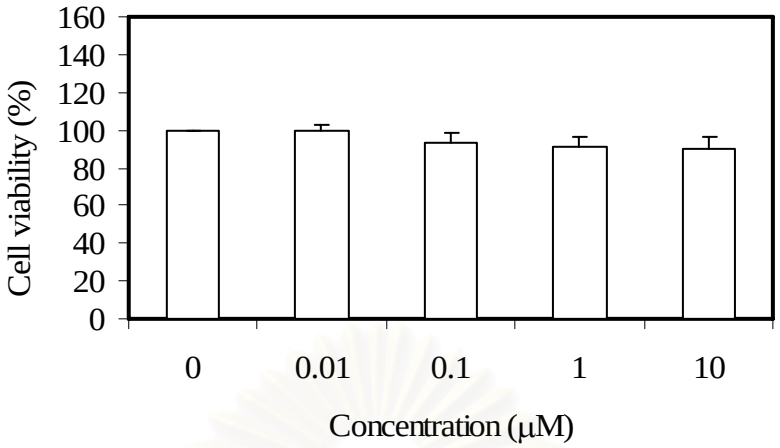

Figure 6 Cytotoxic study of nicotine on rat CECs. The cells were treated with nicotine at concentrations ranging from 0.01 to 10 μM for 24 h. Cell viability was expressed as % of control cell survival measured by XTT assay. Each point represents the mean ± S.E.M. for three different experiments, each performed in triplicate.

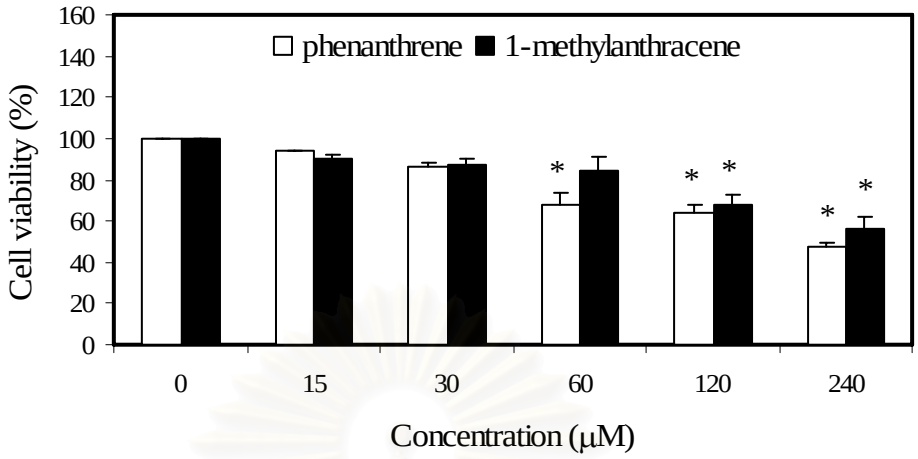

Figure 7 Cytotoxic studies of phenanthrene and 1-methylanthracene on rat CECs. The cells were treated with phenanthrene and 1-methylanthracene at concentrations ranging from 15 to 240 μM for 24 h. Cell viability was expressed as % of control cell survival measured by XTT assay. Each point represents the mean ± S.E.M. for three different experiments, each performed in triplicate. *p<0.05 compared to the cells without phenanthrene and 1-methylanthracene.

Cerebral microvascular junctional protein expression after nicotine and PAH exposure

Previous experimental data suggested that smoking may influence junctional protein expression, which further disturbed BBB functions (Hawkins *et al.*, 2002). In this study, we investigated the effect of nicotine and PAH on the expression of junctional proteins of rat CECs using Western blot analysis.

Preliminary study of the expression of occludin in response to nicotine

First we investigated time- and concentration-dependent changes induced by nicotine on the expression of occludin, one of the transmembrane TJ proteins. Treatment of cerebral endothelial cells with nicotine at concentrations of 0.01, 0.1, 1, and 10 μM for 15 min, 60 min, 5 h, and 24 h did not cause any change in occludin expression even when the highest concentration (10 μM) was used (Figure 8A). To test whether chronic exposure of nicotine could change occludin protein expression, rat CECs were tested for longer period of time. Treatment of the rat CECs with 10 μM nicotine for 3 days did not cause any change in occludin expression as well (Figure 8B). The result suggested that treatment of nicotine at the plasma concentration did not cause any change of occludin expression even at the highest concentration or for chronic treatment. Considering the viability results as well, nicotine at a concentration of 10 μM was used for 24 h in further experiments.

Preliminary study of the expression of occludin in response to PAH

Due to the lack of information involving plasma concentrations of PAH, we therefore preliminary investigated the occludin expression in rat CECs treated with PAH emphasizing at nontoxic and physiological concentration. In order to exclude the possibility that the changes in junctional protein expression were due to cytotoxic effects, a preliminary study of occludin expression was performed with different concentrations of phenanthrene and 1-mehtylanthracene. The treatment of cells with phenanthrene and 1-mehtylanthracene at concentrations of 15, 30, 60, and 120 μM for 24 h were performed (Figure 9A). Western blot analysis revealed that occludin protein expression decreased after the treatment with phenanthrene at the concentration above 60 μM. Treatment with 1-methylanthracene at the concentrations of 15, 30, and 60 μM did not cause any change of occludin protein expression. To study whether chronic treatment of either phenanthrene or 1-methylanthracene could

change occludin protein expression, rat CECs were treated phenanthrene and 1-methylanthracene at the concentration of 30 μM for 6 days. The result showed that there was no change in occludin protein expression compared to control (Figure 9B). Thus to avoid the cytotoxic effect, phenanthrene and 1-methylanthracene treatment at the concentration of 30 μM for 24 h was used for further investigation.

Effect of nicotine and PAH on the expression of junctional proteins

Immunoblots have been used in a number of studies in order to quantitate the amount of TJ-associated proteins: occludin, claudin-5, cadherin, and ZO-1. Tx-100-soluble and -insoluble fractions have been used to biochemically define the localization of tight junction proteins (Nusrat *et al*., 2000; Chen *et al*., 2006). The assembly of structural proteins into the tight junctional complex is a dynamic process that involves changes in their association with components of the cytoskeleton. Biochemically, this association or assembly event can be operationally defined by changes in Tx-100 solubility. The main criterion that is used for the characterization of junctional protein is the recognition of bands of the expected molecular weight.

The reported molecular weight of the bands stained by the antibodies is estimated by comparing to molecular weight standards loaded on the same gel. All antibodies recognize bands at or near the expected molecular weight of target proteins in extracts from rat CECs. Occludin, claudin-5, cadherin, and ZO-1 are detected at 60-65, 22-25, 140, and 210-220 kDa, respectively.

Effect of nicotine on the expression of junctional proteins

To clarify whether nicotine could cause changes of occludin, claudin-5, cadherin, and ZO-1 protein expression, the protein samples were extracted by Tx-100. Treatment of the rat CECs with 10 μM nicotine for 24 h did not change protein expression of occludin and claudin-5 in Tx-100-soluble fraction (Figure 10A and 10C). However, the treatment of rat CECs with nicotine caused a significant decrease in cadherin and ZO-1 protein expression in Tx-100-soluble fraction compared to each control. No change of the expression of occludin, claudin-5, cadherin and ZO-1 was detected in Tx-100-insoluble fraction (Figure 10B and 10D). The results suggested that nicotine significantly decreased in cadherin and ZO-1 protein expression, however nicotine did not affect their association with components of the cytoskeleton.

(A)

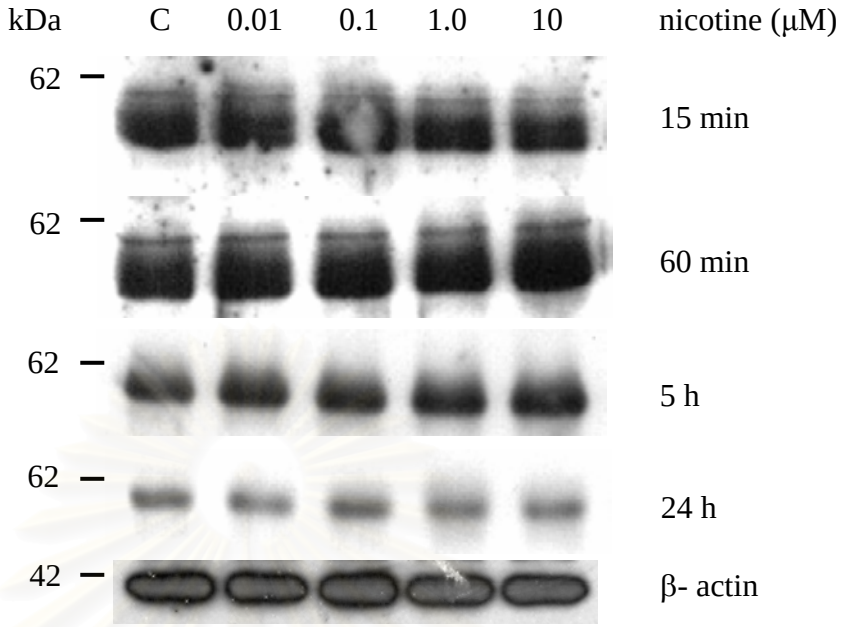

(B)

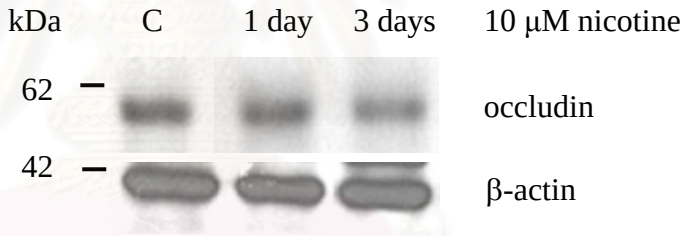

Figure 8 Preliminary study of the expression of occludin in response to nicotine in rat CECs. (A) Cells were treated with 0.01-10 μM nicotine for 15 min, 60 min, 5 h, and 24 h. (B) Cells were treated with 10 μM nicotine for 1 day and 3 days. Cell lysates were separated by 9% SDS-PAGE. Immunoblotting was performed using antibodies for occludin (1:1000). The signals were detected by goat anti rabbit antibody conjugated HRP (1:15,000). n = 1

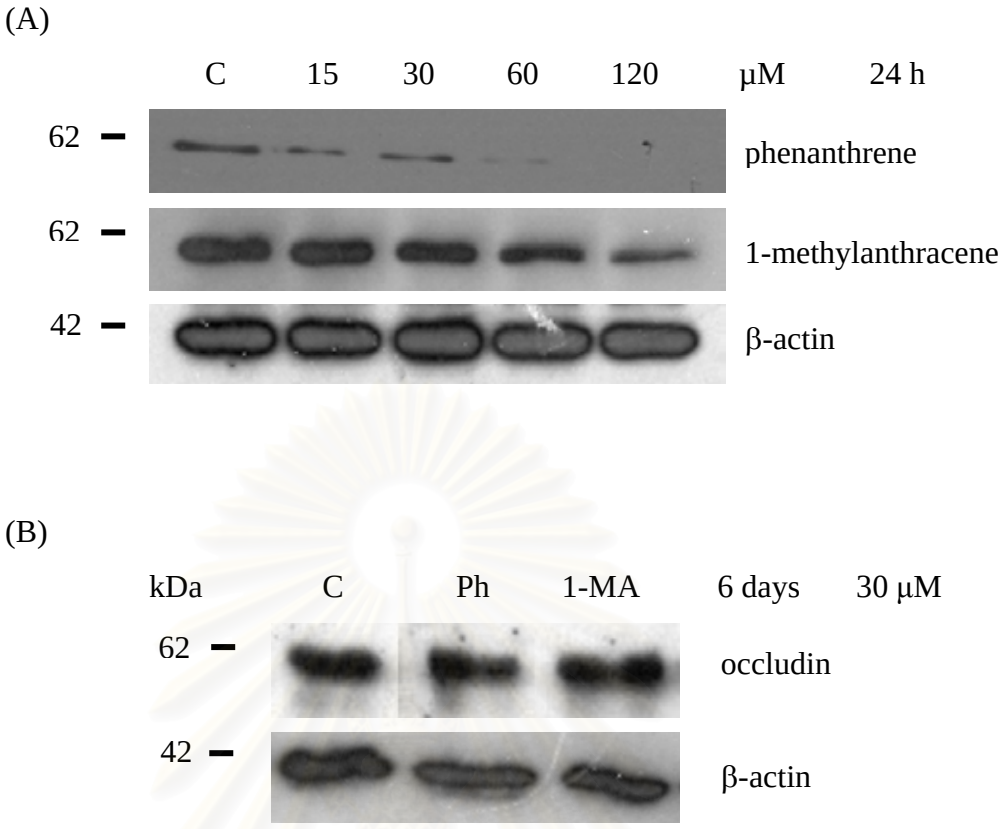

Figure 9 Preliminary study of the expression of occludin in response to phenanthrene and 1-methylanthracene in rat CECs. (A) Cells were treated with 15-120 μM phenanthrene and 1-methylanthracene for 24 h. (B) Cells were treated with either 30 μM phenanthrene (Ph) or 30 μM 1-methylanthracene (1-MA) for 6 days. Cell lysates were separated by 9% SDS-PAGE. Immunoblotting was performed using antibodies for occludin (1:1000). The signals were detected by goat anti rabbit antibody conjugated HRP (1:15,000). n=1.

Effect of PAH on the expression of junctional proteins

To investigate the effect of PAH on the expression of junctional proteins on rat CECs, phenanthrene and 1-methylanthracene at the concentration of 30 μM for 24 h were used. After treatment with phenanthrene, no major change of occludin, claudin-5, cadherin and ZO-1 was detected in neither Tx-100-soluble fraction (Figure 11A and 11C) nor Tx-100-insoluble fraction (Figure 11B and 11D). Similarly, after treatment with 1-methylanthracene, no major change of occludin, claudin-5, cadherin, and ZO-1 was detected in neither Tx-100-soluble fraction (Figure 12A and 12C) nor Tx-100-insoluble fraction (Figure 12B and 12D). The results revealed that phenanthrene and 1-methylanthracene at the concentration of 30 μM had no effect on junctional protein expression.

Cerebral microvascular TJ protein localization after nicotine and PAH exposure

To further investigate the possibility that alterations in BBB junctional protein expression were associated with the pattern of localization of junctional proteins, which were assessed by indirect immunofluorescence microscopy.

Effect of nicotine on the localization of junctional proteins

Immunofluorescent staining of primary rat CECs culture using Cy3-anti-occludin, claudin-5, cadherin, and ZO-1 revealed that rat CECs grown under normal conditions showed a marginal band distribution of those proteins that outlined the cell-cell contact sites. Additionally, rat CECs displayed spindle shaped morphology, which was the characteristic of these cells grown in culture (Figures 13A, 13C, 13E, and 13G). Less intense staining of cadherin was observed, which might be due to cadherin contacting with the neighboring CECs with a single transmembrane characteristic (Figure 13E). No change of occludin and claudin-5 was observed after nicotine treatment (Figure 13B and Figure 13D). Less pronounced effect on the localization of cadherin was observed (Figure 13F). The most pronounced decrease of ZO-1 in response to 10 μM nicotine treatment for 24 h was observed, accompanied by disruption of the continuous membrane staining (Figure 13H). The results were in agreement with those from Western blot analysis.

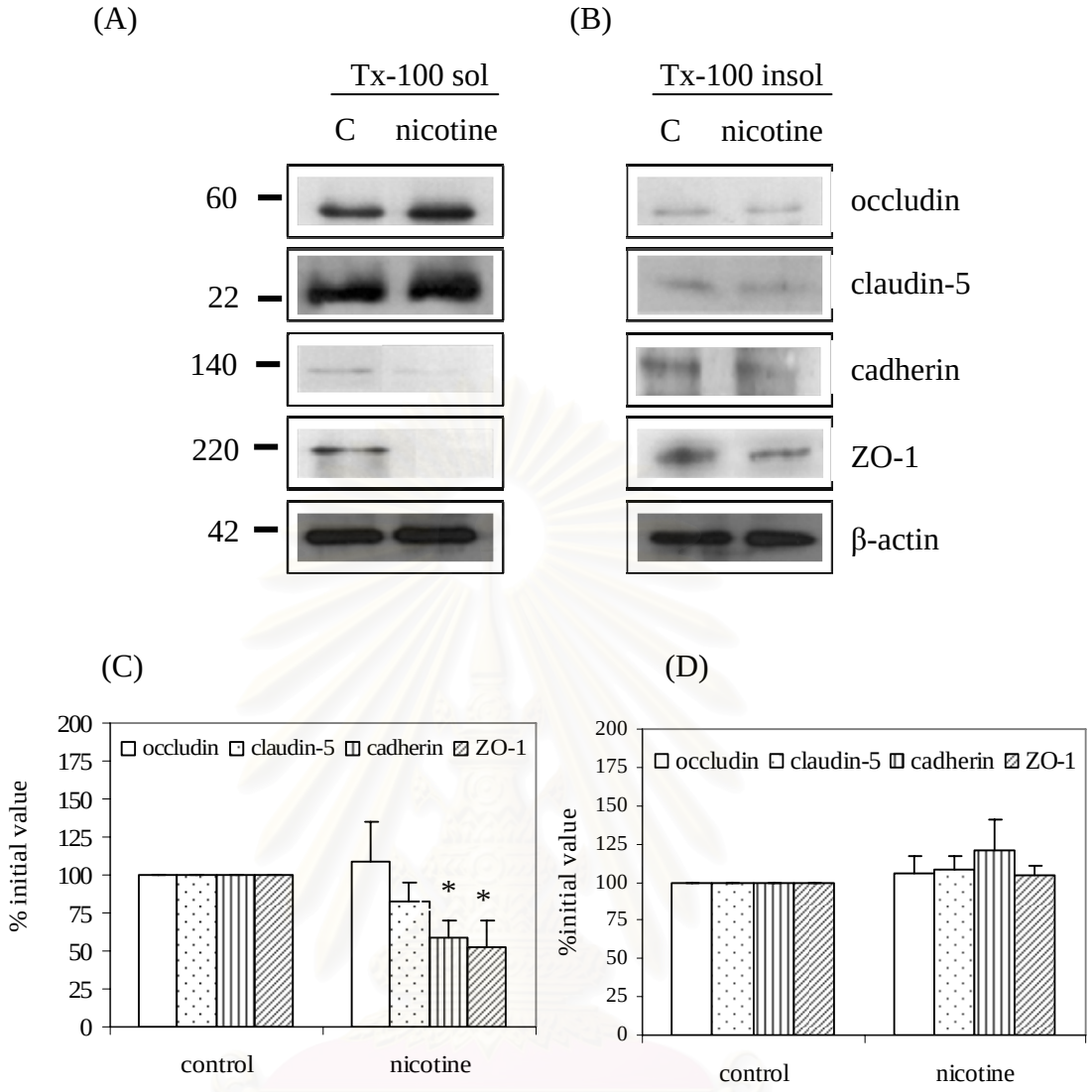

Figure 10 Immunoblots of occludin, claudin-5, cadherin, and ZO-1 proteins in rat CECs in response to nicotine. (A) Tx-100-soluble fraction. (B) Tx-100-insoluble fraction. Cells were subjected to nicotine treatment (10 μM) for 24 h. Cell lysates were separated by 8% (for ZO-1), 9% (occludin and cadherin), and 13% (for claudin-5) SDS-PAGE. Immunoblotting was performed using antibodies for occludin (1:1000), claudin-5 (1:1000), cadherin (1:2000), and ZO-1 (1:250). The signals were detected by goat anti-rabbit antibody conjugated HRP (1:15,000). Densitometrical analysis of immunoblots of (C) Tx-100-soluble fraction, and (D) Tx-100-insoluble fraction. C = control. Each point represents the mean ± S.E.M. for three different experiments. *p<0.05 compared to the cells without nicotine.

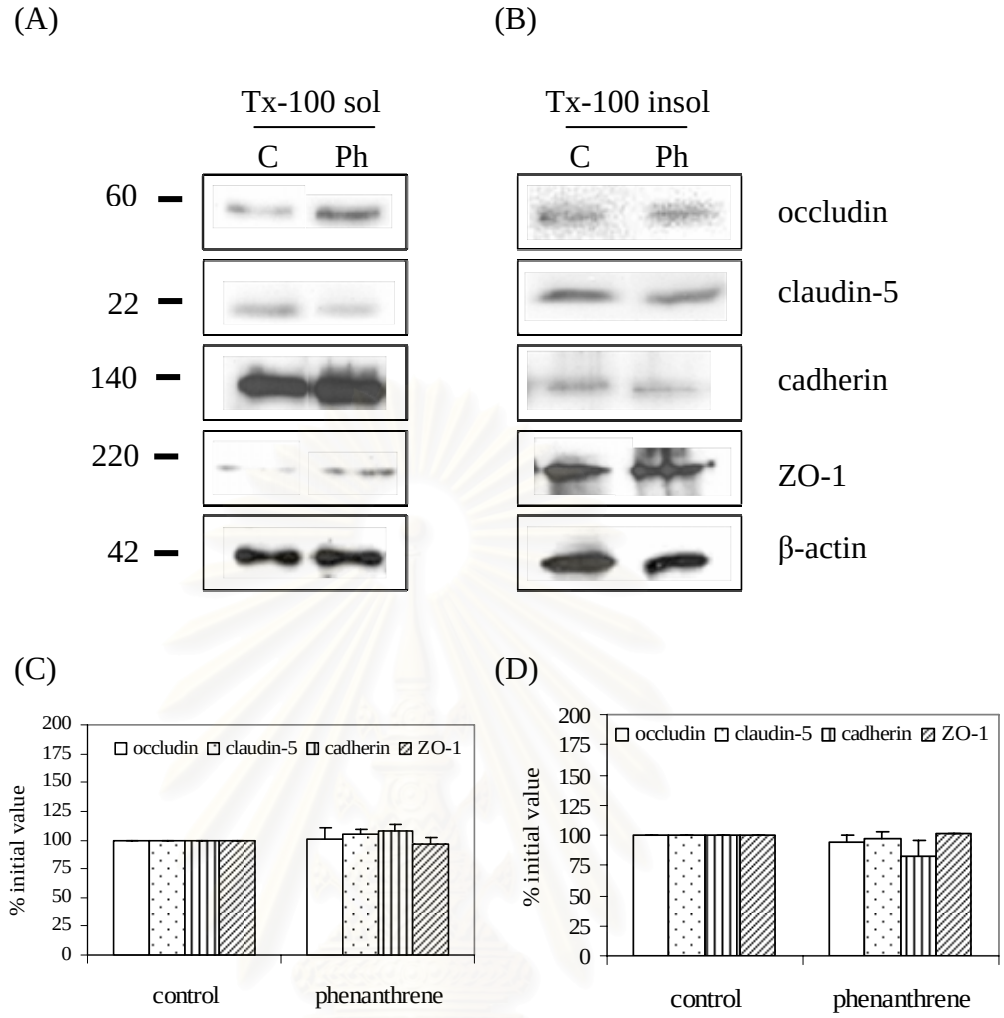

Figure 11 Immunoblots of occludin, claudin-5, cadherin, and ZO-1 proteins in rat CECs in response to phenanthrene. (A) Tx-100-soluble fraction. (B) Tx-100-insoluble fraction. Cells were subjected to phenanthrene (Ph) treatment (30 μM) for 24 h. Cell lysates were separated by 8% (for ZO-1), 9% (occludin and cadherin), and 13% (for claudin-5) SDS-PAGE. Immunoblotting was performed using antibodies for occludin (1:1000), claudin-5 (1:1000), cadherin (1:2000), and ZO-1 (1:250). The signals were detected by goat anti-rabbit antibody conjugated HRP (1:15,000). Densitometrical analysis of immunoblots of (C) Tx-100-soluble fraction, and (D) Tx-100-insoluble fraction. C = control. Each point represents the mean ± S.E.M. for three different experiments.

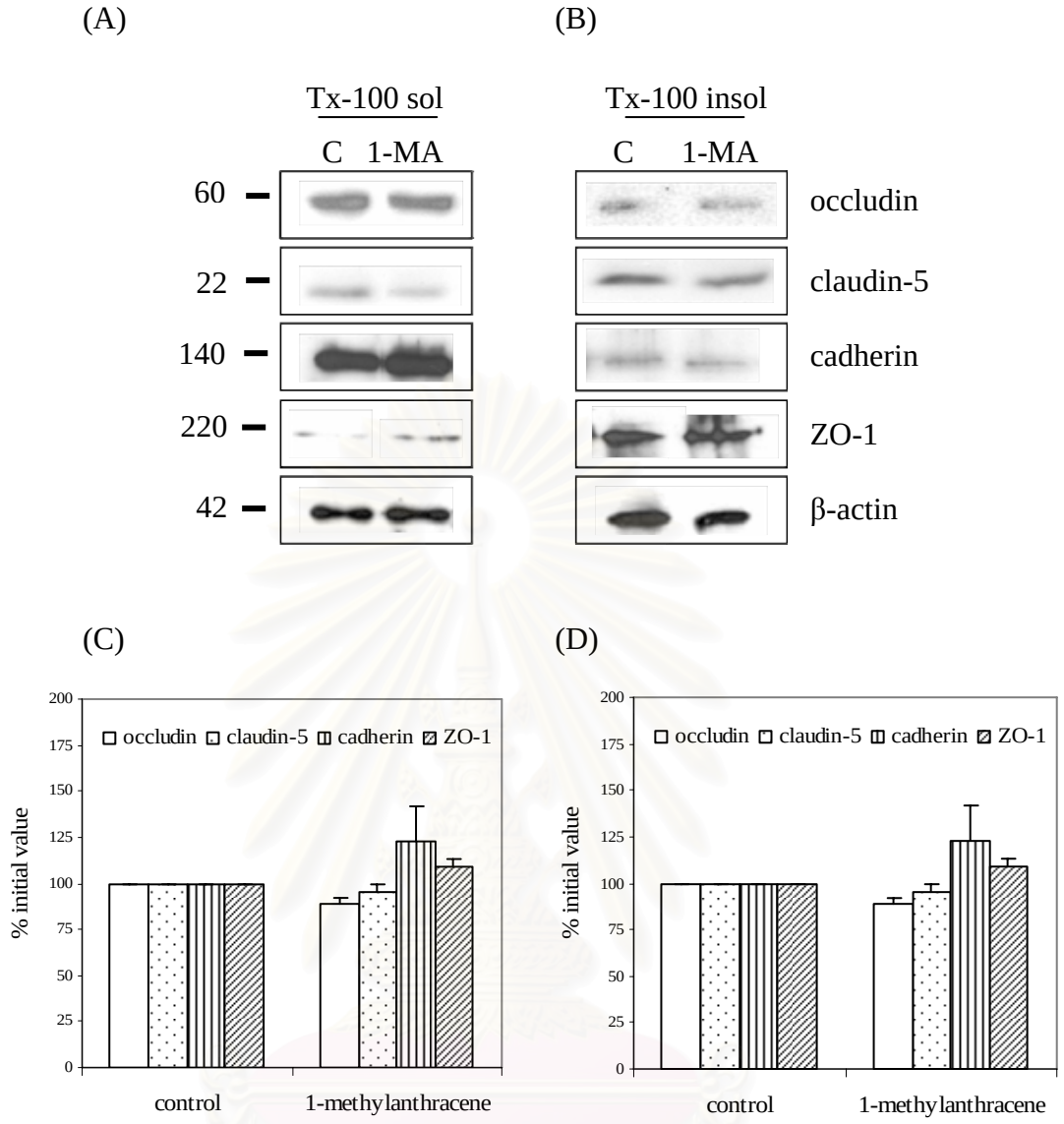

Figure 12 Immunoblots of occludin, claudin-5, cadherin, and ZO-1 proteins in rat CECs in response to 1-methylanthracene. (A) Tx-100-soluble fraction. (B) Tx-100-insoluble fraction. Cells were subjected to 1-methylanthracene treatment (30 μM) for 24 h. Cell lysates were separated by 8% (for ZO-1), 9% (occludin and cadherin), and 13% (for claudin-5) SDS-PAGE. Immunoblotting was performed using antibodies for occludin (1:1000), claudin-5 (1:1000), cadherin (1:2000), and ZO-1 (1:250). The signals were detected by goat anti-rabbit antibody conjugated HRP (1:15,000). Densitometrical analysis of immunoblots of (C) Tx-100-soluble fraction, and (D) Tx-100-insoluble fraction. C = control.

Effect of PAH on the localization of junctional proteins

Treatment with 30 μM phenanthrene for 24 h did not cause significant redistribution of occludin (Figure 14B), claudin-5 (Figure 14D), cadherin (Figure 14F), and ZO-1 (Figure 14H) compared to control. No change could be seen in the localization of junctional proteins in response to 30 μM 1-methylanthracene treatment for 24 h (Figure 15). The results revealed that either phenanthrene or 1-methylanthracene did not change the redistribution of junctional proteins.

Protein- protein interaction after nicotine and PAH exposure

Previous studies showed that nicotine caused a significant decrease in ZO-1 protein expression in Tx-100-soluble fraction (Figure 10). ZO-1 is a peripheral protein that is associated with occludin and tight junctional formation (Saitou et al., 1998). It has been reported that ZO-1 and occludin are components of a molecular complex involved in the formation of junctional structures (Gonzalez-Mariscal *et al*., 2003). To dissect whether nicotine, phenanthrene, and 1-methylanthracene caused a disruption of protein-protein interaction between occludin and ZO-1, the interaction between ZO-1 and occludin was further studied using co-immunoprecipitation in Tx-100-soluble fraction. No difference of anti-occludin staining was observed in control cells and treated cells (Figure 16A). Co-immunoprecipitation staining with anti-ZO-1 antibody showed that the interaction between occludin and ZO-1 was significantly disrupted after exposure to nicotine, phenanthrene, or 1-methylanthracene (Figure 16B). Since nicotine decreased ZO-1 expression in Western blot analysis (Figure 10C), the effect of nicotine on the interaction of ZO-1 and occludin in Tx-100-soluble fraction was investigated using co-immunoprecipitation assay (Figure 16C). The result revealed that relative ZO-1 protein intensity did not change under nicotine treatment (Figure 16D). No change was observed in the phenanthrene treated cells as well. Only the cells treated with 1-methylanthracene significantly caused a decrease in the interaction between ZO-1 and occludin.

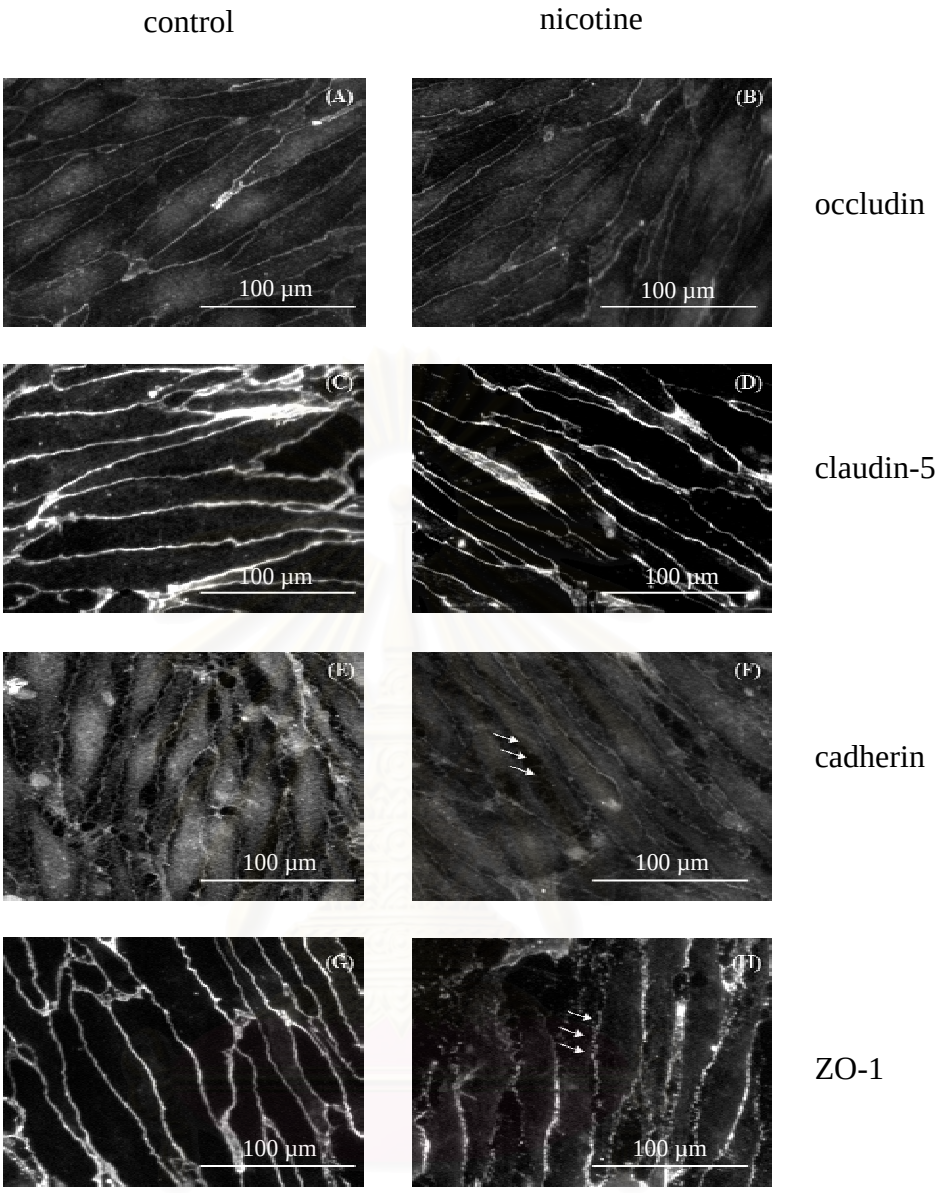

Figure 13 Immunofluorescent localization of the junctional proteins: occludin, claudin-5, cadherin, and ZO-1 in response to nicotine in rat CECs. The CECs were exposed to 10 µM nicotine for 24 h. The cells were fixed and permeabilized with ethanol/acetic acid prior to application of the antibody. Rabbit anti-occludin (A and B), anti-claudin-5 (C and D), anti-cadherin (E and F), and anti-ZO-1 (G and H) antibodies (1:200) were used as first antibodies. The signal was detected by incubation with Cy3-conjugated secondary antibody (1:200). (A, C, E, G) control. (B, D, F, H) nicotine treatment. Arrows marked disruption in staining. Scale bar = 100 µm

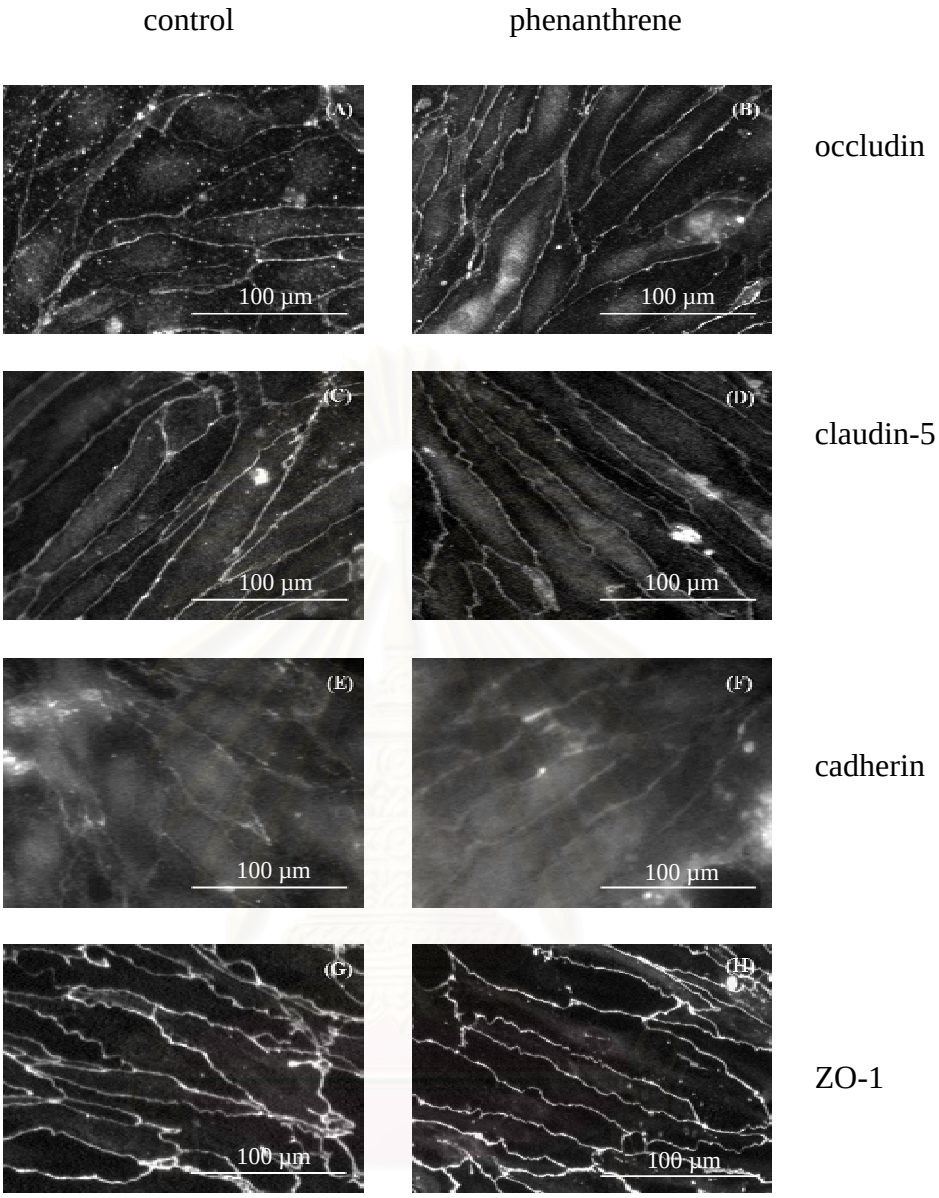

Figure 14 Immunofluorescent localization of the junctional proteins: occludin, claudin-5, cadherin, and ZO-1 in response to phenanthrene in rat CECs. The rat CECs were exposed to 30 µM phenanthrene for 24 h. The cells were fixed and permeabilized with ethanol/acetic acid prior to application of the antibody. Rabbit anti-occludin (A and B), anti-claudin-5 (C and D), anti-cadherin (E and F), and anti-ZO-1 (G and H) antibodies (1:200) were used as first antibodies. The signal was detected by incubation with Cy3-conjugated secondary antibody (1:200). (A, C, E, G) control. (B, D, F, H) phenanthrene treatment. Scale bar = 100 µm

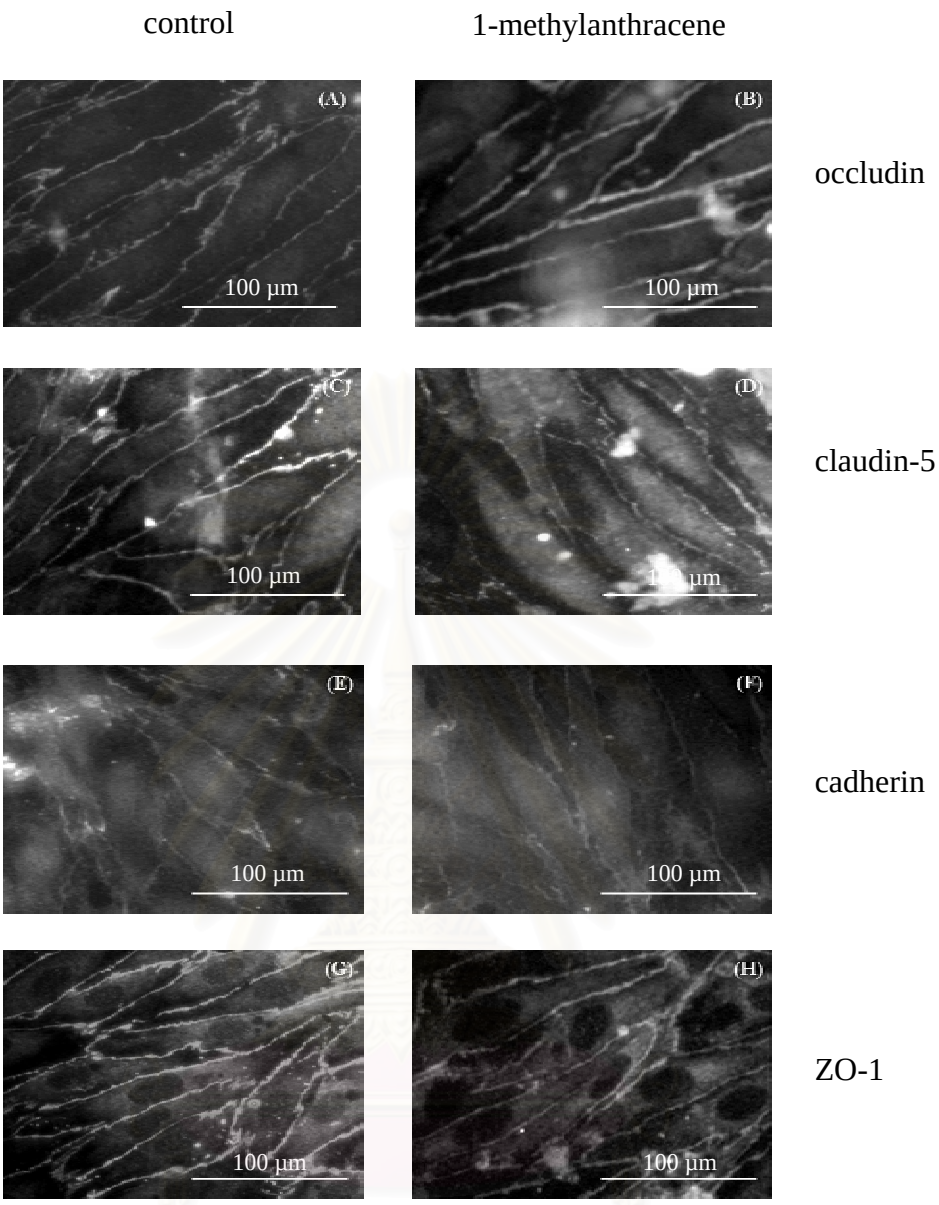

Figure 15 Immunofluorescent localization of the junctional proteins: occludin, claudin-5, cadherin, and ZO-1 in response to 1-methylanthracene in rat CECs. The rat CECs were exposed to 30 µM 1-methylanthracene for 24 h. The cells were fixed and permeabilized with ethanol/acetic acid prior to application of the antibody. Rabbit anti-occludin (A and B), anti-claudin-5 (C and D), anti-cadherin (E and F), and anti-ZO-1 (G and H) antibodies (1:200) were used as first antibodies. The signal was detected by incubation with Cy3-conjugated secondary antibody (1:200). (A, C, E, G) control. (B, D, F, H) 1-methylanthracene treatment. Scale bar = 100 µm

Assessment of the barrier function by TEER measurement

To determine whether the changes in protein expression levels and localization had any functional consequences, a barrier permeability using TEER measurement was performed. For TEER measurements, rat CECs were cocultured with astrocytes on Transwell filters coated with collagen IV/fibronectin and supplemented with physiological concentration of 550 nM hydrocortisone and 250 µM CPT-cAMP (Rubin *et al*., 1991; Weidenfeller *et al*., 2005).

Rat CECs were treated by adding nicotine, phenanthrene, or 1-methylanthracene to the luminal side of the monolayer and incubated for 24 h. The TEER values of the control cells were around 132-273 Ω cm^2, which frequently reported as an *in vitro* BBB model in various laboratories (Gumbletonand Audus, 2001). The results showed that no significant change in TEER was observed after nicotine treatment (101.36 ± 1.78 %) (Figure 17). In addition, no significant decrease in TEER was observed after neither phenanthrene (100.48±12.74%) nor 1-methylanthracene treatment (98.61±8.70%) (Figure 17). The results revealed that nicotine, phenanthrene, or 1-methylanthracene did not change the paracellular permeability as measured by TEER.

Cumulative effect of nicotine treatment under oxidative stress

The previous results showed that nicotine caused severely changes in ZO-1 protein expression (Figure 10A and 10C) and localization (Figure 13H), however, nicotine did not change the paracellular permeability by TEER measurement (Figure 17). Several lines of evidence show that elevated release of oxygen free radicals from brain tissue under pathological conditions might cause severe vascular damage leading to a transient disruption of the BBB (Bresgen *et al*., 2003; Witt *et al*., 2003). The oxidative stress induced change in paracellular permeability may be due to perturbation of TJ complexes (Mark and Davis, 2002; Lee *et al*., 2004; Krizbai *et al*., 2005). Therefore, the combination of nicotine and a redox cycling agent DMNQ, a generator of the hydrogen peroxide oxidant in the cells, was investigated whether nicotine could aggravate TJ damage under oxidative stress.

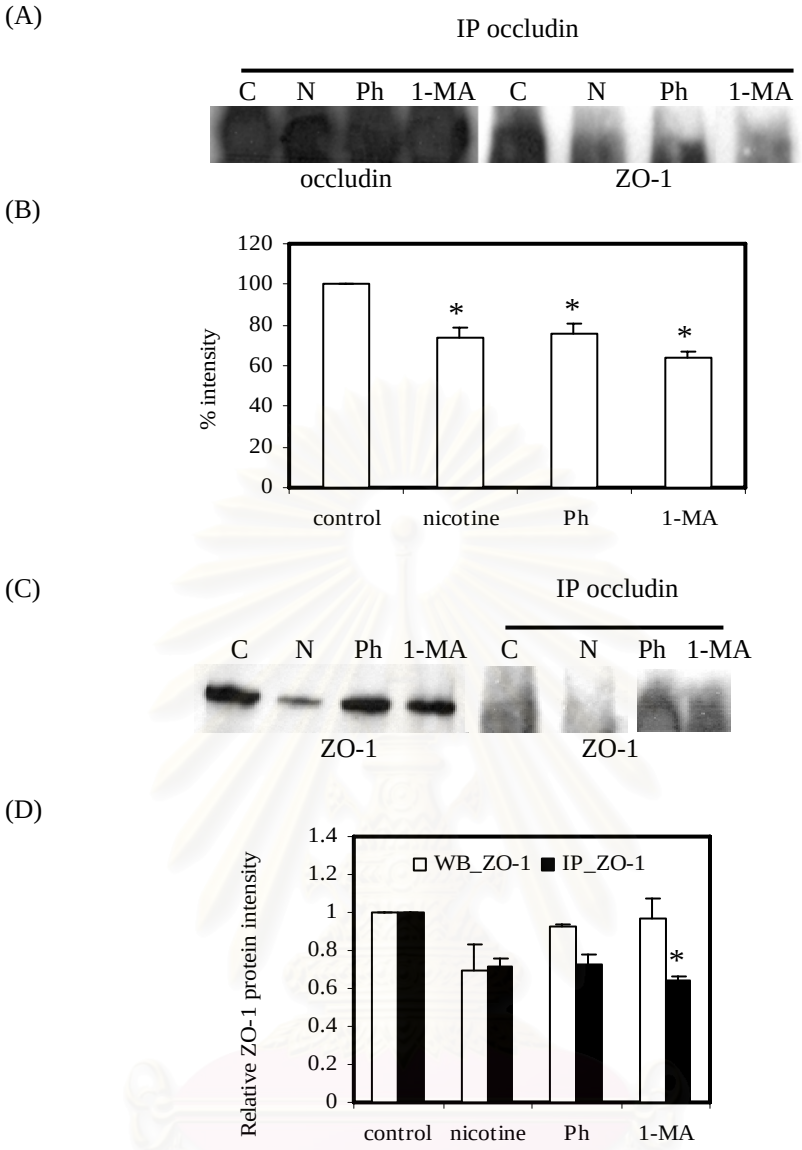

Figure 16 Interaction of occludin and ZO-1 in response to nicotine, phenanthrene, and 1-methylanthracene treatment in rat CECs. (A) occludin was immunoprecipitated from control cells and cells exposed to nicotine at the concentration of 10 μM, phenanthrene and 1-methylanthracene at the concentration of 30 μM. The associated occludin and ZO-1 was detected by immunoblotting. (B) densitometrical analysis of immunoblots of rabbit anti-ZO-1 antibody staining. (C) Western blot analysis of rabbit anti-ZO-1 antibody staining on rat CECs. (D) densitometrical analysis of immunoblots of rabbit anti ZO-1 antibody staining. Each point represents the mean ± S.E.M. for three different experiments. *p<0.05 compared to the cells without treatment.

Cytotoxic effect of DMNQ treatment

To exclude the changes observed after DMNQ arise from nonspecific cell injury, XTT assay was performed on rat CECs treated with DMNQ at the concentrations of 1, 10, 20, 40, 60, 80, and 100 μM for 24 h. The cell viability values according to DMNQ treatment were 107.02±6.11%, 103.97±6.18%, 28.31±1.00%, 8.79±0.49%, 8.38±0.47%, and 7.49±0.42%, respectively. The results showed that no significant difference was observed in endothelial cell viability following DMNQ treatment at the concentration of 1 and 10 μM (Figure 18). Therefore, DMNQ at a concentration of 10 μM was used where the cytotoxic effect was absent.

Cerebral microvascular junctional protein localization after combination of nicotine and DMNQ exposure

We further investigated whether nicotine could cause an alteration of junctional protein localization under oxidative stress condition. The rat CECs were treated with the combination of 10 μM nicotine and 10 μM DMNQ. In control condition, the marginal staining of ZO-1 protein outlining the cell-cell contact was observed (Figure 19A). A disruption of the continuity of ZO-1 expression along the cell-cell contact was observed after 10 μM nicotine exposure (Figure 19B). Treatment with DMNQ had an effect on the ZO-1 protein localization and a retraction of the characteristic spindle shaped morphology (Figure 19C). More pronounced retraction of ZO-1 protein staining was revealed under the combination of nicotine and DMNQ treatment, compared to DMNQ or nicotine treatment alone (Figure 19D). The results showed that nicotine potentially aggravated the disturbance of ZO-1 protein organization under oxidative stress.

Assessment of the barrier function by TEER measurement after combination of nicotine and DMNQ exposure

Nicotine or DMNQ treatment alone did not cause any change of TEER. However, the combination of 10 μM nicotine and 10 μM DMNQ significantly decreased TEER permeability (80±1.43%)compared to the control, nicotine alone (101.36±1.78%), DMNQ alone (95±3.00%) (Figure 20). The result indicated that nicotine under oxidative stress disturbed the localization of ZO-1 (Figure 19D) leading to the significant alteration of BBB permeability compared to nicotine or DMNQ alone.

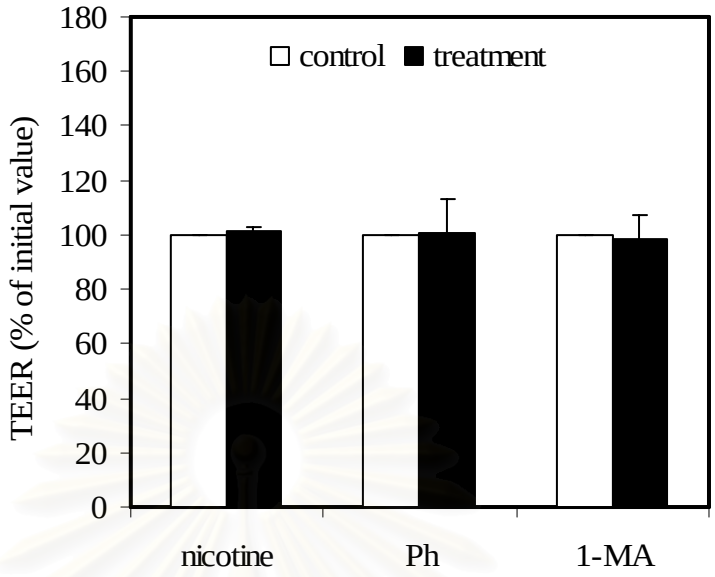

Figure 17 Effect of nicotine, phenanthrene, and 1-methylanthracene on the TEER. Rat CECs, cocultured with astrocytes, were treated with 10 μM nicotine or 30 μM phenanthrene (Ph) or 30 μM 1-methylanthracene (1-MA) for 24 h by adding to the luminal side of the transwell plate. Measurement were started directly after treatment. Each point represents the mean ± S.E.M. for three different experiments.

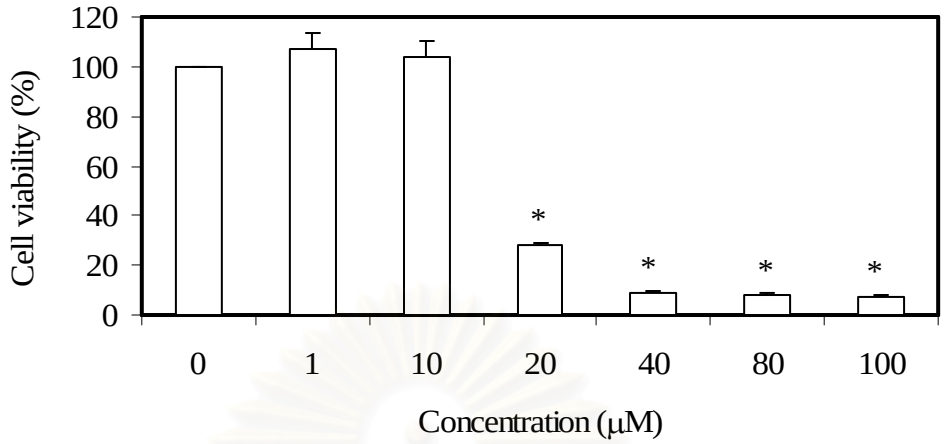

Figure 18 Cytotoxic effect of DMNQ on rat CECs. The cells were treated with various concentrations of DMNQ (1-100 μM) for 24 h. Cell viability was expressed as % of control cell survival measured by XTT assay. Each point represents the mean ± S.E.M. for three different experiments, each performed in triplicate. *p<0.05 compared to the cells without DMNQ.

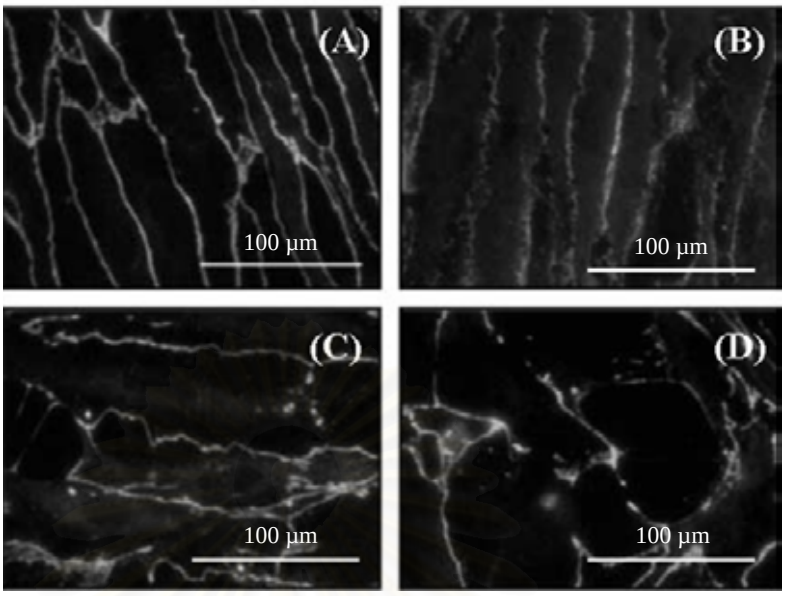

Figure 19 Effects of nicotine and oxidative stress on the localization of ZO-1. (A) control. (B) rat CECs were treated with 10 µM nicotine or (C) 10 µM DMNQ or (D) the combination of 10 µM nicotine and 10 µM DMNQ. The ZO-1 protein was visualized with rabbit anti-ZO-1 primary antibody and Cy3-conjugated secondary antibody. Scale bar = 100 µm.

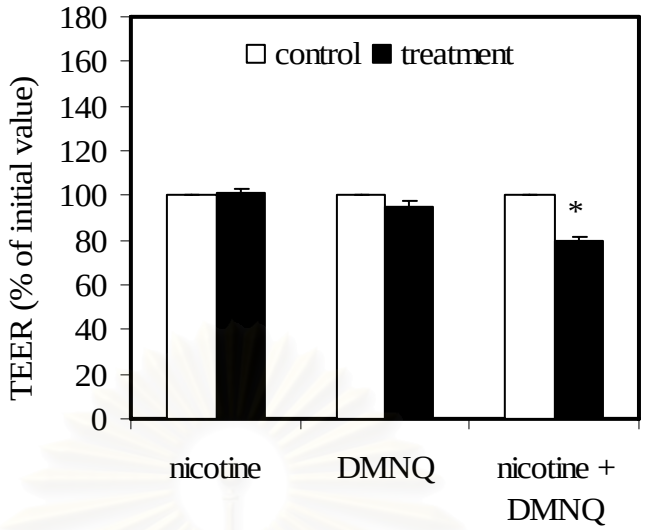

Figure 20 Effect of nicotine and DMNQ on the transcellular electrical resistance. Rat CECs were treated with 10 μM nicotine, 10 μM DMNQ, and the combination of 10 μM nicotine and 10 μM DMNQ for 24 h. Measurement were started directly after treatment. Each point represents the mean ± S.E.M. for three different experiments, each performed in triplicate. *p<0.05 compared to the cells without nicotine or DMNQ treatment.

CHAPTER V

DISCUSSION AND CONCLUSION

Among the well-characterized chemicals, abundant and biologically active components found in tobacco and tobacco smoke are nicotine and PAH. There is overwhelming evidence that smoking associates with a number of neurological and vascular diseases. However, very few information about the effect of cigarette smoke components on rat CECs are available. In the current study, the effect of cigarette smoke components nicotine and PAH on rat CECs was investigated. Since the cerebral endothelium is located at the blood-brain interface, it is the first point of attack of potentially harmful substances to the CNS. In claudin-5-null mice found that they were born with normal-appearing TJ but died a few hours after birth. The experiments were therefore focused on the study of changes affecting the tight and adherens junctional proteins. Primary cultures of brain endothelial cells from different species such as bovine, murine, feline and rat have been widely used for the study of different aspects of BBB function (Abbott *et al.*, 1992; Abbruscato *et al.*, 2002; Megard *et al.*, 2002; Weidenfeller *et al.*, 2005; Perriere *et al.*, 2005; Fletcher *et al.*, 2006). The microvasculature of the CNS can be differentiated from the peripheral tissue endothelia, which possesses uniquely distinguishing characteristics such as cerebral capillary endothelial cells contain tight junctions, the cytoplasm of the endothelial cells is of uniform thickness, with very few pinocytotic vesicles (hollowed out portion of cell membrane fulled with fluid, forming a vacuole, which allows for nutrient transport), and lack fenestrations (*i.e.* openings), a greater number and volume of mitochondria in BBB endothelial cells compared to peripheral endothelial cells, expression of vWF, expression of γ-glutamyl-transpeptidase, P-gp and GLUT (Dorovini-Zis and Huynh, 1992; Domotor *et al*., 1999; Ghazanfari and Stewart, 2001; Calabria *et al*., 2006). The advantage of isolating endothelial cells from large animals is the high yield of endothelial cells. However, our knowledge about the genetic material of bovine and porcine species make them less suitable for molecular characterization compared to the human or rat species (Gumbleton *et al.*, 2001). Furthermore, the access to large animals is usually restricted and cost consuming. The use of human sources raises ethical questions as well. Rat brain endothelial cells are useful components of BBB models and the results can be well correlated with *in*

vivo results (Abbott *et al.*, 1992; Domotor *et al.*, 1999; Parkinson and Hacking, 2005; Perriere *et al.*, 2005; Calabria *et al.*, 2006). An alternative model would have been the use of immortalized brain endothelial cells, however, immortalization usually results in a more de-differentiated phenotype with relatively high paracellular permeability. In addition, cell lines rapidly de-differentiate *in vitro* and losing the characteristics of BBB endothelial cells after a few passages in culture. In our experiments, primary cultures of rat CECs were therefore used to examine the effect of nicotine, phenanthrene, and 1-methylanthracene on junctional protein.

One of the major obstacles in getting good *in vitro* model of the BBB is obtaining a pure endothelial culture. The major difficulty is the presence of contaminating cells such as pericytes, smooth muscle cells, astrocytes, and fibroblasts (Abbott *et al*., 1992). The variation in purity affects the characteristics of the cultures and thus limits reproducibility between different experiments. Several techniques have been used to solve this problem. The use of Ca^{2+}- and Mg^{2+}- free saline washed of cultures has been reported to preferentially remove contaminating cell types leaving the endothelial cells behind (Abbott *et al*., 1992). Furthermore, methods based on complement killing are used as well. A critical step in getting a pure culture is the isolation procedure itself. Two steps of enzymatic digestion were carried out and followed by density gradient centrifugation on Percoll gradient to remove red blood cells and other cell debris, which could interfere with the attachment and the growth of the isolated endothelial cells. To further increase the purity of our cultures, we used puromycin, a broad spectrum antibiotic isolated from *Streptomyces alboniger*, in order to prevent growth of bacteria, protozoa, algae, and mammalian cells (Perriere *et al*., 2005). Rat CECs can stand with puromycin because of their over expression of the efflux transporter P-gp, a multidrug resistance transporter protein, which recognizes puromycin and effluxes it from the cells. By including a puromycin treatment step, we could obtain cultures with high purity as revealed by immunostaining of the cultures with the endothelial specific marker von Willebrand factor (Wu *et al*., 2003). Our results are in line with literature data as well (Perriere *et al*., 2005; Calabria *et al*., 2006). By using this procedure, we could obtain a reasonable yield because brain endothelial cells tend to grow in colonies only. Single cells do not grow well in culture, mainly because the possible lack of survival factors or cell-cell communication with neighbouring cells. It is well-known that endothelial cells adhere poorly to glass and plastic surfaces. In order to promote the adherence of

the brain endothelial cells to the plastic surface of the petri dishes, the surface of the culture dishes was coated with a mixture of collagen IV and fibronectin, which are the major constituents of the endothelial basal lamina (Hamann *et al*., 1995).

To exclude a possible direct toxic effect of cigarette smoke components, we performed viability test. Our results showed that nicotine and PAH at physiologically relevant concentrations did not influence cell viability. Only high concentration above 60 μM of PAH caused a decrease in the viability rat CECs. Occludin and claudin-5 are key TJ proteins, whose expression levels could determine tissue barrier properties. ZO-1 has been shown to be an abundant peripheral tight junctional protein of the BBB associated with occludin and other TJ proteins (Saitou *et al*., 1998). The AJ protein *i.e*. cadherin, plays an important role in maintaining the integrity of the paracellular barrier and the integrity of the BBB as well (Torii *et al*., 2006). Therefore, nicotine and PAH at the nontoxic concentrations were used to investigate the expression of occludin, claudin-5, cadherin, and ZO-1 proteins.

TJ is a micromembrane domain that has both Tx-100-soluble and -insoluble components (Nusrat *et al*., 2000). Detergent fractionation with the use of Tx-100 shows that membrane and cytoplasmic proteins are mostly Tx-100-soluble fraction, whereas proteins incorporated into large protein complexes, such as the cytoskeleton and/or junctional complexes, is Tx-100-insoluble fraction (Wong, 1997). In this study, Western blot analyses of the TJ- and AJ-associated proteins did not show any significant change of occludin and claudin-5 protein expression in neither Tx-100-soluble nor Tx-100-insoluble fractions in response to nicotine treatment at the concentration of 10 μM. On the other hand, treatment with nicotine for 24 h significantly decreased cadherin and ZO-1 protein expression in Tx-100-soluble fraction but not in Tx-100-insoluble fraction. These results suggested that nicotine could affect the subcellular localization of cadherin and ZO-1 and may not involve the incorporation into the large protein complexes. Furthermore, the tight junctional proteins, occludin and claudin-5, may not be a direct target of nicotine action. Our findings were supported by previous reports showing that nicotine treatment was able to reduce ZO-1 content significantly via nAChR (Abbruscato *et al*., 2002; Hawkins *et al*., 2005). The overexpression of α7 nAChR induced cadherin expression (Utsugisawa *et al*., 2002). In addition, α7 nAChR has been shown to be permeable to Ca^{2+} and can generate intracellular Ca^{2+} signals that influence cellular excitability

(Vermino *et al*., 1994), leading to increase endothelial permeability (Tiruppathi *et al*., 2006). Anyway, another possibility of nicotine decreased ZO-1 protein expression might be because ZO-1-associated nucleic acid-binding protein (ZONAB) might bind to the SH3 domain of ZO-1 and further translocated to the nucleus leading to the attenuation of ZO-1 expression (Balda and Matter, 2000). E-cadherin was found to induce contact inhibition of cell growth (St. Croix *et al*., 1998). This effect requires binding of β-catenin to the cadherin cytoplasmic tail (Gottardi *et al*., 2001) and inhibition of the transcriptional activity. Thus, nicotine might decrease cadherin expression via β-catenin. However, non-receptor mediated mechanisms are possible as well (Tonnessen *et al*., 2000). The absence of the effect of PAH on TJ- and AJ-proteins might be due to the lack of AhR expression in rat CECs.

Since nicotine altered junctional protein expression, *i.e.*, cadherin and ZO-1, the distribution of TJ and AJ proteins were further investigated with immunofluorescence microscopy. No changes of occludin and claudin-5 were observed from nicotine treatment. A slight decrease in integrity of the cadherin staining was observed. The most pronounced decrease in response to nicotine treatment was observed in ZO-1 expression demonstrated by the disruption of the continuous membrane staining. These observations were in agreement with our Western blot analysis and previous studies performed on bovine CECs (Abbruscato *et al*., 2002). Our data suggested that only relatively highly physiological concentrations of nicotine were able to induce changes in the structure of the junctional complexes. However, when considering the damaging effect of nicotine, it should be noted that rats are significantly more resistant to nicotine than humans. Furthermore, our *in vitro* model system allowed only for relatively short term monitoring (maximum 24-48 h) of nicotine effect.

The effect of PAH on the barrier characteristics of rat CECs has not been investigated so far. Previous reports showed that 1-methylanthracene and phenanthrene induced apoptosis of human coronary artery endothelial cells by a mechanism that involves PLA2 activation (Tithof *et al*., 2002). Stimulation of human aortic endothelial cells with CSC rich in PAH induced rapid production of IL-4 and IL-8, which might reflect a damaging effect on endothelial cells (Nordskog *et al*., 2005). The mechanism by which PAH affecting on endothelial cells is largely unknown. Our data showed that phenanthrene and 1-methylanthracene had no major effect on junctional proteins. No significant change in the expression of any of the TJ

and AJ protein in the Tx-100-soluble fraction in response to either phenanthrene or 1-methylanthracene treatment could be observed in rat CECs (Figure 12A and 12C). However, a significant decrease in the interaction between occludin with ZO-1 in response to 1-methylanthracene treatment was observed in our co-immunoprecipitation analysis (Figure 16B and 16D). The result suggested that after entering rat CECs, 1-methylanthracene might directly change the conformation of either occludin or ZO-1, leading to a decrease in occludin-ZO-1 complex.

Anatomically, the BBB endothelial cells are surrounded by astrocytes (Abbott *et al*., 2006), when coculture, can increase TEER and decrease paracellular transport (Gaillard *et al*., 2001). There is now strong evidence, particulary from studies in cell cultures, that astrocytes can upregulate many BBB features, leading to tighter TJ (physical barrier) (Rubin *et al*., 1991), the expression and polarized localization of transporters, including P-gp (Schinkel, 1999), and glucose transporter type I (transport barrier) (McAllister *et al*., 2001), and specialized enzyme systems (metabolic barrier) (Subue *et al*., 1999; Abbott, 2002). Stimulation with CPT-cAMP and RO-20-1724 increased TJ functionality, also in the presence of astrocytes (Rubin *et al*., 1991; Gaillard *et al*., 2001). Since changes in the expression of junctional proteins were observed, we assessed the barrier function by the TEER measurement. Criteria for monitoring the quality of monolayers in transport studies include TEER and permeability to hydrophilic markers like [^{14}C]sucrose, which reflect the degree of tight junction formation. Using these criteria, none of the primary endothelial cell culture models matches yet *in vivo* conditions (Bickel, 2005). The TJ significantly restrict even the movement of small ions such as Na^+ and Cl^-, so that the TEER, which is typically 2-20 Ω cm^2 in peripheral capillaries, can be greater than 1,000 Ω cm^2 in brain endothelium (Abbott *et al*., 2006) and sucrose permeability of about 0.3 x 10^{-7} cm x s^{-1} (Bickel, 2005). Values of TEER vary greatly depending on location, which has important functional consequences. In this study, the most impermeable rat CECs cocultured with rat astrocytes typically yield TEER values around 200 Ω cm^2, which was a typical range as reported in *in vitro* BBB model (Perriere *et al*., 2005; Calabria *et al*., 2006). There were no accompanying changes in monolayer integrity as measured with TEER. The observed changes did not lead to a significant decrease in the TEER value. This is in line with data obtained on bovine rat CECs (Abbruscato *et al*., 2002) showing that 12-24 h nicotine treatment had no effect on TEER. However, when the opening of the paracellular route of the BBB was assessed by

[^{14}C]sucrose permeability, a marker for the paracellular pathway across endothelial monolayers, statistically significant increase was observed after 6 x 10^{-8} M nicotine treatment for 12-24 h (Abbruscato *et al*., 2002). This is probably due to the fact that different aspects of junctional permeability are regulated by distinct mechanisms. Low molecular weight molecules such as sucrose can be used to probe the behavior of the paracellular pathway of endothelial monolayers grown *in vitro*. The sucrose permeability of cultured microvascular cells ranged from 10^{-4} to 10^{-5} cm/s compared with 10^{-6} to 10^{-8} cm/s *in vivo* (Grant *et al*., 1998). The previous report indicated that the paracellular pathway in endothelium is strictly regulated and suggested that endothelial junctions can be closed by stimulating adenylate cyclase and opened by stimulating PKC (Oliver, 1990). As endothelial cells have the ability to contract and relax and possess guanylate cyclase responsive to nitric oxide, endothelium-derived relaxing factor decreases [^{14}C]sucrose permeability by relaxing endothelial cells, thereby narrowing the width of endothelial junctions (Oliver, 1992). Both [^{14}C]sucrose permeability and TEER are indicators of paracellular permeability function, however, the mechanism is different. The electrical resistance reflects an amount of ionic molecule flux through cell layer, which depends on the voltage between electrodes across the cell layer. An *in vivo* study showed that only toxic concentrations of nicotine (10^{-4}-10^{-3} M) were able to increase the permeability to 70 kDa FITC-dextran (Schilling *et al*., 1992) and could cause cell apoptosis in high concentration, 100 μM (Yang and Liu, 2004). Previous studies concluded that the expression and localization of ZO-1 did not always correlate with the physiological efficiency of paracellular gate function (Stevenson *et al*., 1988). Low dose of nicotine at plasma levels (0.01 μM), affected endothelial cells by the induction of cell migration (di Luozzo *et al*., 2005).

Changes in protein expression and localization of cadherin and ZO-1 after nicotine treatment cause cerebral endothelial dysfunction. Nicotine has also been known to result in oxidative stress by inducing the generation of ROS in the tissues and leading to cause cellular injury (Kovacic and Cooksy 2005). Thus, nicotine is considered to produce a compromised state in which the brain is potentially more vulnerable to cerebrovascular disease. To prove the hypothesis, a combination between DMNQ and nicotine on rat CECs was performed. DMNQ was used because it generates H_2O_2 in cells while extracellular addition of oxidants such as H_2O_2 requires concentrations often outside the range considered feasible for information in

a biological setting. Furthermore, the redox cycling agent DMNQ was selected since it does not partake in the side reactions with reactive intermediates that occurs with many such reagents (Ramachandran *et al*., 2002). Oxidative stress is known to alter the integrity of the junctions (Witt *et al*., 2003; Krizbai *et al*., 2005; Torii *et al*., 2006). Exposure of endothelial cells to H_2O_2 results in decreased TEER and ZO-1/occludin distribution (Lee *et al*., 2004). Our results revealed that a pronounced decrease of TEER when a combination of nicotine and DMNQ was applied compared to DMNQ and nicotine treatment alone. This suggests a cumulative effect of nicotine abuse and hypoxia. Junctional proteins were much more affected when nicotine treatment was used in combination with DMNQ. However, lack of cell viability test of a combination of nicotine and DMNQ was investigated in this study.

In conclusion, our study performed a complex investigation on the effect of nicotine and PAH on cerebral endothelial cells. Cigarette smoke components did not cause severe acute alterations in the principal functional properties of the cerebral endothelial cells. However, long term exposure of these cells to CSC especially in combination with other damaging effects like oxidative stress may lead to a significantly impaired BBB function. Our results provided important information for the evaluation of smoking associated risk in different neurological disorders involving oxidative stress like cerebral ischemia or hypoxia. However, the limitation of this study is the CECs can not be cultured in longer period of time. The cells can be cultured maximum up to one week. Furthermore, the cells can not be passaged, leading to time and cost consuming process.

REFERENCES

Abbott, N.J., Hughes, C.C.W., Revest, P.A., Greenwood, J. 1992. Development and characterization of a rat brain capillary endothelial culture: towards an *in vitro* blood-brain barrier. J. Cell Sci. 103: 23-37.

Abbott, N.J., Ronnback, L., Hansson, E. 2006. Astrocyte-endothelial interactions at the blood-brain barrier. Nat. Rev. Neurosci. 7: 41-53.

Abbruscato, T.J., Davis, T.P. 1999. Combination of hypoxia/aglycemia compromises *in vitro* blood-brain barrier integrity. J. Pharmacol. Exp. Ther. 289: 668-675.

Abbruscato, T.J., Lopez, S.P., Mark, K.S., Hawkins, B.T., Davis, T.P. 2002. Nicotine and cotinine modulate cerebral microvascular permeability and protein expression of ZO-1 through nicotinic acetylcholine receptors expressed on brain endothelial cells. J. Pharm. Sci. 91: 2525-2538.

Abbruscato, T.J., Lopez, S.P., Roder, K., Paulson, J.R. 2004. Regulation of blood-brain barrier Na,K, Cl-cotransporter through phosphorylation during *in vitro* stroke conditions and nicotine exposure. J. Pharmacol. Exp. Ther. 310: 459-468.

Akiyama, T. 2000. Wnt/beta-catenin signaling. Cytokine Growth Factor Rev. 11: 273-82.

Annas, A., Brittebo, E., Hellman, B. 2000. Evaluation of benzo(a)pyrene-induced DNA damage in human endothelial cells using alkaline single cell gel electrophoresis. Mutat. Res. 471: 145-155.

Asaba, H., Hosoya, K., Takanaka, H., Ohtsuki, S., Tamura, E., Takizawa, T., Terasaki, T. 2000. Blood-brain barrier is involved in the efflux transport of a neuroactive steroid, dehydroepiandrosterone sulfate, via organic anion transporting polypeptide 2. J. Neurochem. 75: 1907-1916.

Asahi, M., Wang, X., Mori, T., Sumii, T., Jung, J-C., Moskowitz, M.A., Fini, M.E., Lo, E.H. 2001. Effects of matrix metalloproteinase-9 gene knockout on the proteolysis of blood-brain barrier and white matter components after cerebral ischemia. J. Neurosci. 21: 7724-7732.

Balda, M.S., Matter, K. 2000. The tight junction protein ZO-1 and an interacting transcription factor regulate ErbB-2 expression. EMBO J. 19: 2024-2033.

Bamforth, S.D., Kniesel, U., Wolburg, H., Engelhardt, B., Risau,W. 1999. A dominant mutant of occludin disrupts tight junction structure and function. J. Cell Sci. 112:1879-1888.

Basuroy, S., Sheth, P., Kuppuswamy, D., Balasubramanian, S., Rayr, R.M., and Rao, R.K. 2003. Expression of kinase-inactive c-Src delays oxidative stress-induced dissembly and accelerates calcium-mediated reassembly of tight junctions in the Caco-2 cell monolayer. J. Biol. Chem. 278: 49239-49245.

Bauer, H., Stelzhammer, W., Fuchs, R., Weiger, T.M., Danninger, C., Probst, G., Krizbai, I.A. 1999. Astrocytes and neurons express the tight junction-specific protein occludin *in vitro*. Exp. Cell Res. 250: 434-438.

Bazzoni, G. 2003. The JAM family of junctional adhesion molecules. Curr. Opin. Cell Biol. 15: 525-530.

Bazzoni, G., and Dejana, E. 2003. Endothelial cell-to-cell junctions: molecule organization and role in vascular homeostasis. Physiol. Rev. 83: 869-901.

Bickel, U. 2005. How to measure drug transport across the blood-brain barrier. NeuroRx. 2: 15-26.

Blasig, I.E., Mertsch, K., Haseloff, R.F. 2002. Nitronyl nitroxides, a novel group of protective agents against oxidative stress in endothelial cells forming the blood-brain barrier. Neuropharmacol. 43: 1006-1014.

Bolton, S.J., Anthony, D.C., Perry, V.H. 1998. Loss of the tight junction proteins occludin and zonula occludens-1 from cerebral vascular endothelium during neutrophil-induced blood-brain barrier breakdown *in vivo*. Neurosci. 86: 1245-1257.

Bresgen, N., Karlhuber, G., Krizbai, I., Bauer, H., Bauer, H.C., Eckl, P.M. 2003. Oxidative stress in cultured cerebral endothelial cells induces chromosomal aberrations, micronuclei, and apoptosis. J. Neurosci. Res. 72: 327-333.

Butt, A,M. 1995. Effect of inflammatory agents on electrical resistance across the blood-brain barrier in pial microvessels of anaesthesized rats. Brain Res. 696: 145–150.

Calabria, A.R., Weidenfeller, C., Jones, A.R., de Vries, H.E., Shusta, E.V. 2006. Puromycin-purified rat brain microvascular endothelial cell cultures exhibit improved barrier properties in response to glucocorticoid induction. J. Neurochem. 97: 922-933.

Chen, J.L., Wei, L., Bereczki, D., Hans, F.J., Otsuka, Y., Acuff, V., Ghersi-Egea, J.F., Patlak, C., Fenstermacher, J.D. 1995. Nicotine raises the influx of permeable solutes across the rat blood-brain barrier with little or no capillary recruitment. J. Cereb. Blood Flow Metab. 15: 687-698.

Chen, M.L., Ge, Z., Fox, J.G., Schauer, D.B. 2006. Disruption of tight junctions and induction of proinflammatory cytokine responses in colonic epithelial cells by *Campylobacter jejuni*. Infect. Immun. 74: 6581-6589.

Citi, S., Volberg, T., Bershadsky, A.D., Denisenko, N., Geiger, B. 1994. Cytoskeletal involvement in the modulation of cell-cell junctions by the protein kinase inhibitor H-7. J. Cell Sci. 107: 683-692.

Conacci-Sorrell, M., Zhurinsky, J., Ben-Ze'ev, A. 2002. The cadherin-catenin adhesion system in signaling and cancer. J. Clin. Invest. 109: 987-991.

Conklin, B.S., Zhao, W., Zhong, D.S., Chen, C. 2002. Nicotine and cotinine up-regulate vascular endothelial growth factor expression in endothelial cells. Am. J. Pathol. 160: 413-418.

Corringer, P-J., Sallette, J., Changeux, J-P. 2006. Nicotine enhances intracellular nicotinic receptor maturation: a novel mechanism of neural plasticity? J. Physiol. Paris 99: 162-171.

Crone, C., Christensen, O. 1981. Electrical resistance of a capillary endothelium. J Gen. Physiol. 77: 349-371.

Cucullo, L., McAllister, M.S., Kight, K., Krizanac-Bengez, L., Marroni, M., Mayberg, M.R., Stanness, K.A., Janigro, D. 2002. A new dynamic *in vitro* model for the multidimensional study of astrocyte-endothelial cell interactions at the blood-brain barrier. Brain Res. 951, 243-254.

Dani, J.A., de Biasi, M. 2001. Cellular mechanisms of nicotine addiction. Pharmacol. Biochem. Behav. 70: 439-446.

De Boer, A.G., Gaillard, P.J., Breimer, D.D. 1999. The transference of results between blood-brain barrier cell culture systems. Eur. J. Pharm. Sci. 8: 1-4.

Dehouck, M.P., Meresse, S., Delorme, P., Fruchart, J.C., Cecchelli, R. 1990. An easier, reproducible, and mass-production method to study the blood-brain barrier *in vitro*. J. Neurochem. 54: 1798-1801.

Dejana, E., Lampugnani, M.G., Martinez-estrada, O., Bazzoni, G. 2000. The molecular organization of endothelial junctions and their functional role in vascular morphogenesis and permeability. Int. J. Dev. Biol. 44: 743-748.

del Zoppo, G.J. and Hallenbeck, J.M. 2000. Advances in the vascular pathophysiology of ischemic stroke. Thromb. Res. 98: 73-81.

Deli, M.A., Abraham, C.S., Niwa, M., Dalus, A. 2003. N,N-diethyl-2[4-(phenylmethyl) phenoxy] ethanamine increases the permeability of primary mouse cerebral endothelial cell monolayers. Inflam. Res. 52: S39-S40.

Denhardt, D.T. 1996. Signal-transducing protein phosphorylation cascades mediated by Ras/Rho proteins in the mammalian cell:The potential for multiplex signaling. Biochem. J. 318: 729-747.

Denker, B.M., Saha, C., Khawaja, S., Nigam, S.K. 1996. Involvement of a heterotrimeric G protein α subunit in tight junction biogenesis. J. Biol. Chem. 271: 25750-25753.

di Luozzo, G., Pradhan, S., Dhadwal, A.K., Chen, A., Ueno, H., Sumpio, B.E. 2005. Nicotine induces mitogen-activated protein kinase dependent vascular smooth muscle cell migration. Atherosclerosis 178: 271-277.

Domotor, E., Sipos, I., Kittel, A., Abbott, N.J., Adam-Vizi, V. 1998. Improved growth of cultured brain microvascular endothelial cells on glass coated with a biological matrix. Neurochem Int. 33: 473-478.

Dorovini-Zis, K., Huynh, H.K. 1992. Ultrastructural localization of factor VIII-related antigen in cultured human brain microvessel endothelial cells. J. Histochem. Cytochem. 40: 689-696.

Eden, H.A., Parkos, C.A. 2000. Modulation of epithelial and endothelial paracellular permeability by leukocytes. Adv. Drug Deliv. Rev. 41: 315-328.

Fanning, A.S., Jameson, B.J., Jesaitis L.A., Anderson, J.M. 1998. The tight junction protein ZO-1 establishes a link between the transmembrane protein occludin and the actin cytoskeleton. J. Biol. Chem. 273: 29745-29753.

Farkas, A., Szatmari, E., Orbok, A., Wilhelm, I., Wejksza, K., Nagyoszi, P., Hutamekalin, P., Bauer, H., Bauer, H-C., Traweger, A., Krizbai, I. 2005. Hyperosmotic mannitol induces Src kinase-dependent phosphorylation of β-catenin in cerebral endothelial cells. J. Neurosci. Res. 80: 855-861.

Fiala, M., Liu, Q.N., Sayre, J., Pop, V., Brahmandam, V., Graves, M.C., Vinters, H.V. 2002. Cyclooxygenase-2-positive macrophages infiltrate the Alzheimer's disease brain and damage the blood-brain barrier. Eur. J. Clin. Invest. 32: 360-371.

Fischer, S., Wobben, M., Marti, H.H., Renz, D., Schaper, W. 2002. Hypoxia-induced hyperpermeability in brain microvessel endothelial cells involves VEGF-mediated changes in the expression of zonula occludens-1. Microvasc. Res. 63: 70-80.

Fletcher, N.F., Brayden, D.J., Brankin, B., Worrall, S., Callanan, J.J. 2006. Growth and characterization of a cell culture model of the feline blood-brain barrier. Vet. Immunol. Immunopathol. 109: 233-244.

Flesher, J.W., Horn, J., Lehner, A.F. 1998a. Carcinogenicity of 1-hydroxy-3-methylcholanthrene and its electrophilic sulfate ester 1-sulfooxy-3-methylcholanthrene in Sprague-Dawley rats. Biochem. Biophys. Res. Commun. 243: 30-35.

Flesher, J.W., Horn, J., Lehner, A.F. 1998b. 9-Sulfooxymethylanthracene is an ultimate electrophilic and carcinogenic form of 9-hydroxymethylanthracene. Biochem. Biophys. Res. Commun. 251: 239-243.

Forster, C., Silwedel, C., Golenhofen, N., Burek, M., Kietz, S., Mankertz, J., Drenckhahn, D. 2005. Occludin as direct target for glucocorticoid-induced improvement of blood-brain properties in a murine *in vitro* model. J. Physiol. 565: 475-486.

Forster, C., Waschke, J., Burek, M., Leers, J., Drenckhahn, D. 2006. Glucocorticoid effects on mouse microvascular endothelial barrier permeability are brain specific. J. Physiol. 573: 413-425.

Friedrich, A., Prasad, P.D., Freyer, D., Ganapathy, V., Brust, P. 2003. Molecular cloning and functional characterization of the OCTN2 transporter at the RBE4 cells, an *in vitro* model of the blood-brain barrier. Brain Res. 968: 69-79.

Furuse, M., Itoh, M., Hirase, T., Nagafuchi, A., Yonemura, S., Tsukita, S., Tsukita, S. 1994. Direct association of occludin with ZO-1 and its possible involvement in the localization of occludin at tight junctions. J. Cell Biol. 127: 1617-1626.

Furuse, M., Hirase, T., Itoh, M., Nagafuchi, A., Yonemura, S., Tsukita, S. 1993. Occludin: a novel integral membrane protein localizing at tight junctions. J. Cell Biol. 123: 1777-1788.

Furuse, M., Fujita, K., Hiiragi, T., Fujimoto, K., Tsukita, S. 1998. Claudin-1 and -2: novel integral membrane proteins localizing at tight junctions with no sequence similarity to occludin. J. Cell Biol. 141: 1539-1550.

Gaillard, P.J., Voorwinden, L.H., Nielsen, J.L., Ivanov, A., Atsumi, R., Engman, H., Ringbom, C., de Boer, A.G., Breimer, D.D. 2001. Establishment and functional characterization of an *in vitro* model of the blood-brain barrier, compromising a co-culture of brain capillary endothelial cells and astrocytes. Eur. J. Pharm. Sci. 12: 215-222.

Gardner, T.W., Dishion, T.J., Posner, N.I. 2006. Attention and adolescent tobacco use: a potential self-regulatory dynamic underlying nicotine addiction. Addict. Behav. 31: 531-536.

Gesto, M., Tintos, A., Soengas, J.L., Míguez, J.M. 2006. Effects of acute and prolonged naphthalene exposure on brain monoaminergic neurotransmitters in rainbow trout (*Oncorhynchus mykiss*). Comp. Biochem. Physiol. C. Toxicol. Pharmacol. 144: 173-183.

Ghazanfari, F.A., Stwewart, R.R. 2001. Characteristics of endothelial cells derived from the blood-brain barrier and of astrocytes in culture. Brain Res. 890: 49-65.

Giannini, A., Mazor, M., Orme, M., Vivanco, M., Waxman, J., Kypta, R. 2004. Nuclear export of α-catenin: overlap between nuclear export signal sequences and the β-catenin binding site. Exp. Cell Res. 295: 150-160.

Goldstein, G.W., Betz, A.L. 1986. The blood brain barrier. Sci. Am. 255: 74-83.

Gonzalez-Mariscal, L., Betanzos, A., Nava, P., Jaramillo, B.E. 2003. Tight junction proteins. Prog. Biophys. Mol. Biol. 81: 1-44.

Gottardi, C.J., Gumbiner, B.M. 2001. Adhesion signaling: how beta-catenin interacts with its partners. Curr. Biol. 11: R792-R794.

Graeber, M.B., Streit, W.J., Kreutzberg, G.W. 1989. Identity of ED-2 positive perivascular cells in rat brain. J. Neurosci. Res. 22: 103-106.

Greenwood, J., Pryce, G., Devine, L., Male, D.K., dos Santos, W.L.C., Calder, V.L., Adamson, P. 1996. SV40 large T immortalized cell lines of the rat blood-brain and blood-retinal barriers retain their phenotypic and immunological characteristics. J. Neuroimmunol. 71: 51-63.

Grevenynghe, J.V., Monteiro, P., Gilot, D., Fest, T., Fardel, O. 2006. Human endothelial progenitors constitute targets for environmental atherogenic polycyclic aromatic hydrocarbons. Biochem. Biophys. Res. Commun. 341: 763-769.

Gumbleton, M., Audus, K.L. 2001. Progress and limitations in the use of *in vitro* cell cultures to serve as a permeability screen for the blood-brain barrier. J. Pharm. Sci. 90: 1681-1698.

Hamann, G.F., Okada, Y., Fitridge, R., del Zoppo, G.J. 1995. Microvascular basal lamina antigens disappear during cerebral ischemia and reperfusion. Stroke 26: 2120-2126.

Haorah, J., Knipe, B., Leibhart, J., Ghorpade, A., Persidsky, Y. 2005. Alcohol-induced oxidative stress in brain endothelial cells causes blood-brain barrier dysfunction. J. Leukoc. Biol. 78: 1223-1232.

Haorah, J., Knipe, B., Gorantla, S., Zheng, J., Persidsky, Y. 2007. Alcohol-induced blood-brain barrier dysfunction is mediated via inositol 1,4,5-triphosphate receptor (IP3R)-gated intracellular calcium release. J. Neurochem. 100: 324-336.

Hassan, B.A., Bellen, H.J. 2000. Doing the MATH: is the mouse a good model for fly development? Genes. Dev. 15:1852-1865.

Hatashita, S., Hoff, J.T. 1990. Brain edema and cerebrovascular permeability during cerebral ischemia in rats. Stroke 21: 582-588.

Hawkins, B.T., Brown, R.C., Davis, T.P. 2002. Smoking and ischemic stroke a role for nicotine? Trends Pharmacol. Sci. 23: 78-82.

Hawkins, B.T., Abbruscato, T.J., Egleton, R.D., Brown, R.C., Huber, J.D., Campos, C.R., Davis, T.P. 2004. Nicotine increases *in vivo* blood-brain barrier permeability and alters cerebral microvascular tight junction protein distribution. Brain Res. 1027: 48-58.

Hawkins, B.T., Egleton, R.D., Davis, T.P. 2005. Modulation of cerebral microvascular permeability by endothelial nicotinic acetylcholine receptors. Am. J. Physiol. Heart Circ. Physiol. 289: H212-H219.

Hawkins, B.T., Thomas, P.D. 2005. The blood-brain barrier/neurovascular unit in health and disease. Pharmacol. Rev. 57: 173-185.

Heeschen, C., Weis, M., Aicher, A., Dimmeler, S., Cooke, J.P. 2002. A novel angiogenic pathway mediated by non-neuronal nicotinic acetylcholine receptors. J. Clin. Invest. 110: 527-536.

Heo, J.H., Han, S.W., Lee, S.K. 2005. Free radicals as triggers of brain edema formation after stroke. Free Radic. Biol. Med. 39: 51-70.

Hirase, T., Staddon, J.M., Saitou, M., Ando-Akatsuka, Y., Itoh, M., Furuse, M., Fujimoto, K., Tsukita, S., Rubin, L.L. 1997. Occludin as a possible determinant of tight junction permeability in endothelial cells. J. Cell Sci. 110:1603-1613.

Hoheisel, D., Nitz, T., Franke, H., Wegener, J., Hakvoort, A., Tilling, T., Galla, H-J. 1998. Hydrocortisone reinforces the blood-brain barrier properties in a serum free cell culture system. Biochem. Biophys. Res. Commun. 244: 312-316.

Hori, S., Ohtsuki, S., Hosoya, K., Nakashima, E., Terasaki, T. 2004. A pericyte-derived angiopoietin-1 multimeric complex induces occludin gene expression in brain capillary endothelial cells through Tie-2 activation *in vitro*. J. Neurochem. 89: 503-513.

Hoschuetzky, H., Aberle, H., Kemler, R. 1994. Beta-catenin mediates the interaction of the cadherin-catenin complex with epidermal growth factor receptor. J. Cell Biol. 127: 1375-1380.

Hoshino, S., Yoshida, M., Inoue, K., Yano, Y., Yanagita, M., Mawatari, H., Yamane, H., Kijima, T., Kumagai, T., Osaki, T., Tachiba, I., Kawase, I. 2005. Cigarette smoke extract induces endothelial cell injury via JNK pathway. Biochem. Biophys. Res. Commun. 329: 58-63.

Huber, J.D., Egleton, R.D., Davis, T.P. 2001. Molecular physiology and pathophysiology of tight junctions in the blood-brain barrier. Trends Neurosci. 24: 719-725.

Huber, J.D., Hau, V.S., Borg, L., Campos, C.R., Egleton, R.D., Davis, T.P. 2002. Blood-brain barrier tight junctions are altered during a 72-h exposure to λ-carrageenan-induced inflammatory pain. Am. J. Physiol. Heart Circ. Physiol. 283: H1531-1537.

Hurst, R.D., Fritz, I.B. 1996. Properties of an immortalised vascular endothelial/glioma cell co-culture model of the blood-brain barrier. J. Cell Physiol. 167: 81-88.

Imamura, Y., Itoh, M., Maeno, Y., Tsykita, S., Nagafuchi, A. 1999. Functional domains of alpha-catenin required for the strong state of cadherin-based cell adhesion. J. Cell Biol. 144: 1311-1322.

Jiang, D.J., Jia, S.J., Yan, J., Zhou, Z., Yuan, Q., Li, Y.J. 2006. Involvement of DDAH/ADMA/NOS pathway in nicotine-induced endothelial dysfunction. Biochem. Biophys. Res. Commun. 349; 683-693.

Jou, T.S., Stewart, D.B., Stappert, J., Nelson, W.J., Marrs J.A. 1995. Genetic and biochemical dissection of protein linkages in the cadherin-catenin complex. Proc. Natl. Acad. Sci. USA. 92: 5067-5071.

Kang, J.J., Cheng, Y.W. 1997. Polycyclic aromatic hydrocarbons induced vasorelaxation through induction of nitric oxide formation in endothelium of rat aorta. Toxicol. Lett. 93: 39-45.

Ke, L., Eisenhour, C.M., Bencherif, M., Lukas, R.J. 1998. Effects of chronic nicotine treatment on expression of diverse nicotinic acetylcholine receptor subtypes. I. Dose- and time-dependent effects of nicotine treatment. J. Pharmacol. Exp. Ther. 286:825-840.

Kevil, C.G., Oshima, T. Alexander, B., Coe, L.L., Alexander, J.S. 2000. H_2O_2-mediated permeability: role of MAPK and occludin. Am J. Physiol. Cell. Physiol. 279: C21-C30.

Kilaru, S., Frangos, S.G., Chen, A.H., Gortler, D., Dhadwal, A.K., Araiam, O., Sumpio, B.E. 2001. Nicotine: a review of its role in atherosclerosis. J. Am. Coll. Surg. 193; 538-546.

Knudsen, K.A., Peralta Soler, A., Johnson, K.R., Wheelock, M.J. 1995. Interaction of α-actinin with the cadherin/catenin cell-cell adhesion complex via α-catenin. J. Cell Biol. 130: 67-77.

Koide, M., Nishizawa, S., Yamamoto, S., Yamaguchi, M., Namba, H., Terakawa, S. 2005. Nicotine exposure, mimiced smoking, directly and indirectly enhanced protein kinase C activity in isolated canine basilar artery, resulting in enhancement of arterial contraction. J. Cereb. Blood Flow Metab. 25; 292-301.

Konu, O., Kane, J.K., Barrett, T., Li., M.D. 2001. Region-specific transcriptional response to chronic nicotine in rat brain. Brain Res. 909; 194-203.

Kovacic, P., Cooksy, A. 2005. Iminium metabolite mechanism for nicotine toxicity and addiction: Oxidative stress and electron transfer. Med. Hypotheses. 64: 104-11.

Krizbai, I.A., Bauer, H., Amberger, A., Hennig, B., Szabo, H., Fuchs, R., Bauer, H.C. 2000. Growth factor-induced morphological, physiological and molecular characteristics in cerebral endothelial cells. Eur. J. Cell Biol. 79: 594-600.

Krizbai, I.A., Deli, M.A. 2003. Signalling pathway regulating the tight junction permeability in the blood-brain barrier. Cell. Mol. Biol. (Noisy-le-grand). 49: 23-31.

Krizbai, I.A., Bauer, H., Bresgen, N., Eckl, P.M., Farkas, A., Szatmari, E., Traweger, A., Wejksza, K., Bauer, H.C. 2005. Effect of oxidative stress on the junctional proteins of cultured cerebral endothelial cells. Cell. Mol. Neurobiol. 25: 129-138.

Kurth, T., Kase, C.S., Berger, K., Schaeffener, E.S., Buring, J.E., Gaziano, M. 2003. Smoking and the risk of hemorrhagic stroke. Stroke 34: 1151-1155.

Lakin, N.D., Jackson, S.P. 1999. Regulation of p53 in response to DNA damage. Oncogene 18: 7644-7655.

Lampugnani, M.G., Resnati, M., Raiteri, M., Pigott, R., Pisacane, A., Houen, G., Ruco, L.P., Dejana, E. 1992. A novel endothelial-specific membrane protein is a marker of cell-cell contacts. J. Cell Biol. 118: 1511-1522.

Lampugnani, M.G., Corada, M., Caveda, L., Breviario, F., Ayalon, O., Geiger, B., Dejana, E. 1995. The molecular organization of endothelial cell to cell junctions: differential association of plakoglobin, beta-catenin, and alpha-catenin with vascular endothelial cadherin (VE-cadherin). J. Cell. Biol. 129: 203-217.

Lampugnani, M.G., Corada, M., Andriopoulou, P., Esser, S., Risau, W., Dejana, E. 1997. Cell confluence regulates tyrosine phosphorylation of adherens junction components in endothelial cells. J. Cell Sci. 110: 2065-2077.

Lee, H.S., Namkoong, K., Kim, D.H., Kim, K.J., Cheong, Y.H., Kin, S.S., Lee, W.B., Kim, K.Y. 2004. Hydrogen peroxide-induced alterations of tight junction protein in bovine brain microvessel endothelial cells. Microvasc. Res. 68: 231-238.

Lee, N.P.Y., Mruk, D.D., Wong, C.H., Cheng, C.Y. 2005. Regulation of sertoli-germ cell adherens junction dynamics in the testis via the nitric oxide synthase (NOS)/cGMP/protein kinase G (PRKG)/β-catenin (CATNB) signaling pathway: an *in vitro* and *in vivo* study. Biol. Reprod. 73: 458-471.

Li, C.H., Lee, C.C., Cheng, Y.W., Juang, H.A., Kang, J.J. 2004. Activation and up-regulation of nitric oxide synthase in human umbilical vein endothelial cells by polycyclic aromatic hydrocarbons. Toxicol. Lett. 151:367-74.

Liaw, C.W., Cannon, C., Power, M.D., Kiboneka, P.K., Rubin, L.L. 1990. Identification and cloning of two species of cadherins in bovine endothelial cells. EMBO J. 9: 2701-8.

Liebner, S., Kniesel, U., Kalbacher, H., Wolburg, H. 2000. Correlation of tight junction morphology with the expression of tight junction proteins in blood-brain barrier endothelial cells. Eur. J. Cell Biol. 79: 707-717.

Lin, S.J., Hong, C.Y., Chang, M.S., Chiang, B.N., Chien, S. 1992. Long-term nicotine exposure increases aortic endothelial cell death and enhances transendothelial macromolecule transport in rats. Artherioscler. Thromb. 12: 1305-1312.

Lindahl. P., Johansson. B.R., Leveen, P., Betsholtz, C. 1997. Pericyte loss and microaneurysm formation in PDGF-B-deficient mice. Science 277: 242–245.

Lippoldt, A., Kniesel, U., Liebner, S., Kalbacher, H., Kirsch, T., Wolburg, H., Haller, H. 2000. Structural alterations of tight junctions are associated with loss of polarity in stroke-prone spontaneously hypertensive rat blood-brain barrier endothelial cells. Brain Res. 885: 251-261.

Liu, R.M., Shi, M.M., Giulivi, C., Forman, H.J., 1998. Quinones increase γ-glutamyl transpeptidase expression by multiple mechanisms in rat lung epithelial cells. Am. J. Physiol. 274: 330-336.

Martin-Padura, I., Lostaglic, S., Schneemann, M., Williams, L., Romano, M., Fruscella, P., Panzeri, C., Stoppacciaro, A., Ruco, L., Villa, A., Simmons, D., Dejana, E. 1998. Junctional adhesion molecule, a novel member of the immunoglobulin superfamily that distributes at intercellular junctions and modulates monocyte transmigration. J. Cell Biol. 142: 117-127.

Mark, K.S., Davis, T.P. 2002. Cerebral microvascular changes in permeability and tight junctions induced by hypoxia-reoxygenation. Am. J. Physiol. Heart Circ. Physiol. 282: 1485-1494.

Matter, K., Balda, M.S. 2003. Holey barrier: claudins and the regulation of brain endothelial permeability. J. Cell Biol. 161: 459-460.

Mayhan, W.G., Sharpe, G.M. 1998. Superoxide dismutase receptors endothelium-dependent arteriolar dilation during acute infusion of nicotine. J. Appl. Physiol. 85: 1292-1298.

McAllister, M.S., Krizanac-Bengez, L., Macchia, F., Naftalin, R.J., Pedley, K.C., Mayberg, M.R., Marroni, M., Leaman, S., Stanness, K.A., Janigro, D. 2001.

Mechanisms of glucose transport at the blood-brain barrier: an *in vitro* study. Brain Res. 904: 20-30.

Megard, I., Garrigues, A., Orlowski, S., Jorajuria, S., Clayette, P., Ezan, E., Mabondzo, A. 2002. A co-culture-based model of human blood-brain barrier: application to active transport of indinavir and *in vivo-in vitro* correlation. Brain Res. 927: 153-167.

Merson, R.R., Franks, D.G., Karchner, S.I., Hahn, M.E. 2006. Development and characterization of polyclonal antibodies against the aryl hydrocarbon receptor protein family (AHR1, AHR2, and AHR repressor) of Atlantic killifish *Fundulus heteroclitus*. Comp. Biochem. Physiol. C. Toxicol. Pharmacol. 142: 85-94.

Mitic, L.L., Anderson, J.M. 1998. Molecular architecture of tight junctions. Annu. Rev. Physiol. 60: 121-142.

Mitic, L.L., Schneeberger, E.E., Fanning, A.S., Anderson, J.M. 1999. Connexin-occludin chimeras containing the ZO-binding domain of occludin localize at MDCK tight junctions and NRK cell contacts. J. Cell Biol. 146: 683-693.

Morita, K., Sasaki, H., Furuse, M., Tsukita, S. 1999. Endothelial claudin:Claudin-5/TMVCF constitutes tight junction strands in endothelial cells. J. Cell Biol. 147: 185-194.

Muller, S.L., Portwich, M., Schmidt, A., Utepbergenov, D.I., Huber, O., Blasig, I.E., Krause, G. 2005. The tight junctional protein occludin and the adherens junction protein α-catenin share a common interaction mechanism with ZO-1. J. Biol. Chem. 280: 3747-3756.

Neunteufl, T., Heher, S., Kostner, K., Mitulovic, G., Lehr, S., Khoschsorur, K., Schmid, R.W., Maurer, G., Stefenellt, T. 2002. Contribution of nicotine to acute endothelial dysfunction in long-term smokers. J. Am. Coll. Cardiol. 39: 251-256.

Newby, D.E., Wright, R.A, Labinjoh, C., Lundlam, C.A., Fox, K.A., Boon, N.A, Webb, D.J. 1999. Endothelial dysfunction, impaired endogenous fibrinolysis, and cigarette smoking: A mechanism for arterial thrombosis and myocardial infarction. Circulation 99: 1411-1415.

Niermann, T., Schmutz, S., Erne, P., Resink, T. 2003. Aryl hydrocarbon receptor ligands repress T-cadherin expression in vascular smooth muscle cells. Biochem. Biophys. Res. Commun. 300: 943-949.

Nitta, T., Hata, M., Gotoh, S., Seo, Y., Sasaki, H., Hashimoto, N., Furuse, M., Tsukita, S. 2003. Size-selective loosening of the blood-brain barrier in claudin-5-deficient mice. J. Cell Biol. 161: 653-660.

Nordskog, B.K., Fields, W.R., Hellmann, G.M. 2005. Kinetic analysis of cytokine response to cigarette smoke condensate by human endothelial and monocytic cells. Toxicology. 212: 87-97.

Nusrat, A., Giry, M., Turner, J.R., Colgan, S.P., Parkos, C.A., Carnes, D., Lemichez, E., Boquet, P., and Madara, J.L. 1995. Rho protein regulates tight junctions and perijunctional actin organization in polarized epithelia. Proc. Natl. Acad. Sci. U.S.A. 92: 10629-10633.

Ohkuma, H., Tabata, H., Suzuki, S., Islam, M.S. 2003. Risk factors for aneurysmal subarachnoid hemorrhage in Aomori, japan. Stroke 34: 96-100.

Okey, A.B, Riddick, D.S, Harper, P.A. 1994. Molecular biology of the aromatic hydrocarbon (dioxin) receptor. Trends Pharmacol. Sci. 15: 226-232.

Oliver, J.A. 1990. Adenylate cyclase and protein kinase C mediate opposite actions on endothelial junctions. J. Cell Physiol. 145: 536-542.

Oliver, J.A. 1992. Endothelium-derived relaxing factor contributes to the regulation of endothelial permeability. J. Cell Physiol. 151: 506-511.

Opdenakker, G., Nelissen, I., Damme, V.J. 2003. Functional roles and therapeutic targeting of gelatinase B and chemokines in multiple sclerosis. Lancet Neurol. 2 : 747-56.

Orlidge, A., D'Amore, P.A. 1987. Inhibition of capillary endothelial cell growth by pericytes and smooth muscle cells. J. Cell. Biol. 105: 1455-1462.

Ou, X., Ramos, K.S. 1992. Proliferative responses of quail aortic smooth muscle cells to benzo[a]pyrene: implications in PAH-induced atherogenesis. Toxicology. 74: 243-258.

Parathath, S.R., Parathath, S., Tsirka, S.E. 2006. Nitric oxide mediates neurodegeneration and breakdown of the blood-brain barrier in tPA-dependent excitotoxic injury in mice. J. Cell Sci. 119: 339-349.

Park, J.H., Okayama, N., Gute, D., Krsmanovic, A., Battarbee, H., Alexander, J.S. 1999. Hypoxia/aglycemia increases endothelial permeability: role of second messengers and cytoskeleton. Am. J. Physiol. 277: C1066-C1074.

Parkinson, F.E., Hacking, C. 2005. Pericyte abundance affects sucrose permeability in cultures of rat brain microvascular endothelial cells. Brain Res. 1049: 8-14.

Parrish, A.R., Fisher, R., Bral, C.M., Burghardt, R.C., Gandolfi, A.J., Brendel, K., Ramos, K.S. 1998. Benzo(a)pyrene-induced alterations in growth-related gene expression and signaling in precision-cut adult rat liver and kidney slices. Toxicol. Appl. Pharmacol. 152: 302-308.

Perriere, N., Demeuse, P.H., Garcia, E., Debray, R.M., Andreux, J-P., Couvreur, P., Scherrmann, J-M., Temsamani, J., Couraud, P-O., Deli, M.A., Roux, F. 2005. Puromycin-based purification of rat brain capillary endothelial cell cultures. Effect on the expression of blood-brain barrier-specific properties. J. Neurochem. 93: 279-289.

Petty, M.A., Lo, E.H. 2002. Junctional complexes of the blood-brain barrier: permeability changes in neuroinflammation. Prog. Neurobiol. 68: 311-23.

Rajasekaran, A.K., Hojo, M., Huima, T., Rodriguez-Boulan, E. 1996. Catenins and zonula occludens-1 form a complex during early stages in the assembly of tight junctions. J. Cell Biol. 132: 451-463.

Ramachandran, A., Moellering, D., Go, Y.M., Shiva, S., Levonen, A.L., Jo, H., Patel, R.P., Parthasarathy, S., Darley-Usmar, V.M. 2002. Activation of c-Jun N-terminal kinase and apoptosis in endothelial cells mediated by endogenous generation of hydrogen peroxide. Biol. Chem. 383: 693-701.

Rao, R.K., Basuroy, S., Rao, V.U., Karnaky, K.L., Gupta, A. 2002. Tyrosine phosphorylation and dissociation of occludin-ZO-1 and E-cadherin-β-catenin complexes fron the cytoskeleton by oxidative stress. Biochem. J. 368: 471-481.

Roux, F., Couraud, P.O. 2003. Rat brain endothelial cell lines for the study of blood-brain barrier permeability and transport functions. Cellular and Molecular Neurobiol. 25: 41-58.

Rubin, L.L., Hall, D.E., Porter, S., Barbu, K., Cannon, C., Horner, H.C., Janatpour, M., Liaw, C.W., Manning, K., Morales, J., Tanner, L.I., Tomaselli, K.J., Bard,

F. 1991. A cell culture model of the blood brain barrier. J. Cell Biol. 115: 1725-1735.

Rummel, A.M., Trosko, J.E., Wilson, M.R., Upham, B.L. 1999. Polycyclic aromatic hydrocarbons with bay-like regions inhibited gap junctional intercellular communication and stimulated MAPK activity. Toxicol. Sci. 49: 232-240.

Saitou, M., Fujimoto, K., Doi, Y., Itoh, M., Fujimoto, T., Furuse, M., Takano, H., Noda, T., Tsukita, S. 1998. Occludin-deficient embryonic stem cells can differentiate into polarized epithelial cells bearing tight junctions. J. Cell Biol. 141: 397-408.

Sakakibara, A. Furuse, M., Saitou, M., Ando-Akatsuka, Y., Tsukita, S. 1997. Possible involvement of phosphorylation of occludin in tight junction formation. J. Cell. Biol. 137: 1393-1401.

Schilling, L., Bultmann, A., Wahl, M. 1992. Lack of effect of topically applied nicotine on pial arteriole diameter and blood-brain barrier integrity in the cat. Clin. Investig. 70: 210-217.

Schinkel, A.H. 1999. P-glycoprotein, a gatekeeper in the blood-brain barrier. Adv. Drug Deliv. Rev. 36: 179-194.

Shelth, P., Basuroy, S., Li, C., Naren, A.P., Rao, R.K. 2003. Role of phosphatidylinositol 3-kinase in oxidative stress-induced disruption of tight junctions. J. Biol. Chem. 278: 49239-49245.

Sobue, K., Yamamoto, N., Yoneda, K., Hodgson, M.E., Yamashiro, K., Tsuruoka, N., Tsuda, T., Katsuya, H., Miura, Y., Asai, K., Kato, T. 1999. Induction of blood-brain barrier properties in immortalized bovine brain endothelial cells by astrocytic factors. Neurosci. Res. 35: 155-164.

St Croix, B., Sheehan, C., Rak, J.W., Florenes, V.A., Slingerland, J.M,, Kerbel, R.S. 1998. E-Cadherin-dependent growth suppression is mediated by the cyclin-dependent kinase inhibitor p27(KIP1). J. Cell Biol. 142: 557-571.

Stuart, R.O., Nigam, S.K. 1995. Regulated assembly of tight junctions by protein kinase C. Proc. Natl. Acad. Sci. USA. 92: 6072-6076.

Stevenson, B.R., Keon, B.H. 1998. The tight junction: morphology to molecules Annu. Rev. Cell Dev. Biol.14: 89-109.

Thirman, M.J. Albrecht, J.H. Krueger, M.A., Erickson, R.R., Cherwitz, D.L., Park, S.S., Gelboin, H.V., Holtzman, J.L. 1994. Induction of cytochrome CYPIA 1

and formation of toxic metabolites of benzo[a]pyrene by rat aorta: a possible role in atherogenesis. Proc. Natl. Acad. Aci. USA. 91: 5397-5401.

Tiruppathi, C., Ahmmed, G.U., Vogel, S.M., Malik, A.B. 2006. Ca^{2+} signaling, TRP channals, and endothelial permeability. Microcirculation 13: 693-708.

Tithof, P.K., Elgayyar, M., Cho, Y., Guan, W., Fisher, A.B., Peters- Golden, M. 2002. Polycyclic aromatic hydrocarbons present in cigarette smoke cause endothelial cell apoptosis by a phospholipase A2- dependent mechanism. FASEB. J. 16: 1463-1464.

Tonnessen, B.H., Severson, S.R., Hurt, R.D., Miller, V.M. 2000. Modulation of nitric-oxide synthase by nicotine. J. Pharmacol. Exp. Ther. 295: 601-606.

Torii, H., Kubota, H., Ishihara, H., Suzuki, M. 2007. Cilostazol inhibits the redistribution of the actin cytoskeleton and junctional proteins on the blood-brain barrier under hypoxia/reoxygenation. Pharmacol. Res. 55: 104-110.

Tsuchiya, M., Asada, A., Kasahara, E., Sata, E., Shindo, M., Inoue, M. 2002. Smoking a single cigarette rapidly reduces combined concentrations of nitrate and nitrite and concentrations of antioxidants in plasma. Circulation 105: 1155-1157.

Tsukita, S., Furuse, M. 2000. Pores in the wall: claudins constitute tight junction strands containing aqueous pores. J. Cell Biol. 2: 285-293.

Tsuneki, H., Ito, K., Sekizaki, N., Ma, E-L., You, Y., Kawakami, J., Adachi, I., Sasaoka, T., Kimura, I. 2004. Nicotinic enhancement of proliferation in bovine and porcine cerebral microvascular endothelial cells. Biol. Pharm. Bull. 27: 1951-1956.

Utsugisawa, K., Nagane, Y., Obara, D., Tohgi, H. 2002. Over-expression of α7 nicotinic acetylcholine receptor induces sustained ERK phosphorylation and N-cadherin expression in PC12 cells. Brain Res. Mol. Brain Res. 106: 88-93.

Van Italia, C.M., Anderson, J.M. 1997. Occludin confers adhesiveness when expressed in fibroblasts. J. Cell Sci. 110: 1113-1121.

Vermino, S., Rogers, M., Radcliffe, K., Dani, J. 1994. Quantitative measurement of calcium flux through muscle and neuronal nicotinc acetylcholine receptors. J. Neurosci. 14: 5514-5524.

Vietor, I., Bader, T., Paiha, K., Huber, L.A. 2001. Perturbation of the tight junction permeability barrier by occludin loop peptides activates beta-catenin/TCF/LEF-mediated transcription. EMBO Rep. 2: 306-312.

Vinggaard, A.M., Hnida, C., Larsen, J.C. 2000. Environment polycyclic aromatic hydrocarbons affect androgen receptor activation *in vitro*. Toxicology 145: 173-183.

Vorbrodt, A.W., Dobrogowska, D.H. 2003. Molecular anatomy of intercellular junctions in brain endothelial and epithelial barriers: electron microscopist's view. Brain Res. Rev. 42: 221-242.

Wan, H., Winton, H.L., Soeller, C., Gruenert, D.C., Thompson, P.J., Cannell, M.B., Stewart, G.A., Garrod, D.R., Robinson, C. 2000. Quantitative structural and biochemical analyses of tight junction dynamics following exposure of epithelial cells to house dust mite allergen Der p 1. Clin. Exp. Allergy 30: 685-698.

Wang, L., Kittaka, M., Sun, N., Schreiber, S.S., Zlokivic, B.V. (1994). Nicotine downregulates alpha2 isoform of Na+, K+ -ATPase at the BBB and brain of rats. Biochem. Biophys. Res. Commun. 199: 1422-1427.

Wang, L., Kittaka, M., Sun, N., Schreiber, S.S., Zlokivic, B.V. (1997). Chronic nicotine treatment enhances focal ischemic brain injury and depletes free pool of brain microvascular tissue plasminogen activator in rats. J. Cereb. Blood Flow Metab. 17: 136-147.

Wang, W., Dentler, W.L., Borchardt, R.T. 2001. VEGF increases BMEC monolayer permeability by affecting occluding expression and tight junction assembly. Am. J. Physiol. Heart Circ. Physiol. 280: H434-H440.

Wang, Y., Wang, L., Ai, X., Zhao, J., Hao, X., Lu, Y., Qiao, Z. 2004. Nicotine could augment adhesion molecule expression in human endothelial cells through macrophages secreting TNF-alpha, IL-1beta. Int. Immunopharmacol. 4: 1675-1686.

Wang, Y., Wang, Z., Zhou, Y., Liu, L., Zhao, Y., Yao, C., Wang, L., Qiao, Z. 2006. Nicotine stimulates adhesion molecule expression via calcium influx and mitogen-activated protein kinases in human endothelial cells. Int. J. Biochem. Cell. Biol. 38: 170-182.

Ward, P.D., Klein, R.R., Troutman, M.D., Desai, S., Thakker, D.R. 2002. Phospholipase C-γ modulates epithelial tight junction permeability through

hyperphosphorylation of tight junction proteins J. Biol. Chem. 277: 35760-35765.

Weidenfeller, C., Schrot, S., Zozulya, A., Galla, H-J. 2005. Murine brain capillary endothelial cells exhibit improved barrier properties under the influence of hydrocortisone. Brain Res. 1053: 162-174.

Weis, L.M., Rummel, A.M., Masten, S.J., Trosko, J.E., Upham, B.L. 1998. Bay or baylike regions of polycyclic aromatic hydrocarbons were potent inhibitors of gap junctional intercellular communication. Environ. Health Perspect. 106: 17-22.

Whyatt, R.M., Bell, D.A., Jedrychowski, W., Santella, R.M., Garte, S.J., Cosma, G., Manchester, D.K., Young, T.L., Cooper, T.B., Ottman, R., Perera, F.P. 1998. Polycyclic aromatic hydrocarbon-DNA adducts in human placenta and modulation by CYP1A1 induction and genotype. Carcinogenesis 19: 1389-1392.

Witt, K.A., Mark, K.S., Hom, S., Davis, T.P. 2003. Effects of hypoxia-reoxygenation on rat blood brain barrier permeability and tight junctional protein expression. Am. J. Physiol. Heart Circ. Physiol. 285: H2820-H2831.

Wittchen, E.S., Haskins, J., Stevenson, B.R. 1999. Protein interactions at the tight junction. Actin has multiple binding partners, and ZO-1 forms independent complexs with ZO-2 and ZO-3. J. Biol. Chem. 49: 35179-35185.

Wong, V. 1997. Phosphorylation of occludin correlates with occludin localization and function at the tight junction. Am. J. Physiol. 273: C1859-C1867.

Wu, Z., Hofman, F.M., Zlokovic, B.V. 2003. A simple method for isolation and characterization of mouse brain microvascular endothelial cells. J. Neurosci. Methods 130: 53-63.

Yamakage, K., Omori, Y., Zaidan-Dagli, M.L., Cros, M.P., Yamasaki, H. 2000. Induction of skin papillomas, carcinomas, and sarcomas in mice in which the connexin 43 gene is heterologously deleted. J. Invest. Dermatol. 114: 289-94.Valerie Ledent, V. and Vervoort, M. 2001. The basic helix-loop-helix protein family: comparative genomics and phylogenetic analysis. Genome Res. 11: 754-770.

Yang, Y.M., Liu, G.T. 2004. Damaging effect of cigarette smoke extract on primary cultured human umbilical vein endothelial cells and its mechanism. Biomed. Environ. Sci. 17: 121-134.

Yildiz, D. 2004. Nicotine, its metabolism and an overview of its biological effects. Toxicon. 43: 619-632.

Zhang, Y. Ramos, K.S. 1997. The induction of proliferative vascular smooth muscle cell phenotypes by benzo[a]pyrene does not involve mutational activation of ras gene. Mutat. Res. 373: 285-292.

Zidovetzki, R., Chen, P., Chen, M., Hofman, F.M. 1999. Endothelin-1-induced interleukin-8 production in human brain-derived endothelial cells is mediated by the protein kinase C and protein tyrosine kinase pathways. Blood 94: 1291-1299.

Zimmerman, G.D., McGeachie, J. 1987. The effect of nicotine on aortic endothelium: a quantitative ultrastructural study. Atherosclerosis 63: 33-41.

APPENDICES

APPENDIX A

PREPARATION OF REAGENTS

Acrylamide gel

50% Acrylamide 49.2% acrylamide, 0.8% methylene bis acrylamide

4 x Separating buffer (100 ml)

1.5 M Tris-HCl (pH 8.8)

0.4 % SDS

Adjust volume with deionized H_2O to 100 ml

4 x Stacking buffer (100 ml)

0.5 M Tris-HCl (pH 6.8)

0.4 % SDS

Adjust volume with deionized H_2O to 100 ml

Ammonium persulfate (APS) 10% APS in DDW

N,N,N',N'-tetramethylenediamine (TEMED)

1. Preparation of separating gel

To make two plates of acrylamide gel, the ingredients of separating gel are

	8%	9%	10%	13%	
DDW	5.9	5.7	5.5	4.9	ml
4% Separating buffer	2.5	2.5	2.5	2.5	ml
50% Acrylamide	1.6	1.8	2.0	2.6	ml
10% APS	50	50	50	50	μl
TEMED	10	10	10	10	μl

All of the ingredients were thoroughly mixed and immediately pour the gel between the glass plates. Before gel was completely polymerized (approximately 20-

30 min), 0.1% SDS in DDW was layered on the top of the separating gel (5 mm thick).

2. Preparation of stacking gel

Once the separating gel has completely polymerized (approximately 20-30 min), 0.1% SDS was removed from the top of the gel. To make stacking gel, the ingredients are

DDW	2.6	ml
4% Separating buffer	1.0	ml
50% Acrylamide	400	µl
10% APS	30	µl
TEMED	5	µl

All of the ingredients were thoroughly mixed and immediately pour the gel between the glass plates. The combs were inserted between the two glass plates of two sets of gel apparatus. The gels were leaved for approximately 30-40 min to polymerize.

3. Application of samples

Once the stacking gel has completely solidated, the combs were gently removed. The wells were flushed out thoroughly with running buffer. The clips and sealing tapes were removed and set up the gel chamber. The air bubbles between layers were removed by gently rolling the chamber.

bFGF (100 µg/ml)

One hundred microgram of bFGF was dissolved in 100 µl steriled PBS. Ten microlitter of solution were aliquoted into microcentrifuge tube and stored at –20 °C.

bFGF working solution (10,000X stock solution)

Ninety microlitter of steriled 1 mg/ml BSA-PBS or BSA-DMEM was added to aliqouted 10 µl bFGF (100 µg/ml). The final concentration was 1 ng/ml. The working solution can be kept for a weeks at 4 °C.

20% BSA-DMEM (weight / volume)

Twenty gram of BSA was dissolved in 100 ml DMEM/ F-12 HAM. The ingredients were put into a sterile glass bottle with wide mouth and stir with steriled magnetic stirrer for a few hours. The solution was steriled with syringe filter (0.45 μM). Twenty-five micromolar of solution was aliquoted into 50 ml-falcon tube and stored at –20 °C.

Collagenase (10 mg/ml)

One hundred milligram of collagenase was dissolved in 10 ml DMEM/ F-12 HAM at 37 ºC (waterbath). The solution was steriled with syringe filter (0.45 μM). One milliliter and 500 microlitter of solution were aliquoted into microcentrifuge tube and stored at –20 °C.

Collagenase-dispase (C/D) (10 mg/ml)

One hundred milligram of C/D was dissolved in 10 ml DMEM/ F-12 HAM at 37 ºC (waterbath). The solution was steriled with syringe filter (0.45 μM). One milliliter and 500 microlitter of solution were aliquoted into microcentrifuge tube and stored at –20 °C.

Commassie Brilliant Blue G-250 for protein determination

To prepare 1 L of Commassie Brilliant Blue G-250 solution, 100 g Commassie Brilliant Blue G-250 was mixed with 50 ml ethanol and 100 ml 85% (w/v) phosphoric acid, and then adjusted volume to 1,000 ml with DDW. After the mixture was mixed well by continuous stirring, the solution was filtrated through Whatman No 10. The solution was kept in container with tight cap and avoid from light.

Coverslip coating

Glass coverslips were washed with 70% ethanol. Both sides of the coverslips were carefully rubbed by cotton bud. Then, the coverslips were put into absolute ethanol and flamed. The coverslips were placed on 35 mm plastic culture dish. The coverslips were were covered by pipetting the coating reagent over the surface (100

μg/ml fibronectin, 250 μg/ml collagen type IV). The coverslips were dried in CO_2 incubator for 3 h.

Culture dishes and filter coating

The coating step was prepared during the second enzyme digestion of the cells. Ten plastic culture dishes, 35 mm diameter (1 dish/1 rat brain), or filters (12 mm Millicell-CM (Millipore) filter insert) were prepared. The coating reagents (50 μg/ml fibronectin, 150 μg/ml collagen type IV, and 800 μl steriled water for culture dish coating and 50 μg/ml fibronectin, 250 μg/ml collagen type IV, and 200 μl steriled water for filter coating) were put into the culture dishes or filters. The dishes or filters were covered by pipetting of the coating reagent over the surface. All dishes or filters were coated one by one and the rest of the coating reagents were discarded. The dishes or filters were dried in CO_2 incubator for 3 h.

DNase I (1 mg/ml) (2,855 U/ml)

Eleven milligram DNase I was dissolved in 11 ml ice-cold PBS. The solution was steriled with syringe filter (0.45 μM). Four hundred milliliter of solution was aliquoted into microcentrifuge tube and stored at –20 °C.

Electrophoresis buffer

To make 1 liter of electrophoresis buffer (250 mM Tris, 1.92 M glycine, and 0.5 % SDS) for stock solution, the ingredients are

Tris	3	g
Glycine	14.4	g
SDS	1	g

All ingredients were dissolved in DDW with continuously stirring. The solution was adjusted volume to 1,000 ml.

Immonoblot

The electrophoresis gel, without staining was equilibrated in transfer buffer solution with shaking for 10 min. A PVDF membrane and 4 pieces of filter paper were cut to the same size as the gel (5 x 8.3 inch). The PVDF membrane was soked by absolute methanol for few seconds before equilibrated by transfer buffer for 10-15 min. The membrane, 4 pieces of filter paper, and 4 pieces of transfer pressure pads were immersed in transfer buffer. The blotting preparation was assembled inserted between the blot restrainer and the blot support frame as shown below:

2 pieces of transfer pressure pad
2 pieces of filter paper
Equilibrated gel
Equilibrated PVDF membrane
2 pieces of filter paper
2 pieces of transfer pressure pad

Lysis buffer for Western blot analysis

The ingredients are:
20 mM Tris-HCl pH 7.4
150 mM NaCl
1% sodium deoxycholate
1% Triton X-100
1 mM sodium orthovanadate
10 mM NaF
1mM Pefabloc

All ingredients were dissolved in DDW. Lysis buffer was freshly prepared.

Percoll gradient centrifugation

For the gradient 10 ml Percoll, 19 ml PBS, 1 ml FBS, and 1 ml 10 x concentrated PBS were mixed, sterile filtered and put into a sterile Oakridge tube. The gradient was prepared by centrifugation at 18,000 rpm for 1.30 h at 4 °C.

Phosphate buffered saline (PBS)

To prepare 1 liter of PBS, the ingredients including 8 g NaCl, 0.2 g KCl, 0.2 g KH_2PO_4, and 1.44 g Na_2HPO_4 were dissolved in deionized water. The solution was mixed well and adjusted the pH to 7.4 with 5 N NaOH. The solution was adjusted volume to 1,000 ml.

PMS stock

To prepare stock solution 10 mM, PMS powder 3.063 mg/ml was solubilized well in PBS. The stock could be kept at 4 ºC for 1 month.

Protein-G-sepharose preparation

Twenty microlitters of beads were used for each protein sample. The beads were washed with 1,000 µl lysis buffer. The beads were incubated on ice for 2 min. The beads were collected by spun down at 2,000 rpm for 10 sec at 4 °C. The supernatant were removed. The beads were washed 5 times. The beads were ready to add to the samples.

Sample buffer

To make 5X sample buffer, for stock solution, the ingredients are

60 mM Tris HCl
25% glycerol
2% SDS
14.4 mM 2-mercaptoethanol
0.1% bromphenol blue

All ingredients were dissolved in DDW with continuously stirring. The solution was adjusted volume to 50 ml. 5X sample buffer was aliquoted into 1 ml/tube and stored at –20 °C.

SDS-PAGE staining

The gel was removed from the gel plaes and shaken in staining solution [0.25% coomassie blue R-250 (w/v), 50% methanol (v/v) and 10% acetic acid (v/v)] for 1 h at RT. The gel was washed to remove dye by shaking with destaining solution [5% methanol (v/v) and 7.5% acetic acid (v/v)]. A sponge was immersed in the washing solution tray to absorb dye until bands of proteins were clearly observed.

Transfer buffer

To make 1 liter of transfer buffer (160 mM Tris, 0.25 M glycine, and 20% methanol), the ingredients are

Tris	1.93	g
Glycine	9	g
Methanol	200	ml

All ingredients were dissolved in DDW with continuously stirring. The solution was adjusted volume to 1,000 ml.

Tris-buffered saline, 0.1 % Tween 20 (TBST)

To make 1 liter of 10X TBST (100 mM Tris, 1 M NaCl, and 0.1 % Tween 20) for stock solution, the ingredients are

Tris	12.114 g
NaCl	58.44 g
Tween 20	10 ml

All ingredients were dissolved in DDW with continuously stirring. The solution was adjusted volume to 1000 ml. Before use, the solution was diluted to 1 X TBST (10 mM Tris, 100 mM NaCl, and 0.01 % Tween 20) with DDW (10X TBST: DDW = 9 : 1).

XTT solution

XTT powder 1 mg/ml was solubilized well in warm DMEM/F-12 Ham. The 25 μM PMS was added into XTT solution and mixed well before used.

APPENDIX B

TABLES OF EXPERIMENTAL RESULTS

Table 1 The percentage of cell viability of nicotine-treated rat CECs in a concentration-dependent manner for 24 h.

Nicotine (μM)	% Cell viability
0	100 ± 0.00
0.01	89.41 ± 3.55
0.1	93.54 ± 5.21
1	90.65 ± 6.17
10	89.66 ± 6.93

Each value represented the mean value with S.E.M. of three independent experiments.

Table 2 The percentage of cell viability of phenanthrene-treated rat CECs in a concentration-dependent manner for 24 h.

Phenanthrene (μM)	% Cell viability
0	100 ± 0.00
15	93.86 ± 0.32
30	86.75 ± 1.97
60	67.95 ± 5.75*
120	64.15 ± 3.28*
240	47.12 ± 2.64*

Each value represented the mean value with S.E.M. of three independent experiments. Asterisks refer significant differences from the control group. Student's *t*-test was used for the comparison of two mean values, and statistical significance was taken as * $p < 0.05$.

Table 3 The percentage of cell viability of 1-methylanthracene-treated rat CECs in a concentration-dependent manner for 24 h.

1-methylanthracene (μM)	% Cell viability
0	100 ± 0.00
15	89.80 ± 2.56
30	87.16 ± 2.98
60	84.54 ± 7.01
120	67.86 ± 4.90*
240	56.56 ± 5.90*

Each value represented the mean value with S.E.M. of three independent experiments. Asterisks refer significant differences from the control group. Student's *t*-test was used for the comparison of two mean values, and statistical significance was taken as * $p < 0.05$.

Table 4 The percentage of expression of junctional proteins in response to nicotine treatment at the concentration of 10 µM

Protein	% Protein expression (compared to control)	
	Tx-soluble	Tx-insoluble
Occludin	109.17 ± 25.59	105.67 ± 11.34
Claudin-5	81.97 ± 12.42	108.20 ± 9.17
Cadherin	58.24 ± 12.12*	120.67 ± 19.76
ZO-1	52.44 ± 17.33*	104.68 ± 5.70

Each value represented the mean value with S.E.M. of three independent experiments. Asterisks refer significant differences from the control group. Student's *t*-test was used for the comparison of two mean values, and statistical significance was taken as * $p < 0.05$.

Table 5 The percentage of expression of junctional proteins in response to phenanthrene treatment at the concentration of 30 µM

Protein	% Protein expression (compared to control)	
	Tx-soluble	Tx-insoluble
Occludin	100.24 ± 11.01	94.06 ± 5.32
Claudin-5	105.25 ± 4.67	96.54 ± 6.12
Cadherin	107.93 ± 5.91	82.27 ± 13.86
ZO-1	96.14 ± 5.91	104.68 ± 5.70

Each value represented the mean value with S.E.M. of three independent experiments.

Table 6 The percentage of expression of junctional proteins in response to 1-methylanthracene treatment at the concentration of 30 µM

Protein	% Protein expression (compared to control)	
	Tx-soluble	Tx-insoluble
Occludin	100.66 ± 1.04	88.650 ± 2.94
Claudin-5	87.32 ± 10.27	95.18 ± 4.26
Cadherin	95.29 ± 2.04	122.49 ± 19.33
ZO-1	107.72 ± 5.55	108.64 ± 4.38

Each value represented the mean value with S.E.M. of three independent experiments.

Table 7 Intensity of protein interaction of occludin and ZO-1 in response to nicotine, phenanthrene, and 1-methylanthracene treatment.

Treatment	% ZO-1 protein expression (compared to control)
control	100 ± 0.00
nicotine	73.59 ± 4.80*
phenanthrene	75.28 ± 5.18*
1-methylanthracene	64.39 ± 2.63*

Each value represented the mean value with S.E.M. of three independent experiments. Asterisks refer significant differences from the control group. Student's *t*-test was used for the comparison of two mean values, and statistical significance was taken as * $p < 0.05$.

Table 8 Relative of ZO-1 protein intensity on occludin and ZO-1 in response to nicotine, phenanthrene, and 1-methylanthracene treatment.

Treatment	Relative ZO-1 protein intensity	
	ZO-1 protein expression (compared to control)	Protein interaction of occludin and ZO-1 (compared to control)
control	1 ± 0.00	1 ± 0.00
nicotine	0.69 ± 0.14	0.71 ± 0.04
phenanthrene	0.92 ± 0.01	0.72 ± 0.05
1-methylanthracene	0.96 ± 0.11	0.63 ± 0.02*

Each value represented the mean value with S.E.M. of three independent experiments. Asterisks refer significant differences from the control group. Student's *t*-test was used for the comparison of two mean values, and statistical significance was taken as * $p < 0.05$. Relative ZO-1 protein intensity was measured by comparing to its control intensity.

Table 9 Effect of nicotine, phenanthrene, and 1-methylanthracene on TEER at 24 h.

TEER	Treatment					
	control	nicotine	control	Ph	control	1-MA
Ω cm^2	273±55.50	219±58.66	132±7.57	125±11.93	233±6.64	248±2.72
% of initial value	100±0.00	101±1.78	100±0.00	100±12.74	100±0.00	98±8.70

Each value represented the mean value with S.E.M. of three independent experiments. Ph = phenanthrene, 1-MA = 1-methylanthracene.

Table 10 Cell viability of DMNQ-treated rat CECs in concentration-dependent manner for 24 h.

DMNQ (μM)	% Cell viability (compared to control)
0	100.00 ± 0.00
1	107.02 ± 6.11
10	103.97 ± 6.18
20	28.31 ± 1.00*
40	8.79 ± 0.49*
80	8.38 ± 0.47*
100	7.49 ± 0.42*

Each value represented the mean value with S.E.M. of three independent experiments. Asterisks refer significant differences from the control group. Student's *t*-test was used for the comparison of two mean values, and statistical significance was taken as * $p < 0.05$.

Table 11 Effect of nicotine and DMNQ on TEER.

TEER	Treatment					
	control	nicotine	control	DMNQ	control	nicotine + DMNQ
Ω cm^2	273±55.50	219±58.66	188±5.50	184±3.76	161±8.98	151±8.33*
% of initial value	100±0.00	101±1.78	100±0.00	95±3.00	100±0.00	80±1.43*

Each value represented the mean value with S.E.M. of three independent experiments. Asterisks refer significant differences from the control group. Student's *t*-test was used for the comparison of two mean values, and statistical significance was taken as * $p < 0.05$.

Study Protocol Approval

The Ethics Committee of the Faculty of Pharmaceutical Sciences, Chulalongkorn University, Bangkok, Thailand has approved the following study to be carried out according to the protocol dated and/ or amended as follows:

Study Title:	Nicotine and polycyclic aromatic hydrocarbons modulate junctional proteins and paracellular permeability of rat cerebral endothelial cells
Centre:	Chulalongkorn University
Principal Investigator:	Miss Pilaiwanwadee Hutamekalin
Protocol Date:	October 18, 2005
No.	209/2005

Vita

Miss Pilaiwanwadee Hutamekalin was born on February 28, 1973 in Nakornpathom Province. She graduated in Bachelor of Science (Biology) in 1995 from Silpakorn University and Master's degree of Science (Neurosciences) in 1998 from Mahidol University. She worked as research assistance at the National Center for Genetic Engineering and Biotechnology (BIOTEC), National Science and Technology Development Agency (NSTDA) from 1998 to 1999. She worked in the Biostructure department at Hoffmann-La Roche AG, Basel, Switzerland from 1999 to 2000. She worked as research assistance at the National Center for Genetic Engineering and Biotechnology (BIOTEC), National Science and Technology Development Agency (NSTDA) from 2000 to 2002.